University of Eastern Piedmont "Amedeo Avogadro"
Department of Science, Technology and Innovation (DiSIT)

From cell to organism:

an overview of responses to simulated hypergravity and microgravity

PhD thesis in Chemistry and Biology – BIO/06
Curricula "Energy, environmental and food sciences"

34th cycle: 2018-2022

PhD tutor

Prof.ssa Maria Angela Masini

PhD student

Valentina Bonetto

PhD Co-tutor

Prof.ssa Simonetta Sampò

PhD program Coordinator

Prof. Gian Cesare Tron

“I was born with an insatiable curiosity about so many things,” she said.
“I thought at some point I was going to have to make a choice between rockets and space — and biology.”

She did not have to make that choice.

Interview to Liz Warren

Table of contents

Introduction

1. Background

The advent of Space programs made it possible to study organisms and cells in a new condition. Outer space represents a unique environment with several abnormal conditions such as, alteration of the gravity vector (hypergravity and microgravity), space radiation, confinement with limited social interactions, hypovaria, extreme temperature, acceleration and space debris (Romsdahl et al., 2018). In particular, gravity vector's changes are essential in the perspective of a long permanence in Space. We focused on this condition and its effects on different organisms and cellular physiology.

The International Space Station (ISS) is an orbiting station; it is a cooperative project between the USA (NASA), Russia (RKA), 11 nations of the European Space Agency (ESA), Canada (CAS-ASC), Japan (JAXA) and Brazil (fig.1). Now, the ISS orbits around our planet in the lowest orbit of Earth and represents the largest and most complex international scientific project ever faced by humanity. It is four times larger than the Russian station Mir, 108 m wide and 88 m long, with more than 4000 m^2 covered with solar panels, which electrically powers six advanced laboratories. The ISS modules were brought in place piece-by-piece and gradually built in orbit using spacewalking astronauts and robotics. Although some individual modules were launched on single-use rockets, NASA's space shuttle used to carry up the heavier pieces. The ISS includes modules and connecting nodes containing living quarters and laboratories, exterior trusses that provide structural support, and solar panels that provide power. In 1998, the first module, the Russian Zarya module, was launched with a Proton rocket. The main construction was completed in 2017, even though the station continually improves to include new missions and experiments.

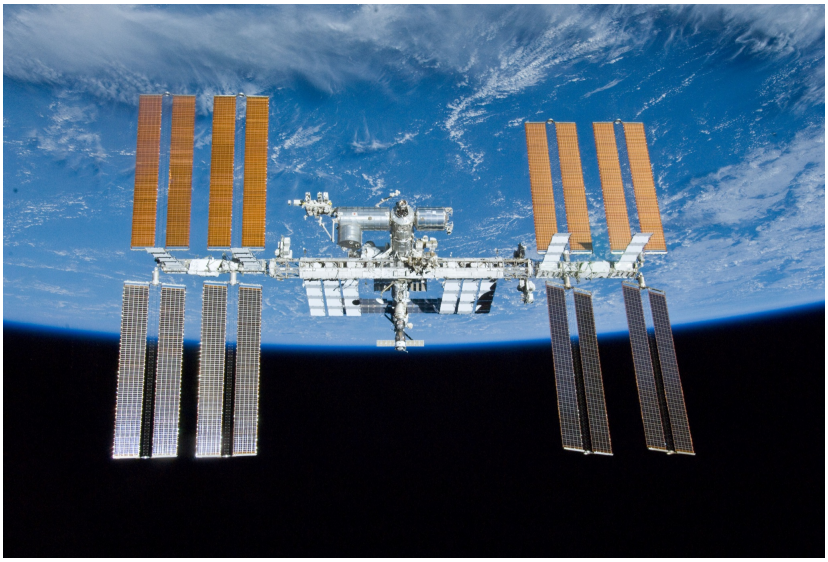

Fig. 1 International Space Station (ISS), European Space Agency photo.

Starting from November 2000, the ISS has been continuously inhabited by a crew of 7 astronauts that usually reached the Space Station by the Russian Soyuz capsule (first launch in 1967). This has for long been the only spacecraft that brought people to the ISS, while in March 2020, SpaceX's Crew Dragon capsule became the first privately-owned spacecraft to transport people to the ISS. Astronauts typically spend a mission period of around 6 months conducting various science experiments and maintaining and repairing the ISS. The astronauts spend at least 2 hours on exercise and personal care to minimise the microgravity side effects on their body and physiology. Currently, the ISS houses a specially designed machine called the Advanced Resistive Exercise Device (ARED). ARED can exercise all the major muscle groups through squats, deadlifts, calf raises and other exercises, using specifically designed resistance machines (Novikova et al., 2005; Trappe et al., 2009).

For decades the Space Agencies have promoted the study of Space travel effects on different organisms and cells. Thanks to the data collected, during the space missions, some questions arose about the side effect of altered gravity conditions in outer Space on living organisms, particularly hypergravity, during take-off and landing, and microgravity, along the mission. Throughout the launch, forces varied from 1 to 3g. While in the orbit re-entry phase, forces varied from nearly zero to 1.6g, over approximately 33 minutes. Thus, hypergravity and microgravity are two of the leading research topics in Space Biology since gravity perturbations may affect morphological and physiological traits, also compromising survival or fecundity of different organisms (Saldanha et al., 2016; Mora et al., 2019).

Except for cargo spacecraft that support the Space Station operations by transporting food and other supplies and the arrival of new crew members, the ISS is completely isolated from any other biological ecosystem and represents a unique extreme enclosed environment. The presence of humans on board entails the presence of microorganisms such as contaminants from the Earth environment, components of experiments, or the normal microbiota of the crew members. The ISS environment is a hermetically closed system subject to microgravity, cosmic radiation and high concentration of carbon dioxide. The internal temperature is constant, approximately around 22°C, and the humidity is stable at approximately 60%; the astronauts live and work in this orbiting isolated environment (Mora et al., 2019), which is highly controlled in order to protect as much as possible the health of the astronauts living there (Novikova et al., 2005). Life Support Systems (LSS) were developed and placed on the ISS to sustain humans living and working, far away from Earth's protective atmosphere and resources like water, air and food. LSS technologies control the atmosphere, with air revitalisation that includes oxygen generation and recovery, removal of carbon dioxide and control of trace contaminants and particulates, and water. The water management systems are designed to recycle crewmember urine, wastewater, and humidity for reuse as clean water, reducing the amount of water and consumables needed from Earth. Nowadays, we are on the cusp of significant advances in human interplanetary Space exploration advances. Long-term Space missions to reach Mars and the Moon require to preserve Space Station materials integrity, ensure a more reliable and effective system, and become independent from Earth supplies. It will also be more and more important to maintain long-term health in space and keep astronauts functioning at a high level during future longer flights (Voorhies et al., 2019).

2. Gravity Vector Changes: hypergravity and microgravity

Hypergravity

Gravity force is a universal force of attraction acting between all matter. It is by far the weakest known force in nature, and it does not play a pivotal role in determining the internal properties of matter. On the other hand, gravity is one of the constant factors guiding and affecting the evolution of all organisms living on Earth. It is difficult to understand what role this vector force may have on life as we know it, but it is accepted that it plays a fundamental role in regulating tissue and cell homeostasis, inducing mechanical stresses at the cellular level. The effect of its variation presents a fascinating topic in biology and medicine. Every (living and nonliving) object on the surface of the

Earth, due to the force of gravity, experiences weight (or force of gravity), proportionally to their mass and proportionally to the Earth's mass.

2.1. Gravity Vector Changes: Hypergravity

Hypergravity is a condition with an increased force of gravity, greater than 1g, namely the one experimented on the surface of Earth. Hypergravity is usually artificially created by researchers, in particular circumstance, to test materials or during recruitment for airforce and space missions. During hypergravity experiments, the resultant acceleration on a body is different from the acceleration due to the Earth gravity. The unit of the ratio of an applied acceleration to the gravitational constant is conventionally called G, with an approximate value of 6.67×10^{-11} N m^2/kg^2 units in the International System. In general:

$$F = G\frac{m1\ m2}{d^2}$$

Force (F) equals a gravitational constant (G) times the product of the masses divided by the square of the distance (d) between the masses (m). The gravitational constant (G) is calculated by the expression:

$$G = \frac{applied\ acceleration}{\mathrm{g}}$$

On Earth the acceleration of gravity (g) is 9.8 m/s^2 and it can be calculated by the expression:

$$g = G\frac{m}{d^2}$$

Hypergravity conditions can be experimented on Earth in a number of ways. Apart from using masses to produce a hypergravitational field (which is not practical), the typical methods to experiment with increased g-conditions are linear acceleration or centrifugation (Frett et al., 2016).

Every time that a vehicle accelerates continuously along a straight line all objects inside this vehicle are affected by a force that pushes them towards the opposite direction. This happens when a Space Shuttle is taking off. This is a linear acceleration and it is commonly used for crash simulators, for cars or aeroplanes. In the 1950's linear acceleration was used to examine the effects of high acceleration and deceleration forces on humans (Bonnefoy et al., 2021).

Another way to experiment with hypergravity conditions is centrifugation. Centrifugal force is an outward force that pushes a rotating body away from the rotation axis. This

centrifugal force (F) is the product of the centripetal acceleration, that means the magnitude of the tangential and the angular velocities ($r \times w^2$) times the mass (m) of the rotating object:

$$F = m \times w^2 \times r$$

This force has similar effects on cells, tissues, organs and whole organisms and can therefore be used to explore the effects of hypergravity but also to identify gravity-induced processes.

Centrifugation is technically easier to use, with respect to the linear acceleration, in order to achieve hypergravity both in ground-based and in space applications (Frett et al., 2016).

2.2. Gravity Vector Changes: Microgravity

When the forces of gravity are no longer opposed by elastic or other real forces and thus free to accelerate an object, the object becomes weightless. “Real weightlessness”, when gravity force reaches 0g, is also described as “free fall” by physicists. This is the condition where gravity is not opposed by any other forces rather than the virtual forces of inertia, and thus it is free to develop its full impact upon a mass (Albrecht-Buehler, 1992).

It is well known that, once in orbit and in the ISS, astronauts, as all living forms on board, experiment a decrease of the gravity vector that does not achieve 0g, thus is known as microgravity (with values around 10^{-6}g). This happens because the gravity force, as the force between two different masses, is inversely proportional to the square of the distance, so that it decreases with the distance:

$$F = g \frac{m1 \cdot m2}{r^2}$$

Thus, spacecrafts can reach a sufficient distance from Earth, where an individual or an object, inside the vessel, will experiment with microgravity, in other words individuals and objects are subject to a small fraction of the gravitational force. Nevertheless, this is not why things “float” on a vessel in orbit. Gravity causes all objects to fall with the same velocity in vacuum conditions. This force is measured due to the acceleration that freely falling objects experience, in other words, without frictional forces. This speed is irrespective of the object's mass, as it is only dependent upon the height of fall and the gravitational acceleration. The International Space Station (ISS) orbits our planet at an altitude between 320 and 400 km, where Earth’s gravity is approximately 90%. This orbiting spacecraft moves at 27,500 km/hour, and the orbit of its “fall” follows the orbit

and gravitational force of the Earth. Due to this fact, a spacecraft keeps falling toward the earth and never “hits” it. Thus, every spacecraft that is in a circular orbit around the Earth is actually in a free fall around the planet (Albrecht-Buehler, 1992; Frett et al., 2016).

2.3. Ground-based facilities for simulation of altered gravity environments

Interest in the effects of altered gravity on living organisms and cells has also intensified in recent years, due to the scenario of interplanetary travels. Planets suitable to inhabitation by Earth-based life are of actual interest, and most of them are predicted to have variable gravitational forces (Kalb et al., 2007; Horneck, 2008; Oczypok et al., 2012). Most of the papers cited are studies conducted both in real and simulated microgravity, thus exploiting facilities based on Earth (Saldanha et al, 2016; Bonnefoy et al., 2021). Scientists have developed ground-based microgravity simulators to study the physiological and molecular responses to altered gravity and develop effective countermeasures for spaceflight. As a matter of fact, ground-based facilities play a prominent role in gravitational biology. These platforms allow us to change gravity vectors and study the effect of gravity’s vector variation on organisms and cells on Earth. Furthermore, facilities for ground-based research can be used to identify possible effects of gravity changing before performing costly and time-consuming real microgravity experiments on board the ISS or the Space Shuttle. Biological experiments regarding gravity, that use ground-based facilities, provide a way to gain more knowledge about the experimental system's response in altered gravitational conditions. However, concerning microgravity, information and results obtained exploiting these facilities have to be verified under real microgravity conditions.

2.3.1 Hypergravity simulator: Large Diameter Centrifuge

Hypergravity can be simulated using a Large Diameter Centrifuge (LDC, fig.2). The LDC is a new centrifuge developed for the Life and Physical Sciences Instrumentation and Life Support Laboratory (LIS) project at the European Centre for Space Research and Technology (ESTEC), ESA's main research and development centre for space technologies, based in Noordwijk, the Netherlands (Van Loon, 2008).

Fig. 2 View of the LDC when rotating at full speed (i.e. 67 rpm) with the 6 gondolas swinging out. In the centre of rotation is the 7th enclosure for rotation control in case of animal studies. Next to the 7th enclosure is room to store dedicated liquid or gas bottles (Van Loon et al., 2008).

The idea of a large radius centrifuge was already postulated by Konstantin Tsiolkovsky, the Russian Space pioneer at the beginning of the 1900s. Other researchers have since worked on large rotating systems to apply chronic acceleration, but such a system has never been produced (Hall, 2016; Howe et al., 2019). Although there are challenges, realising an in-flight rotating station is feasible from a technological perspective. It does not have to be as expensive as a regular static spacecraft. The current focus in research is on short arm centrifuges. The main reason is that such in-flight centrifuges should fit into the hull diameter of the spacecraft in the range of 3 - 4.5 m. However, rotating in such a limited space results in huge body gravity gradients when rotating (Goswami et al., 2021).

This particular centrifuge allows the acquisition of data in a gravitational force range between 1 and 20 g, thus providing a condition of hypergravity for cell cultures, small animals, plants, but also to support physical and technological experiments or in the field of biology, materials science, geology or plasma physics. The LDC can perform experiments lasting one minute to six months without interruption. The development of hyper-gravity is guaranteed by the centripetal forces implemented in the rotation, and the minimum acceleration time from 1 to 20g is 60 seconds. In contrast, the maximum acceleration time is unlimited. It has a maximum diameter of 8 metres with four arms with a total of 6 free-swinging gondolas equipped with a series of utilities for the payloads (Van Loon, 2001; Van Loon, 2008), each of which has a maximum capacity of 80 kg. Gondolas are equipped with video connections and sensors capable of maintaining temperature and acceleration within predetermined ranges and sensors at the doors and fixing points for safety reasons. An additional gondola is located in the central axis to carry out control and comparison measures. For long-term animal studies, it is possible to provide the gondolas with drinking water and air; moreover, it is also possible to use specific pure gases or gas mixtures for combustion studies (Van Loon, 2008).

Special centrifuges lead to an increase in the gravitational force. The first purpose is to allow experimental manipulation of the gravitational field in order to study the response of the different samples (cell or organism) in depth. The second is to mitigate the adverse effects of space flight. Data collected will help us understand the effects of increased gravitational forces.

2.3.2. Microgravity simulator: from clinostats to Random Positioning Machine (RPM)

Given the difficulty of obtaining the possibility to expose cells and organisms to real microgravity, many experiments are conducted on Earth, using tools that simulate the reduction of the gravity vector. The so-called microgravity simulators do not reproduce real microgravity conditions but rather achieve unilateral stimulation by randomising the direction of gravity over time (clinostat and random positioning machine) or compensating the gravitational force with a counteracting force (magnetic levitation).
Random Positioning Machine (RPM) is a ground-based facility developed in the Netherlands (Airbus, Defence & Space, ADS, former Dutch Space, Leiden, NL); it is a clinostat with two axes, also called 3D-clinostat.
Clinostats are the most straightforward and affordable tool used to manipulate gravity on Earth. Clinostats were introduced in the late 19th century by the pioneers of plant gravitropism (Van Loon, 2007) and, along the years, have evolved to be applied to new technologies and new needs. Clinostats simulate the absence of a directional gravity field by averaging to zero the gravity vector through random rotations over time (Dedolph et al., 1971). Clinostats rotate around the main axis. Despite their limitations, clinostats remain an in-axis (1D or 2D clinostat) or two axes (3D clinostats). Two gimbal-mounted frames constitute three-dimensional clinostats turned independently by two dedicated motors. In Japan, they were first introduced by T. Hoson for plant research and later improved by Dutch Space in the Netherlands (Van Loon, 2007).
The term 3D clinostat means that the frames operate with constant speed and direction; when speed and direction are different and randomised, the clinostat takes the name of a "random positioning machine" (RPM, fig. 3) (Herranz et al., 2013). Dedicated algorithms drive the frames rotation, such that the biological samples, fixed on the inner frame, are constantly reoriented, rotating along two independent axes that change their orientations at constant speed and direction, so the gravity vector is averaged over time. Thus, even if 1g is constantly acting on the sample, the averaged gravity vector is close to zero (Brungs et al., 2016). Supposed the rotation is faster than the response time of

the biological system, the continuous reorientation will allow the sample to experience a condition very close to microgravity (Wuest et al., 2015).

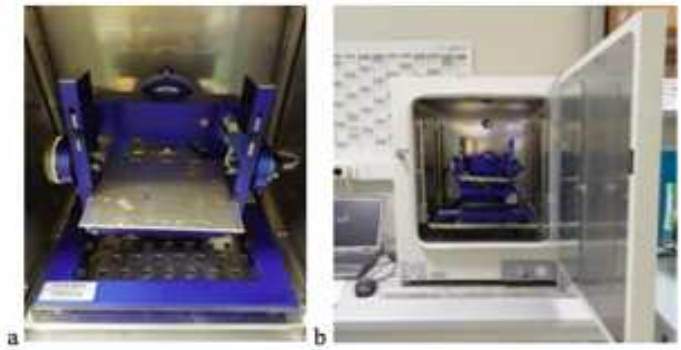

Fig 3. Random Positioning Machine (RPM). The RPM (Dutch Space, Leiden, Netherlands) (a) was run in a commercially available incubator to keep constant temperature and CO_2 (b).

Rotation induces accelerative forces. Therefore, sample positioning within the RPM is critical to consider when using this simulator. Where the two rotational axes cross, the forces acting on the sample are negligible; further from the centre, the forces acting on the outer edges of the sample become more relevant (Borst and van Loon, 2009). Therefore, the choice of an RPM setup imposes limits to sample volume. In addition, compared with static and real microgravity experiments, sample rotation introduces additional fluid motion in the culture flask, producing shear forces and enhancing convection (van Loon, 2007). Moderate rotations should be combined with smooth transitions to reduce shear stress. Enhanced convection leads to improved nutrients and gas provision and waste product removal, which allow it to work with higher cell densities. Higher cell density and gravitational unloading increase the chance of cell-cell interaction and the formation of multicellular aggregates. Thus, RPM can also be used to induce three-dimensional growth and to obtain a spheroid-like structure (Ingram et al., 1997; Grimm et al., 2018). Another practical aspect to consider when using the RPM is to avoid the formation of air bubbles in the liquid medium. Air bubbles produce unwanted fluid motion and shear stress and can cause the detachment of adherent cells (van Loon, 2008).

Even if this platform has been extensively used to simulate microgravity for Space Biology studies (preparatory tests for flight experiments, pre-and post-flight experiments, etc.), the RPM has been shown to mimic microgravity effects only partially. In reality, discrepancies in gene regulation were found between cells exposed to the RPM and those exposed to real microgravity in Space (Wuest et al., 2015).

Therefore, data from RPM experiments have to be interpreted carefully and, if possible, compared to experiments in real microgravity.

In summary, in order to obtain reliable data with the RPM, the experimental conditions must be carefully set. However, depending on the combination of rotation speed and the distance from the centre, high-quality microgravity conditions can be obtained, in the order of 10^{-6}g (Grimm et al., 2014). Moreover, thanks to recently introduced algorithms, RPM machines can also only partially average Earth gravity in order to simulate Moon- (0.16 g) or Mars-like (0.33 g) gravity conditions (Wuest et al., 2015).

It should be noted that simulated microgravity is not similar to the real microgravity experimented within the space environment. The fundamental difference with real weightlessness lies in inconstancy, because simulation devices have an alternating impact that prevents near zero gravity. However, it should also be noted that even in a real space flight, at least in low Earth orbit, it is almost impossible to achieve 0 gravity. This is due to a number of technogenic factors, for example the turning on of the ISS engines to correct the orbit (Ogneva et al., 2020).

3. Hypergravity-induced changes and adaptive responses:

3.1. Physiological effects of hypergravity

Gravity deeply influences several biological events in the living organisms. Variations in gravity values induce adaptive reactions that have been shown to play important roles, for example, in cell survival, growth and spatial organisation. During a Shuttle flight, astronauts experience a multitude of gravitational forces; the most studied for its effect on human physiology is microgravity. However, hypergravity has also demonstrated the ability to influence different systems. Additionally, astronauts and biological samples sent into Space are routinely subjected to hypergravity of 1.5–3.5 g when exiting and re-entering the Earth's atmosphere, and to microgravity, once in orbit after reaching the Space Station (Hu et al., 2008; Wu et al., 2012). Hypergravity facilities can be used to show sounding rocket launch effects, to identify gravitational imprint at the cellular level as well as to define alterations in organism’s physiology on mammals, also to derive a test protocol for the Space Adaptation Syndrome in humans and as a new therapeutic approach (van Loon, 2001).

All life forms existing on Earth have evolved to maximise their fitness at 1g, but they can also adapt to greater gravitational forces (Saldanha et al., 2016). The effects of gravity values larger than 1g exert biological either positive or negative consequences

on the living beings. Moreover, the physiological effects of long-duration exposures to hypergravity, especially on integrative physiology and systems, are poorly understood. The majority of researches focus on small parts and do not evaluate their interactions and consequences onto other related subsystems. Any tissue, organ, or receptor that depends on a continuous hydrostatic pressure gradient will experience changes if exposed to an altered gravitational environment.

For example, when exposed to hypergravity, many cells exhibit different proliferation and energy consumption than at 1 g. Tschopp and Cogoli (1983) demonstrated that hypergravity (10g, 48h) improves cell proliferation by 20–30% in different cell types. In contrast, glucose consumption is reduced at 10g compared to 1g, which means an increase of the anaerobic metabolism. This hypergravity-induced enhancement of proliferation can be related to DNA polymerase α, which is crucial in eukaryotic replication, and shows increased activity by hypergravity stimulation after 1h (Takemura and Yoshida, 2001). These results could be helpful to *in vitro* production of stem cells prior to commitment and following their implantation in regenerative medicine protocols and tissue engineering. Thus, hypergravity may be used as a new therapeutic approach. Significant changes were also observed in the cytoskeleton organisation and integrin distribution, accompanied by a great increase of the expression of genes related to actin, microtubules and intermediate filaments. The hyper-gravitational stress induces a significant reorganisation of the cytoskeleton, with upregulation of the genes encoding for actin, vimentin and tubulin, and redistribution of αvβ3 integrin (Monici et al., 2006).

How multicellular organisms respond to increased g-loading has been long studied to evaluate the effects of increased g-forces on pilots, especially those who perform manoeuvres in combat or aerobatics. Nowadays, the interest in the short-term and long-term effects of altered gravity on diverse organisms has also intensified with advances in interplanetary travels. Planets suitable to inhabitation by humanity are of particular interest, and most of them are predicted to have variable gravitational forces. Studies conducted in model organisms can help fill the gaps in our understanding of the consequences of gravitational forces more significant than 1g. Many reviews have shown the ability of diverse biological model organisms, such as mice, to face higher gravitational forces to feel these gaps. Different works have reported changes in mice body composition with an increase of muscle mass and a reduction of fat mass and body weight (Wade, 2005; Morita et al., 2015; Tominari, 2019). Low-speed hypergravity regimens, also tested on humans, can increase bone density and circulation related to

overexpression of bone formation markers such as Bone Morphogenetic Protein-2 (Bmp2), Collagen type 1α1 (Col1a1), Osterix (Osx) e Sclerostin (Sost) (Tomari, 2019). Other studies showed that hypergravity exposure induces more discrepancy between vestibular, visual, and sensorimotor signals, affecting performance, spatial abilities, and movements. Mice subjected to centrifugation showed an increase of heart rate due to increased sympathetic tone activity, with a consequent increase of urinary catecholamine levels. An increase of heart rate can therefore lead to morphological and structural changes of the organ (Morita et al., 2015). Alterations to the vestibular system are caused by a different distribution of otoliths and a decrease of signal transduction level (Frett et al., 2016; Wade, 2005; Morita et al., 2015). Studies on effects of gravitational acceleration can be useful as reference to improve knowledge in orientation mechanism and for cardiovascular regulation.

3.2. Effects of hypergravity on reproductive system

Some studies focused on the effect of hypergravity on the male reproductive system, have revealed that the human testis is an exceptionally sensible organ and it is easily overwhelmed by enviromental alteration and physiological disturbance (Saldanha et al, 2016). In mice subjected to 2g, a low sperm motility was recorded due to changes in the cytoskeleton and a decrease in tubulin production. These variations caused a decrease of ATP consumption: in the early stages of adaptation to hyper-gravity, there is a transient accumulation of ATP that leads to a suppression of the phosphofructokinase activity by the "Pasteur effect", and to the transition from glycolysis to oxidative phosphorylation. The oxygen consumption rate increases resulting in ROS accumulation. This results in a lower motor capacity of the spermatozoa and a decrease in male fertility (Ogneva et al., 2020). Additional effects of hyper-gravity towards the hypothalamus-pituitary-testis axis were observed, with increased testosterone levels in monkeys subjected to 2 g for three weeks (Strollo et al., 2000). Other studies conducted on sea urchin sperm have shown that they are sensitive to hyper-gravity, this was proved by a reduction of sperm velocity and fertilisation capabilities (Tash and Bracho, 1999; Tash et al., 2001; Ogneva et al., 2020). Changes of sperm motility were more pronounced under hypergravity than in microgravity, which is consistent with the data obtained on human sperm in parabolic flights; the observed changes in motility may be associated with changes in cell respiration and with a decrease of ATP consumption. The motor activity of sperm is also determined by the microtubule cytoskeleton state related to a decrease of the tubulin content.

Fertilisation and embryogenesis, like mating, are complex processes, and hypergravity could affect any of the several essential stages, influencing reproduction, development and survival.

However, these and other studies highlight differences in the responses to increased g-loading in various organisms based on size and physical contexts, as a deep comprehension of the adaptive responses is missing (Saldanha et al., 2016).

As reported in literature, hypergravity could be used as a countermeasure to minimise the effect of weightlessness conditions. Prior exposure to hypergravity can improve the condition of bodies for space travel, especially for long-term travel in a near-weightless environment, such as the ISS. Before and after space travel, hypergravity treatment for astronauts seems to be an excellent countermeasure to mitigate some health problems experienced after space travel. In fact, "gravity doping" (sudden acute exposure to small bouts of hypergravity) might be more effective than a more prolonged exposure to 1g or partial gravity. Also, artificial gravity, especially with intermittent exposure of about 30 min to 1 hour a day, in itself is presumably not enough to ensure full fitness. Even with short-arm simulated gravity, exercise capabilities will be needed for maintaining bone, muscle, and aerobic fitness during exposure to mechanical unloading (Goswami et al., 2021). The use of a hypergravity simulator, as LDC, would accelerate or stimulate all systems to the same way while there is a more physiological pressure and force distribution within the body in a large diameter centrifuge. Long radius chronic artificial gravity also does not require specific episodes of countermeasure training per day. Currently, the crew spends about 1.5–2h a day, at least 5 days a week, exercising to work against the microgravity pathologies exploiting the Resistance Exercise Device and also hypergravity simulator, while not fully counteracting its effects (Vico and Hargens, 2018).

Functional studies of effects to acute hypergravity and microgravity exposure has been perfomed exploiting parabolic flight, wich follow the ballistic trajectory of a parabola. Parabolic fight produce short successive periods of altered gravity within the range 0 and 1.8 g. (Zheng et al., 2017; Acharya et al., 2019).

A deep knowledge of the biological responses to hypergravity is deficitary, mainly since the body of evidence in the literature comprises significantly different and hardly relatable hypergravity conditions. We have a wealth of data regarding human physiology under long-duration microgravity conditions, but we do not know anything about chronic hypergravity. Applying prolonged hypergravity stimuli it could be possible to explore the impact of very long rotation duration on human physiology and

behaviour, address specific flight requirements, explore the Reduced Gravity Paradigm or identify minimum gravity thresholds (Goswami et al., 2021).

4. Microgravity-induced changes and adaptive responses

Nowadays, it is well known that microgravity can induce pathophysiological modifications described in astronauts (fig.4). During spaceflight, organisms face three periods of physiological adaptation: (1) changes upon entry to microgravity (initial adaptation), (2) changes after prolonged exposure to microgravity, and (3) readaptation to 1g gravity on Earth once returned from Space. The initial adaptation consists in impairing the cardiovascular and musculoskeletal systems, muscle atrophy and reductions in bone density, immune function, cardiovascular system and endocrine disorders (Winnard et al., 2017). Endocrine and reproductive tissues are key elements in the animal and human pathophysiology on the ground and, by extrapolation, in Space. Moreover, alterations to human physiology, sleep changes, living in confined environments with limited social interactions could pose mental health problems during space flight and once back on Earth. This set of gravity-related symptoms is called "Space Adaptation Syndrome" and they represent a threat after the return to Earth, where astronauts face the third period previously cited, a readaptation period to 1g gravity that could have different features. Maintaining good health, in general, requires the maintenance of homeostasis, this equilibrium is very likely to be subject to significant perturbations in Space, as already proven by the several pathological variations in several body functions regularly reported by astronauts.

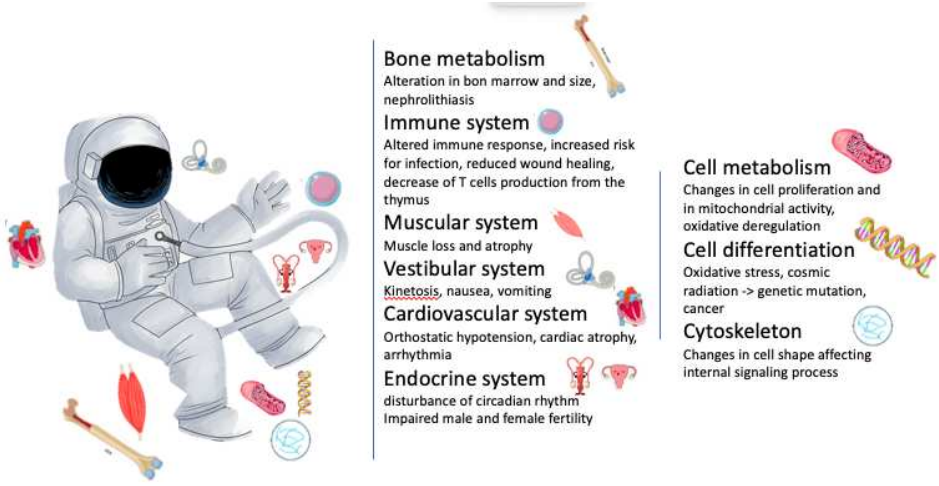

Fig. 4 Impact of microgravity and space radiation on astronauts (modified from Moroni et al., 2022)

The effects of space travel can endure for some time postflight and recovery time is closely influenced by the duration of missions and the exposure time to space conditions. Therefore, assessing how organisms could be affected by long-term spaceflight became more and more important.

4.1. Impact of microgravity on both normal and cancer cells

Early investigations of microgravity effects on human cells were carried out during the US Skylab Program in the 1970s. The main goal of this series of experiments was to gain more information about physiological changes that occur at the cellular level during extended exposure to microgravity in low Earth orbit, ranging from 28 days to 84 days. First results showed that living biological systems, from organisms to single cells, can readily adapt and grow in the space environment (Becker et al., 2013).
Coina et al. (2006) observed a drop of different metabolic activities, such as glucose uptake, methionine uptake/incorporation and thymidine incorporation, and an increase in stress protein expression (HSP-60, HSP-70 and 14-3-3 protein) suggesting that cells can feel the alteration in gravity conditions, simulated using a 3D-clinostat. The adaptive response to spaceflight is due to the effect exerted by near weightlessness at the cellular level. Indeed, alterations in cell shape, size, volume, and adherence properties were observed in cells cultured under microgravity conditions (Bradbury et al., 2020). Morphological alterations reflect changes in cytoskeletal organisation. The absence of mechanical loading induced a disaggregation in actin and tubulin filaments affecting cellular adherence, migration capacity, gene expression, force-sensing proteins, as mechanically activated ion channels, and signalling of the mechanotransduction pathways that depend on the combined interaction between cytoskeleton and cell adhesion molecules (Uva et al., 2002; Masini et al., 2007). Moreover, previous studies on primary cell culture, from mouse testis, showed correlations between cytoskeletal alteration, sex hormone production and exposure to simulated weightlessness. Mechanical unloading can also compromise signalling pathways, affecting signalling response, cell's metabolism and proliferation rate (Strollo et al., 2004; Vidyasekar et al., 2015). Biological properties changes and cells exposed to microgravity can be profoundly affected by the physical modifications in this unique environment (fig.5). Cytoskeleton rearrangement and reduced cell adhesion result in the ability of cells to form complex multicellular aggregates called spheroids (Unsworth and Lelkes, 1998; Costa et al., 2016). Three-dimensional (3D) cell culture technologies more closely represent *in vivo* cell environments.

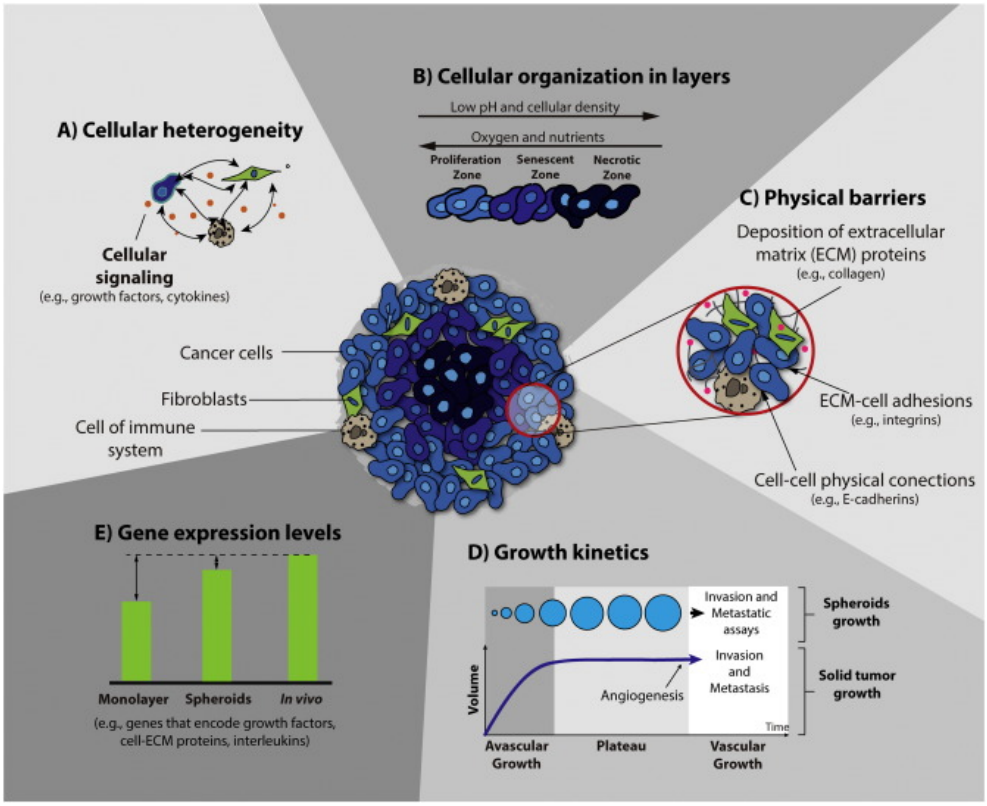

Fig. 5 Main characteristics of spheroids obtained with 3D cell culture technologies (Costa et al., 2016)

Breast, thyroid, and prostate cancer cells differentiate and show various morphological alterations, changing their growth behaviour when grown in space or under simulated microgravity. In the last years, a significant interest was developed regarding the impact of microgravity on tumour cells and 3D spheroids obtained exploiting low gravity conditions represent ideal in vitro systems for examining aspects of the tumour microenvironment that are observed *in vivo* (Kimlin et al., 2013; Topal et al., 2021). The cancer cells differentiate into two phenotypes in the microgravity environment. One part grows adherently on the bottom of the cell culture flasks and the other one assembled to 3D spheroids. 3D cell culture represents an intermediate metastasis model in its complexity between a monolayer culture and the *in vivo* tumour with the features of the primary tumour and also exhibit stem-like features (Zhang et al., 2020). Therefore, microgravity-engineered spheroids of different cancer types may represent an excellent model for detailed cancer stem cell's research.

In gravity altered conditions, cancer cells behave differently from normal ones: some processes, including apoptosis, adhesion, proliferation and migration, are differently activated (Kimlin et al., 2013; Vidyasekar et al., 2015). Indeed, it has been demonstrated that microgravity induces apoptosis in thyroid cancer cells, through the up-regulation of the pro-apoptotic factors Bax, PARP and p53, and inhibition of proliferation in Burkitt lymphoma cells, but not in normal cells. In addition, in simulated microgravity conditions tumour cells are subjected to a profound morphological rearrangement (Vidyasekar et al., 2015). Kopp et al. (2016) demonstrated that this phenomenon is linked to F-actin accumulation. Other authors have shown that the cytoskeleton, particularly the microfilamentous and microtubular components, become disorganised after a very short time of exposure to microgravity (Masini et al., 2006; Ulbrich et al. 2011). This alteration may affects many genes involved in the regulation of cancer cell proliferation, susceptibility to drugs (Mukhopadhyay et al., 2016), DNA repair (e.g. PARP), cell damage and invasion, through metastasis (Zhao et al., 2016; Kimlin et al, 2013).

Cancer cell migration causes metastasis and in lung cancer cell line A459 microgravity induces a decrease in matrix metalloproteinase expression this resulting in a reduction of cell migration. Cancer metastasis process correlates to Epithelial Mesenchymal Transition (EMT) (Topal et al., 2021). EMT is the capacity of epithelial cells to acquire mesenchymal traits under the influence of specific environmental signals, to trigger local invasion into surrounding tissues and systemic dissemination to distant organ sites (Sampieri and Fodde, 2012).

Vimentin plays an important role in this event, as a marker of EMT and a necessary regulatory factor for the migration of mesenchymal cells, whose activity is interrelated with E-cadherin expression. Previous studies have shown that decreased expression of E-cadherin could result in aggressiveness, dedifferentiation, and metastasis in many cancers. The available evidence suggests that microgravity can rearrange vimentin, reducing the number of vimentin molecules that exert physiological effects, compromising cancer cells' migration. On the other side, microgravity was found to promote cell migration and expression of genes related to different sub-types of non-small cell lung cancers, in particular alterations in TIMP-1, MMP-2, and MMP-9 expression levels were observed (Ahn et al., 2019).

EMT can induce differentiated cancer cells into a stem cell-like state. It has largely been accepted that resistance to conventional anti-cancer treatments can be attributed to a small cell subset called cancer stem cells (CSCs). CSCs represent a subpopulation

of tumour cells endowed, just like normal stem cells, with self-renewal and multi-lineage differentiation capacity, but with an altered homeostatic equilibrium that results in unbalanced cell growth and the formation of the tumour mass. This subset of cells is the main orchestrator of tumour establishment, metastatic progression and relapse (fig.6). Already identified in most of the neoplastic tissues, differently from the other tumour cells, CSCs are endowed with great plasticity, capability to enter quiescence and survive to microenvironment changes adapting metabolism, energy machinery and proliferation.

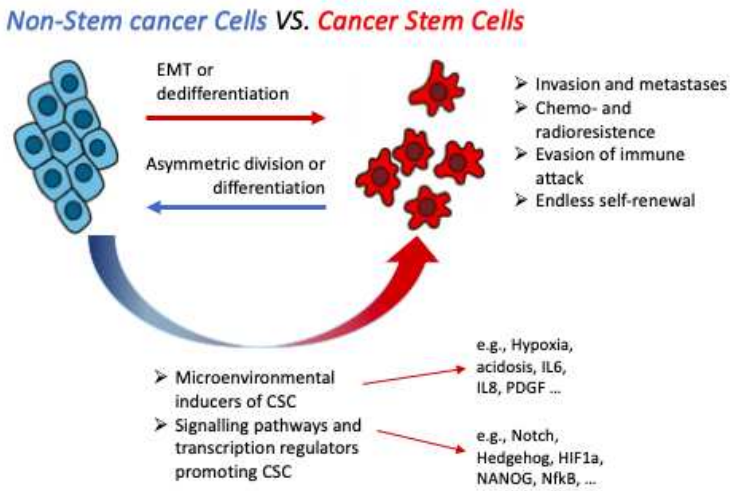

Fig. 6 Illustration of the reversible transitions between the pools of non-stem cancer cells and CSCs and main characteristics of CSCs that are critical for the tumorigenicity and cancer pathogenesis. The figure includes some extracellular and intracellular stimuli, factors, and pathways that can contribute to the cancer stemness development and progression (modified from Kabakov et al., 2020).

Up until now, there are only a few studies investigating CSCs response to microgravity. Moreover, results gained are quite different, depending on cell type and the choice of experimental design. Pisanu et al. (2014) showed that CSCs from non-small lung cancer cells are rescued from their quiescent state and lose their stemness when subjected to microgravity, whereas human colorectal cancer cells HCT116, under the same condition, showed an elevated autophagic rate and increased stemness (Arun et al., 2019). Anyway, both simulated and real microgravity condition induce CSCs generation from different cancer cell types, this could be interesting for the identification of new target structures involved in CSCs proliferation and differentiation that may furthermore lead to the development of novel tumour-suppressing drugs (Grimm et al., 2020).

As reported, to date the results of microgravity effects on cancer cells and CSCs are contradictory mainly due to different setup, experimental designs and time-points

analysed. However, combining the insight gained from space-based investigations together with data from on-ground culture models could improve our knowledge on cancer and support the development of novel anti-cancer therapies.

4.1.1. Pancreatic Ductal Adenocarcinoma (PDAC): epidemiology and driver-mutations

Despite its incisiveness, pancreatic ductal adenocarcinoma (PDAC) has not been examined so far in microgravity conditions. This neoplasia is one of the most severe malignancies, characterised by early spread to local and distant organs, representing the 4th-5th cause of death from cancer in the western world. The therapeutic options currently available for PDAC treatment are surgery, alone or in combination with radio or chemotherapy; however, only 8% of patients are alive 5 years after diagnosis due to late diagnosis and/or resistance to conventional treatments. The only curative therapy available for pancreatic cancer is surgical resection, after which the median survival of patients is 15–20 months and 5-year survival is 7%–25%, depending, among others, on the presence of positive margins at the time of surgery (Konstantinidis et al., 2013).

The incidence of PDAC is on the rise and early diagnosis is essential to improve the prognosis of patients with this tumour. It is rare for PDAC to be diagnosed at an early stage, with only 2% of all PDAC being diagnosed at stages 0 and I. Since PDAC does not present specific symptoms, it is difficult to use clinical symptoms for early detection; determining risk factors for PDAC may enable early detection of PDAC by conducting periodic examinations in patients who are especially at risk. The major risk factors can be broadly classified into family history, genetic disorders, complications, and behaviour.

Bad habits, such as habitual consumption of junk food, alcohol and cigarettes, as an increase in body mass index (BMI) increase the risk of onset of PDAC. Another risk factor is diabetes type II, in patients with this disorder the risk of developing PDAC is increased. Moreover, cigarette smoking synergistically increases the risk of developing PDAC in patients with other risk factors.

Smoking and chronic pancreatitis increase the risk of developing PDAC in patients with diabetes mellitus. Chronic pancreatitis has been reported to be a risk factor for developing PDAC. A meta-analysis revealed a correlation between acute pancreatitis and the development of PDAC (Malka et al., 2002). Patients with a history of acute pancreatitis require accurate evaluations from the perspective of pancreatic carcinogenesis.

Invasive cancer, as PDAC, can also develop from cystic precursor lesions of the pancreas such as intraductal papillary mucinous neoplasms (IPMNs) or mucinous cystic neoplasms (MCNs) (Matthaei et al., 2011). IPMN is characterised by ductal dilatation caused by the proliferation of a papillary epithelial neoplasm capable of producing mucus. The most prevalent precursor of PDAC is pancreatic intraepithelial neoplasia (PanIN) that start from low-grade lesions (PanIN-1A and PanIN-1B) to intermediate (PanIN-2) and high-grade lesions (PanIN-3) in which minimal cytological and architectural atypia develops in severe atypia. Progression is accompanied by molecular changes and can develop into invasive carcinoma (Distler et al., 2014). In over 90% of PDACs the driver mutation is V-Ki-ras2 Kirsten Rat Sarcoma viral oncogene homolog (KRAS) activation, which is the earliest mutation and increases cell proliferation rate. Subsequent early events occurring are telomere shortening and inactivation of tumour suppressor genes cyclin-dependent kinase inhibitor p16 (p16), Cyclin-Dependent Kinase inhibitor 2A (CDKN2A) and the inactivation of tumour suppressor genes SMAD4/DPC4 and TP53 (Hruban et al., 2004). Each of these mutations causes deregulation of a specific signalling pathway, resulting in the initiation or evolution of cancer clones.

Recent data have challenged this model of gradual accumulation of mutations. Notta et al. (2016) revealed that a subset of pancreatic cancers were not the result of sequential mutations but simultaneous mutations, thereby setting up invasive tumour growth.

Up to 10% of PDAC cases are hereditary and familial in origin; the risk ratio of developing PDAC is reportedly 6.79 times greater in families with a member who has PDAC. Hereditary pancreatitis is a genetic condition characterised by recurrent episodes of acute pancreatitis starting in infancy. Moreover, it seems associated with mutations in the PRSS1 and SPINK1 genes.

Besides the known mutations involved in the development of pancreatic cancer, studies also demonstrate that PDAC has a complex landscape of low-frequency mutations and considerable intratumoural heterogeneity. Jones et al. (2008) demonstrated an average of 63 genetic alterations in a core set of 12 cellular signalling pathways, while data collected in other works reported 32 significantly mutated genes in 10 gene programmes (Yachida et al., 2010; Bailey et al., 2016).

Traditionally, like many other malignant diseases, pancreatic cancer results from an accumulation of mutations in genes (i.e., tumour suppressor genes, oncogenes, and genomic maintenance genes) and altered cellular signalling pathways resulting in progression from intraepithelial neoplasia to invasive cancer (Sakorafas et al., 2001).

The loss of tissue integrity, which characterised cancer development, carcinogenesis, and further progress, occurs due to reciprocal interactions between tumour cells and the non-cellular and cellular components of the Tumour Microenvironment (TME). The immunoarchitectural characteristics of the TME interact and cooperate with the tumour cells in a dynamic way to affect tumour progression. TME consists of tumour cells, tumour stromal cells including stromal fibroblasts, endothelial cells and immune cells like microglia, macrophages and lymphocytes and the non-cellular components of the extracellular matrix such as collagen, fibronectin, hyaluronan, laminin, among others. Tumour cells control the function of cellular and non-cellular components of TME through complex signalling networks to use the non-malignant cells to work for their own benefit. The consequence of such cross-talks is reflected in tumour formation and maintenance as well as deficient response to therapy and multidrug resistance. Recently, genomic and transcriptomic profiling has allowed the characterization of distinct molecular PDAC subtypes with unique genetic signatures, widespread intra-tumoural heterogeneity. The differences in genetic alterations result in different subtypes of PDAC, which differ in their response to therapy, tumour invasiveness, and survival (Bailey et al., 2016; Collisson et al., 2011; Moffitt et al., 2015).

4.2. Physiological effects of microgravity on fungal organism: an overview

In 2013, the US National Aeronautics and Space Administration (NASA) announced plans for a human mission to Mars, which increased the interest on effects of long-duration space missions on human physiology and spacecraft materials. So far, NASA has not found behavioural emergencies during US space flights, but as we extend our reach into Space, it is likely a matter of time before something like this will occur. Private organisations, such as SpaceX, have announced plans to launch their own crews into Space. NASA aims to send humans back to the Moon and subsequently to Mars in the 2030. Spacecrafts are usually inhabited by crewmembers, the presence of humans on board entails the presence of other organisms: microorganisms (fig.7). Microbial contamination was observed on piping and equipment behind panels on board Salyut 6; water recycling system, rubber of hatch locks, electrical connectors, and the thermal control system's radiator on board Salyut 7; and air conditioning, oxygen electrolysis block, EVA suit's headphone, water recycling unit, and thermal control system on board Mir (Novikova et al., 2005).

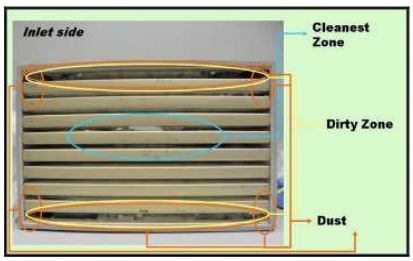

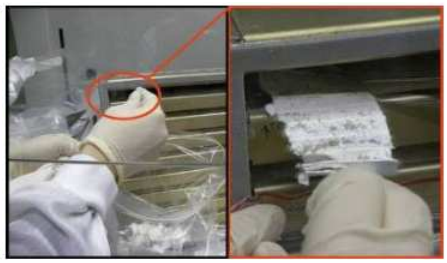

Sample location	Total Count (CFU/100 cm^2) TC 36°C	Details	Total fungal Count (CFU/100 cm^2) YM 22°C	Details
Inlet side Close to edge	1,90 x 10 ^{2}	5% bacteria (identified species: *Acinetobacter calcoaceticus*)	1. 1 x 10 ^{2}	73,3% Penicillia
		95% fungi		26,7% Aspergilli
Inlet side Middle zone	n.e †.	Invasive colonies of yeast (identified species: *Rhodotorula rubra*)	0.2 x 10 ^{2}	100.0% Penicillia
Outlet side Close to edge	n.g.*			

* n.g : no growth † n.e.: not enumerable colonies

Fig.7 Columbus cabin HEPA filter (High Efficiency Particulate Air) and results of microbiological and fungal analyses (Grizaffi et al, 2011).

In entering this new era of human spaceflight, a thorough understanding of how microorganisms respond and adapt to the various stimuli encountered while in Space will play an important role in ensuring a healthy living environment for crew members and spacecraft components.

Microbial species from the ISS can be both beneficial and detrimental to human health (Checinska Sielaff et al., 2019). Therefore, responses of microorganisms will be of paramount importance in future space exploration activities. Exposure to spaceflight conditions and the immunocompromised state of astronauts might still induce some commensal microorganisms to become pathogenic, compromising crew members health outcomes and safety of the Space Station environment. Then, understanding how these microorganisms can adapt themselves to space conditions could be useful to develop strategies to mitigate the risk posed by possible pathogenic microorganisms (Lesnyak et al., 1996; Taylor et al., 1997). In addition, space environment has to be considered as extreme environments and microorganisms enable to survive there can show space-induced alteration that could have an impact not only on crew's health but also on spacecraft's components (Romsdahl et al., 2018, 2019). On the other hand, microorganisms could be employed to sustain life in the space environment during long-term missions carrying out life support utilities, such as waste degradation, water recovery, and oxygen production. In particular, fungal biotechnology can be harnessed, so that Space Stations are self-sustaining with respect to food, pharmaceuticals, waste recycling, and plastic degradation for long-term missions (Cortesao et al., 2020).

The first experiments involving exposure of microorganisms to space conditions started in 1935 with balloon flights and rocket payloads (Dickson, 1991; Nickerson et al., 2004). Then in 1966 the National Aeronautics and Space Administration (NASA), during the Gemini IX and XII missions, began experiments in which spores of the fungi *Penicillium roqueforti* were directly exposed to space conditions for 6.5h. This study was one of the first to evaluate the survival limits of microorganisms upon exposure to space conditions. Nowadays it is well known that fungi include species that show higher resistance in comparison to prokaryotes (Romsdahl et al., 2019). Fungi can be found in various extreme conditions, such as: different temperatures and pH (Amaral Zettler et al. 2002; Gunde-Cimerman et al. 2009), in dry environments (Barnard et al. 2013), in environments with ionising radiation (Dadachova and Casadevall 2008), Mars-like conditions (Onofri et al. 2008; Blachowicz et al., 2019), and spacecraft environment (Onofri et al. 2007; Checinska et al. 2015). Through adaptation, fungi have developed the capacity to sense and respond to external stimuli, enabling their survival in a wide variety of ecological niches (Onofri et al. 2007; Onofri et al. 2019; Dadachova and Casadevall 2008; de Crecy et al. 2009; Checinska et al. 2015).

Fungi, with their ability to adapt, survive and reproduce in extreme environments, represent a fascinating topic with an impressive amount of interesting applications, as said before. The space environment is characterised by multiple stress factors that could have an impact on fungal morphology and physiology, as described for all eukaryotic organisms that undergo this condition. Horneck et al. (2006) in previous works investigated the effect of microgravity and radiation on different fungal strains. They demonstrate that microgravity decreases the transfer of extracellular nutrients and metabolic by-products, altering the chemical environment to which the hyphae are exposed to. Although, solar and cosmic radiation alters biological processes by acting as a promoter of mutagenesis, which may result in an increased rate of biological evolution and lead to the development of adaptive responses (Horneck et al. 2006; 2010). Our understanding of how fungi respond and adapt to the various conditions encountered during spaceflight remains in its infancy. We just can say that fungi are ubiquitous in spacecraft environments. Microgravity and carbon source deficiency can alter their metabolism inducing fungi to adapt themselves to digest complex polymer present on spacecraft causing the mechanical or electrical problem without possibilities to change some components that need to be supplied from Earth (Pierson 2001; Novikova et al. 2006; Venkateswaran et al. 2014; Checinska et al. 2015; Romsdahl et al., 2019).

4.2.1 Impact of gravity vector on Fungal Growth and Morphology

Environmental stimuli control and determine the development, growth and survival of many living organisms such as plants, animals and fungi. Mobile organisms respond to environmental stimuli by implementing movement strategies, while in sessile organisms, especially in plants and fungi, the effects of environmental stimuli are often evident in a phenomenon called tropism that involves directional growth of stem, roots or hyphae in response to the stimulus direction (Moore, 1991). Gravity is a homogeneous stimulus that induces a non-uniform response involving several mechanisms resulting in morphological and physiological alterations. Many organisms sense gravity as a guiding signal for directed growth, sometimes in combination with other environmental signals, such as light. Fungi use the information provided by the measurement of gravity to orient the growth of morphological structures. Gravity perception is quite different from the perception of other environmental stimuli (e.g. light, temperature, pH). It is ubiquitous in the fungal kingdom and is manifested as gravi-morphogenesis and gravitropism. Gravitropism is widespread in fungi and has been studied in part in the 1800s and in the 1900s, although cellular and molecular mechanisms underlying gravioriented growth are still poorly known (Moore, 1991).

The system that allows the perception of gravity in living organisms is characterised by three components: a sensory mechanism to detect gravity; a reaction mechanism that responds to stimuli deriving from the sensory mechanism, as initiating changes in growth pattern; a communication mechanism that leads signals from the sensory mechanism to the reaction mechanism (Moore, 1991).

The response to gravity is fundamental in the basidiome development to ensure release of spores. Hymenium of basidiomycetes is the characteristic structure that permits the liberation of spores protected below the hat. The spores must fall vertically from the basidiome and be dispersed in the air, as reported in studies carried out on *Coprinus spp* (Moore, 1996). This mechanism depends on gravity perception and modulation of growth processes in relation to the direction of the vector gravity. Fungi are able to sense gravity and show, in some cases (e.g. aerial sporangia), strong gravitropism or gravity-based morphogenic patterns. Gravity perception in fungi has been also studied extensively in *Phycomyces blakeensianus* (Mucorales), where it is mediated by a combination of statoliths made of oxalate crystals and buoyant lipid structures (Göttig and Galland, 2014). Gravitropism in *Phycomyces* seems to be mediated by a differential flux of H^+ and Ca^{2+} in the mycelium (Živanović, 2005, 2012, 2013; Göttig and Galland, 2014). However, statoliths in this fungus apparently have originated from

a recent bacterial gene transfer (Nguyen et al., 2018). In the absence of crystalline structures in other lineages, it has been proposed that nuclei themselves might act as statolith-like structures in *Agaricomycotina* (Monzer, 1995, 1996; Moore et al., 1996; Kern et al., 1997). However, biophysical data suggest that the density of the nuclei in Ascomycota might not be sufficient for them to function as statoliths (Grolig et al., 2006). Buoyancy systems have been identified in *Ascomycota*, *Basidiomycota*, *Mucoromycotina*, *Mortierellomycotina* and *Glomeromycota* and the identified components seem to be well conserved across long evolutionary distances (Grolig et al., 2006). These responses are well described in both filamentous and zoosporic fungi, suggesting a considerable degree of evolutionary conservation, but unfortunately little is known about their molecular mechanisms.

Nowadays, a clear sensor of gravity in fungal hyphae candidate has not yet been found and does not appear to be a structural, mechanical, electrophysiological or chemical mechanism to communicate the response of this supposed sensor through the fungal structure, making it difficult to understand fungal gravisensing mechanism.

A thorough understanding of how fungi respond and adapt to the various stimuli encountered during spaceflight presents many economic benefits and is imperative for the health of crew.

In general, it is thought that microgravity alters biological processes by initially altering the physical forces acting on the cell and its environment. This results in decreased transfer of extracellular nutrients and metabolic by-products, causing the cell to be exposed to a completely different chemical environment

Study based on *Aspergillus niger* strain isolated from ISS, exposed to real microgravity, shows differential growth and conidiation patterns, starvation response, oxidative stress resistance, cell wall modulation, and nutrient acquisition compared to a terrestrial strain. The ISS isolate exhibits a higher growth rate than the terrestrial strain, an increase in protein involved in melanin production pathway. Moreover, the ISS isolate displayed enrichment of starvation-induced nutrient acquisition enzymes of carbon starvation, an adaptation to the low-nutrient environment that exists as a result of stringent microbial monitoring and remediation by NASA. During starvation, *A. niger* produces a lot of glycoside hydrolases that facilitate the release of nutrients from biopolymers and the recycling of cell wall components to generate energy and building blocks that can be used for maintenance and conidiogenesis (Jiròn-Lazos et al., 2018).

Chunmei et al. (2019) investigated the effect of simulated microgravity on the metabolism of the corrosive filamentous fungi *Aspergillus carbonarius*. Results show

an increase in organic acids production, especially those intermediates in the TCA cycle, such as citric acid and isocitric acid. Moreover, production of oxalic acid results increases when *A. carbonarius* grows under standard conditions. Studies performed on *A. niger* showed that oxalic acid exhibits chelating properties toward metal ions by producing metal oxalates. This property may also contribute to the formation of copper oxalate crystals, resulting in a higher copper tolerance, that enable acidogenic fungi to carry on extensive deterioration of clays, micas, and feldspars due to the production of oxalic, citric, and gluconic acids (De La Torre et al., 1993; Mai et al., 2016). The increased accumulation of these organic acids in this study provides strong evidence of the corrosion ability of moulds in space environments, as the organic acids produced by fungi occupy a central position in the process of corrosion of metal and rock.

These results, together with those of Huang et al. (2018), show important effects on microorganism metabolism induced by a decrease in gravity vector, including aminoacid metabolism and pathways associated with energy production.

In addition, mechanical unloading was found to induce cell wall modification altering intracellular vesicular transport necessary for the synthesis of the cell wall. It has also been reported that microgravity influences intracellular organelles: several hyphae, in fact, were empty or poor of organelles. All these disorders in hyphal morphology are probably related to changes in cytoskeleton-associated proteins, microfilaments and microtubules (Chunmei et al., 2019).

4.2.2. Effects of microgravity vector on Fungal Degradative activity

Most of the isolated fungi are potential biodegraders of polymers and thus present a potential hazard to structural materials and components of several systems on the Space Station. Some of these microorganisms are also called “technophiles", the term referred to microorganisms that can grow and degrade materials such as glass, metals or plastics, becoming a possible hazard when they develop in a confined environment, such as the Space Station, thus they must be controlled (van Tongeren et al., 2007). Technophiles can be organised into structures that make them less vulnerable to the extreme conditions of a Space Station. These structures are called biofilms and are characterised by groups of organisms that adhere to each other by synthesising extracellular substances (Zea et al., 2018).

Microorganisms able to form biofilm show new morphological characteristics, with specific mechanisms to adhere to surfaces and to respond to external signals. Biofilm formation is a highly organised and complex process that allows microorganisms to

resist in an extreme environment. A fundamental role in biofilm formation is performed by the extracellular matrix composed by polysaccharides, macromolecules and water, that protects the structure from the external environment (Pathak et al., 2017). Moreover, the hydrophobicity of cellular structures plays a key role allowing biofilm formation and its adhesion to a surface. Even if the term "biofilm" is not commonly used to describe the growth of filamentous fungi, similar structures have been observed in the species *Aspergillus fumigatus* and *Aspergillus niger* and for genus *Penicillium*. In fungal biofilms, the growth of mycelium is associated with the surface and has an aggregated morphology with stratified hyphae producing polymeric extracellular matrices that package hyphae together. In fungi growth as biofilm, genetic changes involving increased tolerance to antimicrobials and biocidal products, variations in the production and secretion of enzymes or metabolites and physiological changes are detected (Harding et al., 2009). These biofilms are ubiquitous and present both in natural environments and in industrial environments. Their formation increases the spread of fungal and bacterial contaminations both in structures where food is handled, as well as in drinking water filtering systems and also in sanitary devices. The presence of biofilm on surfaces leads to a decrease in efficiency and duration of equipment such as heat exchangers and water and air recycling systems (Zea et al., 2018).

Synthetic polymers are water resistant due to their hydrophobic properties and their apolar nature that prevent water absorption, showing limitations on biodegradation and biofilm formation (Pathak et al., 2017). These materials have an important structural function for spacecraft, and some of these polymers, used as electrical insulators, are fundamental in operating systems that control the flight of the vehicle (Gu et al., 2007). Anyhow, it was found that both fungi and bacteria are able to colonise a wide range of high-strength polymer materials. An example of this process is *Penicillium fretans* and *Bacillus mycoides* able to form biofilm and degrade polyethylene. *B. mycoides* is able to colonise the mycelium of *P. fretans* forming a biofilm on polyethylene surfaces. The degradation of the material was observed by assessing the percentage of lost weight, the production of CO_2 and the gas chromatography (Sangale et al., 2012).

In orbit, biological-induced corrosion is a very important risk factor, especially in long-term missions (Klintworth et al., 1999). Studies carried out on Mir station indicated that some structural equipment and materials are damaged due to the accumulation and proliferation of fungi and bacteria (Novikova et al., 2004; Novikova, 2005). A well documented example of this phenomenon was the progressive degradation of a quartz window of a Mir station module. This event was largely due to the growth of *Bacillus*

polymira, *Penicillium chrysogenum* and several species of *Aspergillus* (Zaloguyev et al., 1985; Pierson et al., 1994). Fungal species identified as responsible for deterioration of materials on Mir are the same isolated from ISS and belong to the genera *Penicillium*, *Aspergillus* and *Cladosporium* (Alekhova et al., 2005). In order to investigate the biodegradative activity of isolated mushrooms, the same have been inoculated on different types of materials and monitored over time (Alekhova et al., 2005).

Another example of degraded material caused by activity of biological agents are polyamides used as electrical insulators and fibro-reinforced composites. It is now known that, following the formation of fungal biofilm, deterioration and dielectric changes in the polymer occurs. Using impedance electrochemical spectroscopy (EIS) it was possible to observe fungal growth and progressive material degradation. Two phases were described: an initial decline in the coating resistance, due to the partial input of water and ionic species in the polymer matrix, and a second deterioration of the polymer by the activity of the fungus resulting in a large decrease of polymer resistance. The microorganisms involved in this process were: *Aspergillus versicolor, Cladosporium cladosporioides* and *Chaetomium*, commonly present in the atmosphere (Gu et al., 2007).

Based on information reported and considering the advent of long-duration space missions, it is necessary to consider the possible effect of prolonged microgravity conditions on ubiquitous fungi degradation activity. They can adapt their metabolism becoming able to use alternative sources of food, altering in rather substantial ways materials and instruments.

References

Acharya A, Brungs S, Lichterfeld Y, Hescheler J, Hemmersbach R, Boeuf H, Sachinidis A. Parabolic, Flight-Induced, Acute Hypergravity and Microgravity Effects on the Beating Rate of Human Cardiomyocytes. Cells. 2019 Apr 14;8(4):352. doi: 10.3390/cells8040352

Ahn CB, Lee JH, Han DG, Kang HW, Lee SH, Lee JI, Son KH, Lee JW. Simulated microgravity with floating environment promotes migration of non-small cell lung cancers. *Sci Rep.* 2019 Oct 10; 9(1):14553. doi: 10.1038/s41598-019-50736-6.

Albrecht-Buehler G. The simulation of microgravity conditions on the ground. *ASGSB Bull*. 1992 Oct; 5(2):3-10. PMID: 11537639.

Alekhova TA, Aleksandrova AA, Novozhilova TIu, Lysak LV, Zagustina NA and Bezborodov AM. Monitoring of microbial degraders in manned space stations. *Prikl Biokhim Mikrobiol*. 2005 Jul-Aug; 41(4):435-43. Russian. PMID: 16212041.

Amaral Zettler LA, Gómez F, Zettler E, Keenan BG, Amils R, Sogin ML. Microbiology: eukaryotic diversity in Spain's River of Fire. *Nature.* 2002 May 9; 417(6885):137. doi: 10.1038/417137a.

Arun RP, Sivanesan D, Patra B, Varadaraj S, Verma RS. Simulated microgravity increases polyploid giant cancer cells and nuclear localization of YAP. *Sci Rep*. 2019 Jul 23; 9(1):10684. doi: 10.1038/s41598-019-47116-5.

Bailey P, Chang DK, Nones K, Johns AL, et al. Genomic analyses identify molecular subtypes of pancreatic cancer. *Nature*. 2016 Mar 3; 531(7592):47-52. doi: 10.1038/nature16965.

Barnard RL, Osborne CA, Firestone MK. Responses of soil bacterial and fungal communities to extreme desiccation and rewetting. *ISME J.* 2013 Nov; 7(11):2229-41. doi: 10.1038/ismej.2013.104.

Becker JL AND Souza GR. Using space-based investigations to inform cancer research on Earth. *Nat Rev Cancer*. 2013 May;13(5):315-27. doi: 10.1038/nrc3507.

Bonnefoy J, Ghislin S, Beyrend J, Coste F, Calcagno G, Lartaud I, Gauquelin-Koch G, Poussier S, Frippiat JP. Gravitational Experimental Platform for Animal Models, a New Platform at ESA's Terrestrial Facilities to Study the Effects of Micro- and Hypergravity on Aquatic and Rodent Animal Models. *Int J Mol Sci.* 2021 Mar 15; 22(6):2961. doi: 10.3390/ijms22062961.

Borst AG and van Loon JJWA. Technology and Developments for the Random Positioning Machine, RPM. *Microgravity Sci. Technol.* 2009; 21, 287 https://doi.org/10.1007/s12217-008-9043-2.

Bradbury P, Wu H, Choi JU, Rowan AE, Zhang H, Poole K, Lauko J, Chou J. Modeling the Impact of Microgravity at the Cellular Level: Implications for Human Disease. *Front Cell Dev Biol*. 2020 Feb 21; 8:96 doi: 10.3389/fcell.2020.00096.

Brungs S, Egli M, Wuest SL *et al.* Facilities for Simulation of Microgravity in the ESA Ground-Based Facility Programme. *Microgravity Sci. Technol.* 2016; 28, 191–203 doi: 10.1007/s12217-015-9471-8

Chechiska Sielaff A, Urbaniak C, .Mohan GBM, Stepanov VG. *et al.* Characterization of the total and viable bacterial and fungal communities associated with the International Space Station surfaces Microbiome, 2019; 7:50

Checinska A, Probst AJ, Vaishampayan P, White JR, et al. Microbiomes of the dust particles collected from the International Space Station and Spacecraft Assembly Facilities. Microbiome. 2015 Oct 27; 3:50. doi: 10.1186/s40168-015-0116-3.

Chunmei J, Dan G, Zhenzhu L, Junling S, Dongyan S. Clinostat Rotation Affects Metabolite Transportation and Increases Organic Acid Production by Aspergillus carbonarius, as Revealed by Differential Metabolomic Analysis. *Applied and Enviromental Microbiology*. 2019; 85 (18): 1-16.

Collisson EA, Sadanandam A, Olson P, Gibb WJ, Truitt M, Gu S, Cooc J, Weinkle J, Kim GE, Jakkula L, Feiler HS, Ko AH, Olshen AB, Danenberg KL, Tempero MA, Spellman PT, Hanahan D, Gray JW. Subtypes of pancreatic ductal adenocarcinoma and their differing responses to therapy. *Nat Med*. 2011 Apr; 17(4):500-3. doi: 10.1038/nm.2344.

Cortesão M, Schütze T, Marx R, Moeller R and Meyer V. Fungal Biotechnology in Space: Why and How? In: Nevalainen, H. (eds) Grand Challenges in Fungal Biotechnology. Grand Challenges in Biology and Biotechnology. *Springer, Cham* 2020 doi: 10.1007/978-3-030-29541-7_18

Costa EC, Moreira AF, de Melo-Diogo D, Gaspar VM, Carvalho MP and Correia IJ. 3D tumor spheroids: an overview on the tools and techniques used for their analysis.

Biotechnol Adv. 2016 Dec; 34(8):1427-1441. doi: 10.1016/j.biotechadv.2016.11.002.

Dadachova E and Casadevall A. Ionizing radiation: how fungi cope, adapt, and exploit with the help of melanin. *Curr Opin Microbiol*. 2008 Dec; 11(6):525-31. doi: 10.1016/j.mib.2008.09.013.

De la Torre M, Gomez-Alarcon G, Palacios J. "In vitro" biofilm formation by *Penicillum frequentans* strains on sandstone, granite, and limestone. *Appl Microbiol Biotechnol* 1993; 40:408–415. doi:10.1007/BF00170402

Dickson KJ. Summary of biological spaceflight experiments with cells. *ASGSB Bulletin: Publication of the American Society for Gravitational and Space Biology*. 1991; *4*(2), 151-260.

Distler M, Aust D, Weitz J, Pilarsky C, Grützmann R. Precursor lesions for sporadic pancreatic cancer: PanIN, IPMN, and MCN. *Biomed Res Int.* 2014; 2014:474905. doi: 10.1155/2014/474905.

Frett T, Petrat G, WA van Loon JJ *et al.* Hypergravity Facilities in the ESA Ground-Based Facility Program – Current Research Activities and Future Tasks. *Microgravity Sci. Technol.* 2016; 28, 205–214.

Goswami N, White O, Blaber A, Evans J, van Loon JJWA, Clement G. Human physiology adaptation to altered gravity environments. *Acta Astronautica*. 2021; 89, 216–221 doi:10.1016/j.actaastro.2021.08.023.

Göttig M. and Galland P. Gravitropism in *Phycomyces*: violation of the so-called resultant law - evidence for two response components. *Plant Biology.* 2014; 16, 158–166.

Grimm D, Egli M, Krüger M, Riwaldt S, Corydon TJ, Kopp S, Wehland M, Wise P, Infanger M, Mann V, Sundaresan A. Tissue Engineering Under Microgravity Conditions-Use of Stem Cells and Specialized Cells. *Stem Cells Dev*. 2018 Jun 15; 27(12):787-804. doi: 10.1089/scd.2017.0242.

Grimm D, Wehland M, Corydon TJ, Richter P, Prasad B, Bauer J, Egli M, Kopp S, Lebert M, Krüger M. The effects of microgravity on differentiation and cell growth in stem cells and cancer stem cells, *Stem Cells Translational Medicine*. 2020 Aug; 9(8), 882–894. doi:10.1002/sctm.20-0084.

Grimm D, Wehland M, Pietsch J, Aleshcheva G, Wise P, van Loon J, Ulbrich C, Magnusson, NE, Infanger M and Bauer J. Growing tissues, in real and simulated microgravity: new methods for tissue engineering. *Tissue Eng. Part B Rev*. 2014; 20, 555–566.

Grolig F, Döring M and Galland P.Gravisusception by buoyancy: a mechanism ubiquitous among fungi? *Protoplasma.* 2006; 229, 117–123.

Gu JD. Microbial colonization of polymeric materials for space applications and mechanisms of biodeterioration: A review. *International Biodeterioration and Biodegradation*. 2007; 59: 170-179.

Gunde-Cimerman N, Ramos J, Plemenitas A. Halotolerant and halophilic fungi. *Mycol Res*. 2009 Nov;113(Pt 11):1231-41. doi: 10.1016/j.mycres.2009.09.002. Epub 2009 Sep 10. PMID: 19747974.

Hall TW. Artificial gravity in theory and practice 46th International Conference on Environmental Systems (2016) 46th International Conference on Environmental Systems, Vienna, Austria

Harding MW, Marques LR, Horward RJ and Olson ME. Can filamentous fungi form biofilms?, *Trends in Microbiology*. 2009; 17(11): 475-479.

Herranz, R., Boonstra, Anken, R.H., Braun, M., 2013, Ground-Based Facilities for Simulation of Microgravity: Organism-Specific Recommendations for Their Use, and Reccommended Terminology, Astrobiology, 13 (1): 1-17.

Horneck G, Facius R, Reichert M, Rettberg P, et al. HUMEX, a study on the survivability and adaptation of humans to long-duration exploratory missions, part I: lunar missions. Adv Space Res. 2003;31(11):2389-401. doi: 10.1016/s0273-1177(03)00568-4. PMID: 14696589.

Horneck G, Stöffler D, Ott S, Hornemann U, Cockell CS, Moeller R, Meyer C, de Vera JP, Fritz J, Schade S and Artemieva NA. Microbial rock inhabitants survive hypervelocity impacts on Mars-like host planets: first phase of lithopanspermia experimentally tested. *Astrobiology*. 2008 Feb; 8(1):17-44. doi: 10.1089/ast.2007.0134.

Horneck, G., Klaus, D.M., and Mancinelli R.L., 2010, Space Microbiology, Microbiology and Molecular Biology Review, 74 (1): 121-156.

Howe ASS, B., Hall TW and Landau DF Gateway gravity testbed (GGT). 49th International Conference on Environmental Systems (2019) Boston, Massachusetts, USA.

Hu C, Hao H, Ma B, Yuan Y, Liu F, Li L. A new respiratory training system for astronauts. In: Peng, Y., Weng, X. (eds) 7th Asian-Pacific Conference on Medical and Biological Engineering. *IFMBE Proceedings*. 2008; vol 19. Springer, Berlin, Heidelberg. Doi:10.1007/978-3-540-79039-6_46

Huang B, Li DG, Huang Y and Liu CT. Effects of spaceflight and simulated microgravity on microbial growth and secondary metabolism. *Mil Med Res* 2018;5, 18.

Ingram M, Techy GB, Saroufeem R, Yazan O, Narayan KS, Goodwin TJ, et al. Three-dimensional growth patterns of various human tumor cell lines in simulated microgravity of a NASA bioreactor. *In Vitro Cell Dev Biol Anim*. 1997; 33(6), 459-466. doi: 10.1007/s11626-997-0064-8.

Jirón-Lazos U, Corvo F., De la Rosa SC, García-Ochoa EM, Bastidas DM, Bastidas JM. Localized corrosion of aluminum alloy 6061 in the presence of Aspergillus niger, Int. *Biodeterior. Biodegrad*. 2018;133:17-25, doi:10.1016/j.ibiod.2018.05.007.

Jones S, Zhang X, Parsons DW, Lin JC, et al. Core signaling pathways in human pancreatic cancers revealed by global genomic analyses. Science. 2008 Sep 26;321(5897):1801-6. doi: 10.1126/science.1164368.

Kalb R, Solomon D. Space exploration, Mars, and the nervous system. Arch Neurol. 2007 Apr;64(4):485-90. doi:10.1001/archneur.64.4.485.

Kabakov A, Yakimova A, Matchuk O. Molecular Chaperones in Cancer Stem Cells: Determinants of Stemness and Potential Targets for Antitumor Therapy. Cells. 2020; 9(4):892. https://doi.org/10.3390/cells9040892

Kern VD, Mendgen K and Hock B. *Flammulina* as a model system for fungal graviresponses. *Planta*. 1997; 203, 23–32.

Kimlin LC, Casagrande G, Virador VM. In vitro three-dimensional (3D) models in cancer research: an update. *Mol Carcinog*. 2013; 52(3):167-82. doi: 10.1002/mc.21844.

Klintworth R, Reher HJ, Viktorov AN, Bohle D. Biological induced corrosion of materials II: new test methods and experiences from MIR station. *Acta Astronaut*.

1999;44(7-12):569-78. doi: 10.1016/s0094-5765(99)00069-7.

Konstantinidis IT, Warshaw AL, Allen JN, Blaszkowsky LS, Castillo CF, Deshpande V, Hong TS, Kwak EL, Lauwers GY, Ryan DP, Wargo JA, Lillemoe KD, Ferrone CR. Pancreatic ductal adenocarcinoma: is there a survival difference for R1 resections versus locally advanced unresectable tumors? What is a "true" R0 resection? *Ann Surg*. 2013 ;257(4):731-6. doi: 10.1097/SLA.0b013e318263da2f.

Lesnyak A, Sonnenfeld G, Avery L, Konstantinova I, Rykova M, Meshkov D, Orlova T. Effect of SLS-2 spaceflight on immunologic parameters of rats. *J Appl Physiol*. 1996; 81, 178-182.

Mai HTN, Lee KM and Choi SS. Enhanced oxalic acid production from corncob by a methanol-resistant strain of *Aspergillus niger* using semi solid-sate fermentation. *Process Biochem.* 2016; 51:9–15. doi:10.1016/j.procbio.2015.11.005.

Malka D, Hammel P, Maire F, Rufat P, Madeira I, Pessione F, Lévy P, Ruszniewski P. Risk of pancreatic adenocarcinoma in chronic pancreatitis. Gut. 2002;51(6):849-52. doi: 10.1136/gut.51.6.849.

Masini, M. A., Strollo, F., Ricci, F., Pastorino, M., & Uva, B. M. (2007). Microtubule disruptions and repair phenomena in cultured glial cells under microgravity. *Gravitational and Space Research*, *19*(2).

Matthaei H, Hong SM, Mayo SC, dal Molin M, et al. Presence of pancreatic intraepithelial neoplasia in the pancreatic transection margin does not influence outcome in patients with R0 resected pancreatic cancer. *Ann Surg Oncol*. 2011 ;18(12):3493-9. doi: 10.1245/s10434-011-1745-9.

Moffitt RA, Marayati R, Flate EL, Volmar KE, et al. Virtual microdissection identifies distinct tumor- and stroma-specific subtypes of pancreatic ductal adenocarcinoma. *Nat Genet*. 2015 ; 47(10):1168-78. doi: 10.1038/ng.3398.

Monici M, Marziliano N, Basile V, Romano G, Conti A, Pezzatini S and Morbidelli L. Hypergravity affects morphology and function in microvascular endothelial cells. *Microgravity-Science and Technology* 2006; *18*(3), 234-238.

Monzer J. Actin filaments are involved in cellular graviperception of the basidiomycete *Flammulina velutipes*. *European Journal of Cell Biology* 1995; 66, 151–156.

Monzer J. Cellular graviperception in the basidiomycete *Flammulina velutipes* – Can the nuclei serve as fungal statoliths? *European Journal of Cell Biology.* 1996; 71, 216–220.

Moore D. Graviresponses in fungi. *Adv in Space Res*, Grain Britain. 1996; 6/7: 73-82.

Moore D. Perception and response to gravity in higher fungi-a critical appraisal. *New Phytol*. 1991; 117: 3-23.

Mora M, Wink L, Kogler I, Mahnert A, et al., The International Space Station selects for microorganisms adapted to the extreme environment but does not induce genomic and physiological changes relevant for human health, *Bio Rxiv*. 2019: 533752

Morita H, Obata K, Abe C, Shiba D, Shirakawa M, Kudo T, Takahashi S. Feasibility of a Short-Arm Centrifuge for Mouse Hypergravity Experiments. *PlosOne* 2015. Doi:10, e0133981.

Moroni L, Tabury K, Stenuit H, Grimm D, Baatout S, Mironov V. What can biofabrication do for space and what can space do for biofabrication? Trends

Biotechnol. 2022 Apr;40(4):398-411. doi: 10.1016/j.tibtech.2021.08.008.

Mukhopadhyay S, Frias MA, Chatterjee A, Yellen P, Foster DA. The Enigma of Rapamycin Dosage. Mol Cancer Ther. 2016 Mar;15(3):347-53. doi: 10.1158/1535-7163.MCT-15-0720. Epub 2016 Feb 25. PMID: 26916116; PMCID: PMC4783198.

Nguyen T A, Greig J, Khan A, Goh C and Jedd G. Evolutionary novelty in gravity sensing through horizontal gene transfer and high-order protein assembly. *PLoS Biology.* 2018; 16, 1–16.

Nickerson CA, Ott CM, Wilson JW, Ramamurthy R, and Pierson DL. Microbial responses to microgravity and other low-shear environments. *Microbiology and Molecular Biology Reviews*. 2004; *68*(2), 345-361.

Notta F, Chan-Seng-Yue M, Lemire M, Li Y, et al. A renewed model of pancreatic cancer evolution based on genomic rearrangement patterns. Nature. 2016 Oct 20;538(7625):378-382. doi: 10.1038/nature19823

Novikova N, De Boever P, Poddubko S, Deshevaya E, Polikarpov N, Rakova N, Coninx I, Mergeay M. Survey of environmental biocontamination on board the International Space Station *Research in Microbiology* 2006, 157 (1), 5–12. doi:10.1016/j.resmic.2005.07.010.

Novikova ND. Review of the knowledge of microbial contamination of the Russian manned spacecraft. *Microbial Ecology*. 2004; 47 (2): 127-132.

Oczypok EA, Etheridge T, Freeman J, Stodieck L, Johnsen R, Baillie D, Szewczyk NJ. Remote automated multi-generational growth and observation of an animal in low Earth orbit. J R Soc Interface. 2012 Mar 7;9(68):596-9. doi: 10.1098/rsif.2011.0716.

Ogneva IV, Usik MA, Loktev SS, Zhdankina YS, Biryukov NS, Orlov OI, Sychev VN. Testes and duct deferens of mice during space flight: cytoskeleton structure, sperm-specific proteins and epigenetic events. Sci Rep. 2019 Jul 5;9(1):9730. doi: 10.1038/s41598-019-46324-3.

Onofri S, Barreca D, Selbmann L, Isola D, Rabbow E, Horneck G, de Vera JP, Hatton J, Zucconi L. Resistance of Antarctic black fungi and cryptoendolithic communities to simulated space and Martian conditions. *Stud Mycol*. 2008;61:99-109. doi: 10.3114/sim.2008.61.10.

Onofri S, Selbmann L, de Hoog GS, Grube M, Barreca D, Ruisi S, Zucconi L, Evolution and adaptation of fungi at boundaries of life. *Adv in Space Res.* 2007; 40(11):, Pages 1657–1664, doi:10.1016/j.asr.2007.06.004.;

Onofri S, Selbmann L, Pacelli C, Zucconi L, Rabbow E, de Vera JP. Survival, DNA, and Ultrastructural Integrity of a Cryptoendolithic Antarctic Fungus in Mars and Lunar Rock Analogs Exposed Outside the International Space Station. Astrobiology. 2019 Feb;19(2):170-182. doi: 10.1089/ast.2017.1728.

Pathak, V.M., Navneet Review on the current status of polymer degradation: a microbial approach. *Bioresour Bioprocess.* 2017;**4,** 15 doi:10.1186/s40643-017-0145-9

Pierson DL, McGinnis MR, Viktorov AN. Space Biology and Medicine, Vol. II: Life Support and Habitability in: F.M. Sulzman, A.M. Genin (Eds, American Institute of Aeronautics and Astronautics,Washington, DC, 2004; pp. 77–93.

Pierson DL. Microbial contamination of spacecraft. *Gravit Space Biol Bull.* 2001;14, 1-6.

Romsdahl J, Blachowicz A, Chiang AJ, Chiang YM, Masonjones S, Yaegashi J, Countryman S, Karouia F, Kalkum M, Stajich JE, Venkateswaran K, Wang CCC. International Space Station conditions alter genomics, proteomics, and metabolomics in Aspergillus nidulans. Appl Microbiol Biotechnol. 2019 Feb;103(3):1363-1377. doi: 10.1007/s00253-018-9525-0.

Romsdahl J, Blachowicz A, Chiang AJ, Singh N, Stajich JE, Kalkum M, Venkateswaran K, Wang CCC. Characterization of Aspergillus niger Isolated from the International Space Station, mSystems. 2018; 3(5): 1-13.

Sakorafas GH, et al. Molecular biology of pancreatic cancer: potential clinical implications. Bio Drugs 2001; 15, 439–452.

Saldanha JN, Pandey S, Powell-Coffman JA. The effects of short-term hypergravity on Caenorhabditis elegans. *Life Sci Space Res* (Amst). 2016 ;10:38-46. doi: 10.1016/j.lssr.2016.06.003.

Sampieri K, Fodde R. Cancer stem cells and metastasis. Semin Cancer Biol. 2012 ;22(3):187-93. doi: 10.1016/j.semcancer.2012.03.002. PMID: 22774232.

Sangale MK, Shahnawaz M, Ade AB (2012) A Review on Biodegradation of Polythene: The Microbial Approach. J Bioremed Biodeg 3:164. doi: 10.4172/2155-6199.1000164

Strollo F, Barger L, Fuller C. Testosterone urinary excretion rate increases during hypergravity in male monkeys. J Gravit Physiol 2000;7:181–82.

Strollo F, Masini MA, Pastorino M, Ricci F, Vadrucci S, Cogoli-Greuter M, Uva BM. Microgravity-induced alterations in cultured testicular cells. J Gravit Physiol. 2004 Jul;11(2):P187-8. PMID: 16237831.

Takemura M, Yoshida S. Stimulation of DNA polymerase alpha by hypergravity generated by centrifugal acceleration. Biochem Biophys Res Commun. 2001 Nov 30;289(2):345-9. doi: 10.1006/bbrc.2001.5986. PMID: 11716478.

Tash JS, Bracho GE. Microgravity alters protein phosphorylation changes during initiation of sea urchin sperm motility. FASEB J. 1999;13 Suppl:S43-54. doi: 10.1096/fasebj.13.9001.s43.

Tash JS, Kim S, Schuber M, Seibt D, Kinsey WH. Fertilization of sea urchin eggs and sperm motility are negatively impacted under low hypergravitational forces significant to space flight. Biol Reprod. 2001 Oct;65(4):1224-31. doi: 10.1095/biolreprod65.4.1224. PMID: 11566747.

Taylor GR, I. Konstantinova, G. Sonnenfeld, R. Jennings Changes in the immune system during and after spaceflight Adv. Space Biol. Med., 6 (1997), pp. 1-32

Tominari T, Ichimaru R, Taniguchi K, Yumoto A, Shirakawa M, Matsumoto C, Watanabe K, Hirata M, Itoh Y, Shiba D, Miyaura C, Inada M. Hypergravity and microgravity exhibited reversal effects on the bone and muscle mass in mice. Sci Rep. 2019 29; 9(1):6614. doi: 10.1038/s41598-019-42829-z.

Topal U, Zamur C. Microgravity, Stem Cells, and Cancer: A New Hope for Cancer Treatment. Stem Cells Int. 2021 Apr 29;2021:5566872. doi: 10.1155/2021/5566872.

Trappe S, Costill D, Gallagher P, Creer A, Peters JR, Evans H, Riley DA, Fitts RH. Exercise in space: human skeletal muscle after 6 months aboard the International Space Station. J Appl Physiol 2009;106(4):1159-68. doi: 10.1152/japplphysiol.91578.2008.

Tschopp A, Cogoli A. Hypergravity promotes cell proliferation. Experientia. 1983 Dec

15;39(12):1323-9. doi: 10.1007/BF01990088.

Ulbrich C, Pietsch J, Grosse J, Wehland M, Schulz H, Saar K, Hübner N, Hauslage J, Hemmersbach R, Braun M, van Loon J, Vagt N, Egli M, Richter P, Einspanier R, Sharbati S, Baltz T, Infanger M, Ma X, Grimm D. Differential gene regulation under altered gravity conditions in follicular thyroid cancer cells: relationship between the extracellular matrix and the cytoskeleton. Cell Physiol Biochem. 2011;28(2):185-98. doi: 10.1159/000331730.

Unsworth BR, Lelkes PI. Growing tissues in microgravity. Nat Med. 1998 Aug;4(8):901-7. doi: 10.1038/nm0898-901.

Uva BM, Masini MA, Sturla M, et al. Clinorotation-induced weightlessness influences the cytoskeleton of glial cells in culture. *Brain. Res.* 2002;934:132–39.

van Loon JJ. Hypergravity studies in the Netherlands. J Gravit Physiol. 2001 ;8(1):P139-42.

Van Loon, J. J. W. A., "A Large Radius Human Centrifuge: The Human Hypergravity Havitat", in Life in Space for Life on Earth, 2008, vol. 553.

van Loon, J.J. W. A. 2007: Some history and the use of random positioning Machine, RPM, in gravity related research, Advances in Space Research, 39: 1161-1165.

van Tongeren SP, Krooneman J, Raangs GC, Gjalt R, Welling W, Harmsen HJM. Microbial Detection and Monitoring in Advanced Life Support Systems like the International Space Station. *Microgravity Science and Technology* 2007; 20(2): 45-48.

Venkateswaran K, Vaishampayan P, Cisneros J, Pierson DL, Rogers SO, Perry J. International Space Station environmental microbiome - microbial inventories of ISS filter debris. *Appl Microbiol Biotechnol*. 2014 ;98(14):6453-66. doi: 10.1007/s00253-014-5650-6.

Vico L, Hargens A. Skeletal changes during and after spaceflight. *Nat Rev Rheumatol* **14,** 229–245 (2018). https://doi.org/10.1038/nrrheum.2018.37

Vidyasekar P, Shyamsunder P, Arun R, Santhakumar R, Kapadia NK, et al. (2015) Genome Wide Expression Profiling of Cancer Cell Lines Cultured in Microgravity Reveals Significant Dysregulation of Cell Cycle and MicroRNA Gene Networks. PLOS ONE 10(8): e0135958. https://doi.org/10.1371/journal.pone.0135958

Voorhies AA, Mark Ott C, Mehta S, Pierson DL, et al.. Study of the impact of long-duration space missions at the International Space Station on the astronaut microbiome. *Sci Rep*. 2019 Jul 9;9(1):9911. doi: 10.1038/s41598-019-46303-8.

Wade, C.: Responses across the Gravity Continuum: Hypergravity to Microgravity. Adv. Space Biol. Med. 2005; 10, 225–245.

Winnard A, Nasser M, Debuse D, Stokes M, Evetts S, Wilkinson M, Hides J, Caplan N. Systematic review of countermeasures to minimise physiological changes and risk of injury to the lumbopelvic area following long-term microgravity. *Musculoskelet Sci Pract.* 2017;27 Suppl 1:S5-S14. doi: 10.1016/j.msksp.2016.12.009.

Wu B, Xue Y, Wu P, Gu Z, Wang Y, Jing X. Physiological responses of astronaut candidates to simulated +Gx orbital emergency re-entry. *Aviat Space Environ Med*. 2012;83(8):758-63. doi: 10.3357/asem.3109.2012.

Wuest SL, Richard S, Kopp S, Grimm D, Egli M. Simulated microgravity: critical review on the use of Random Positioning Machines for mammalian cell culture. *BioMed Res Int.* 2015, 971474

Yachida S, Jones S, Bozic I, Antal T, et al. Distant metastasis occurs late during the genetic evolution of pancreatic cancer. *Nature*. 2010 28;467(7319):1114-7. doi: 10.1038/nature09515.

Zaloguyev SN, Viktorov AN, Bohle D. Results of Microbiological Studies Performed during the Use of Salyut-6 Space Station, Kosmicheskaya Biologiyai Aviakosmicheskaya Meditsina, 1985; 3: 64-66.

Zea L, Zeena N, Rubin P, Cortesao M, Luo J, McBride SA, Moeller R, Klaus D, Muller D, Varanasi KK, Muecklich F, Stodieck L. Design of spaceflight biofilm experiment. *Acta Astronautica*, 2018 148: 294-300.

Zhang C, Yang Z, Dong DL, Jang TS, Knowles JC, Kim HW, Jin GZ, Xuan Y. 3D culture technologies of cancer stem cells: promising ex vivo tumor models. J Tissue Eng. 2020; 24;11:2041731420933407. doi: 10.1177/2041731420933407.

Zheng Y, Gliddon CM, Aitken P, Stiles L, Machado ML, Philoxene B, Denise P, Smith PF, Besnard S. Effects of acute altered gravity during parabolic flight and/or vestibular loss on cell proliferation in the rat dentate gyrus. Neurosci Lett. 2017 Jul 27;654:120-124. doi: 10.1016/j.neulet.2017.06.033.

Živanović BD. Ca^{2+} and H^{+} ion fluxes near the surface of gravitropically stimulated *Phycomyces* sporangiophore. *Annals of the New York Academy of Sciences* 2005; 1048, 487-490.

Živanović BD. Intracellular reorganization and ionic signaling of the *Phycomyces* stage I sporangiophore in response to gravity and touch. *Communicative & Integrative Biology* 2013;6, 1-4.

Živanović BD. Surface tip-to-base Ca2+ and H+ ionic fluxes are involved in apical growth and graviperception of the *Phycomyces* stage I sporangiophore. *Planta* 236, 1817-1829.

Outline of the Thesis

Today Space is more accessible than ever. In the International Space Station (ISS) era, we move closer to the reality of Space inhabitation. Colonisation of Space and extended spaceflight missions require prolonged exposure to decreased gravity (microgravity, i.e., weightlessness), whereas lift-off and re-entry of the spacecraft are associated with exposure to increased gravity (hypergravity). Physiological changes may reflect recovery or landing (acute hypergravity) responses rather than in-flight (microgravity) effects.

There is growing scientific interest in how different gravitational states influence organism physiology and adaptive cellular response. Long-term space missions and the eventual goal of Space colonisation, lead space biology research to pay more attention to investigations of both acute and chronic responses of altered gravity.

A more comprehensive understanding of the effects of altered gravity on mammalian reproduction is needed, if Space is to be successfully colonised. In addition, an understanding of the effects of altered gravity on reproductive physiology is imperative for the development of countermeasures.

Hypergravity has been used for a long time as training for pilots and astronauts, and now is proposed as a Space Adaptation Syndrome countermeasure. It becomes increasingly important to understand the effects of increased gravity on mammalian reproductive physiology and function. The testes are basic organs of the male reproductive system with the dual function of spermatogenesis and steroidogenesis. Today it is well known that microgravity is associated with a set of changes in male reproductive physiology and function, significant body fluid shift causing facial edema, cardiovascular responses and disturbance in hormones and reproductive organs.

In the present studies, we studied the effects of gravity vector variation (hypergravity and microgravity conditions) on different organisms and cell lines models as shown below.

The effect of hypergravity was investigated on the morphological structure and endocrine regulation of testis in mice kept in a hypergravity environment for 14 days, using LDC to simulate 3g conditions. In parallel, the first stages of simulated microgravity response were evaluated on primary cell culture from rat testis, to evaluate the possibility of spermatogenesis failure in the space environment.

Interest in the long-term effects of altered gravity on cells and living organisms has intensified in recent years with an increase in interplanetary travels. Since the first studies carried out in space conditions it has been possible to observe alterations of

biological systems primarily due to the absence of weight force. In this research, the effects of long-term simulated microgravity were evaluated on two different biological systems, cancer cell line and fungal organisms.

Previous studies in cell biology have indeed shown evidence that cellular function and morphology can be altered by microgravity, compared to normal gravity, of both normal cells and cancer cells (Jhala et al., 2014; Aleshcheva et al., 2016). These results provide some inspiration for cancer research. Exploiting the 3D-clinostat, Random Positioning Machine (RPM) tool, we decided to perform a comprehensive analysis of the long-term effects of simulated microgravity (simulated microgravity) on pancreatic ductal adenocarcinoma (PDAC) cells. Pancreatic cancer remains the tumour with the worst overall survival worldwide with little progress in terms of novel treatments. Despite its incisiveness, PDAC has not been examined so far in microgravity conditions. The aim of this study was the development and characterization of an in vitro 3D-pancreatic cancer model, performing a comprehensive morphologic, transcriptomic, proteomic and lipidomic analysis in PDAC cells at different time points of simulated microgravity exposure (1, 7 and 9 days).

Since the presence of humans in Space entails the presence of microorganisms it becomes really important to know the effects of long-term microgravity on these ubiquitous hosts to preserve crewed spacecraft safety and to prevent biodegradation of spacecraft materials. The purpose of these sets of tests is to start to evaluate the effect of microgravity on fungal growth rate and morphology at different time-points (4 and 10 days) in normal and in simulated microgravity conditions, reproduced using RPM. To preserve completeness of technological characteristics of spacecraft materials in long-term missions, we investigated after two months if the fungal degradative activities are influenced by simulated microgravity.

Technopolymer materials were provided by the ETANS lab (Engineering Technological Area for Nanotechnologies for Space; Thales Alenia Space, Torino). The information gained can be applicable to the safety and preservation of spacecraft crews, and last but not least can provide new and sustainable solutions for the plastic pollution challenges.

Chapter 1

The Importance of Gravity Vector on Adult Mammalian Organisms: Effects of Hyper-Gravity on Mouse Testis

The Importance of Gravity Vector on Adult Mammalian Organisms: Effects of Hyper-Gravity on Mouse Testis

Article submitted to *Microgravity Science and Technology,* 21/02/2022

INTRODUCTION

Space exploration represents the upcoming frontier of human being, in particular regarding the incoming project on Mars, that means long stay in the space environment with prolonged gravity alterations (Misha and Luderer, 2019). In this scenario, the influence of exposure to a gravity environment other than Earth's for a prolonged time is becoming an important topic to consider for its influence on the human physiology. The force of gravity is an essential physical component of the Earth's environment, and it is known that gravity exerts a strong influence on the cellular level. Experimental investigations have been found cell cytoskeleton to be mainly affected (Uva et al., 2002), and changes in intracellular molecular pathways were also observed (Bonfiglio et al., 2019). In the last years the cellular and physiological effects of microgravity have gained more attention, following the concerns about a progressive increasing time spent by astronauts at low gravity (Heer and Paloski, 2006; Sharma et al., 2008; Misha and Luderer, 2019**;** Afshinnekoo et al., 2020). But rather a few have been the studies about hypergravity (Genchi et al., 2015; Frett et al., 2016). Hypergravity, which ranges between 2-4 *g*, is experimented for a very short time compared to microgravity environment during the whole space mission. Probably, because of this last reason a trend to minimise the reported consequences was observed during the last years, as can be assessed by the scarce scientific papers available. Nevertheless, astronauts have several experiences of hypergravity during their mission such as during the exit from terrestrial orbit or during a return to earth ground, where the potential use of space-shuttle, can enforces a prolonged fly at high gravity (Wade, 2005). The hypergravity condition mainly affects hormonal balance and homeostasis regulation together with body liquid compartment disturbances and, even though the details of the hormonal dysregulation are not known, spaceflight clearly induces multiple changes in the interrelationship among hormones and alterations in the sensitivity of responding systems (Clement et al., 2019). Casey et al. (2012) reported a complex change in circadian rhythm which caused a decreased rate of mammary metabolic activity and increased pup mortality in rats, following exposure to hypergravity. Hypergravity consequences have been proved also on calcitonin released by thyroid parafollicular

cells together with significant reduction in the thickness of cortical bone (Albi et al., 2012).

Testis, the male organ of the reproductive system, is an organ gland, but, for its correct functionality, it is also dependent on a correct relationship with several endocrine factors. Following this particularly dependence on endocrine and reactive environment of the body, testis is considered a good candidate to study in general the occurrence of homeostasis alteration. Indeed, spaceflight has been shown to significantly affect the physiology of the testis (Sapp et al., 1990; McLachlan et al., 2002). One of the main hitches in studying the biological responses to hypergravity has been in the past the lack of experimental devices to reproduce gravity changes and the impossibility to recruit animal models for long time periods, as well. Now, in contrast to microgravity studies on animals, which can be adopted only in accordance with international space mission on International Space Station (ISS), the hypergravity experiments can now be quite easily performed on live animals in the Large Diameter Centrifuge machine. Centrifugation is, in fact, a good ground-based model to simulate altered gravity which occurs during space missions (Morita et al., 2015).
In the present work we have investigated the effect of hyper-gravity on morphological structure and endocrine regulation of testis in mice, hold in a hypergravity environment for several days.

MATERIALS AND METHODS

Animal care

In all phases of the hypergravity experiment animals were handled according to internationally accepted principles for care of laboratory animals (E.E.C. Council Directive 86/609, OJL358,1, Dec. 12, 1987). Formal approval to conduct the described experiments was obtained from by the Public Veterinary Health Department of the Italian Ministry of Health (prot. n. 4347-09/03/2009-DGSA.P.) and the University of Genoa (Genoa, Italy), where the naïve group mice were stabularized. The authors of this article were not directly involved in executing the animal maintenance part of the experiments. Instead, they were allowed to the mice at the end of the hypergravity experiment and participating in the specific tissue collection and analysis.

Experimental design

Experiment in hypergravity was performed at the Large Diameter Centrifuge, located at European Space Research and Technology Centre (ESTED, Noordwijk, NL). This

instrument is composed by several peripheral cages coupled by an arm to a central rotor. A gage located up to the body of central rotor is used as control. The rotor activity induces to the peripheral cages a rotatory movement responsible to develop a centrifuge force mimicking the increased gravity. Each cage is equipped by camera and control device for observing animal behaviour, holding standard environmental condition and monitoring vital parameters (van Loon et al., 2008). In this experiment 6 mice (C57BL/10J, 8 weeks-old), individually housed in the peripheral cages, were used, underput to a 3*g* of hypergravity for 14 days. Six mice holding the same time in the central cages up to the rotor, to which hypergravity was not imposed, was used as control (sham)-group of hypergravity experiment. A naïve control group was made in institutional stabularium of University of Genoa, where five mice (C57BL/10J,8 weeks-old) were housed in standard stabularium cages for 14 days. At the end of the experimental period, mice were euthanised by anaesthesia under 0.5-2% isoflurane gas (O_2: 95.0%), sacrificed by decollation. Testes, including epididymis, were removed bilaterally. The right samples were quickly frozen in liquid nitrogen and stored in dry ice. The left testes were divided in two halves: one was fixed in 4% paraformaldehyde and stored in phosphate-buffered saline (PBS 1X), the other was quickly frozen in liquid nitrogen and stored in dry ice. Specimens were then shipped to dep. of Science and Technological Innovation (DISIT) of University of Eastern Piedmont (UPO), where the investigative protocols were performed, and data analysed. The fixed samples were processed for embedding in paraffin wax. Consecutive serial sections were cut (5 μm thick) and mounted on silanized-slides. Then slides were dewaxed, rehydrated through descending series of ethanol and alternate slides were submitted to investigative protocols as detailed below. The frozen samples were used for PCR protocol. Histological microarchitecture of the organ was investigated by Masson's trichromic staining.

Immunohistochemistry and Immunofluorescence

Three slides for each sample were decorated with each primary antibodies detailed below. Immunohistochemical protocol was applied to investigate the distribution of 3β-steroid dehydrogenase (3β-HSD) and 17β-steroid dehydrogenase (17β-HSD). Briefly the dewaxed and hydrated slides were incubated overnight at 4°C with primary antibody against 3β-HSD (raised in mouse; Santa Cruz Biotechnology Inc.; dilution of 1:50); and 17β-HSD (raised in mouse; Santa Cruz Biotechnology Inc.; dilution of 1:50); after washing in PBS respectively anti-mouse secondary antibody, mouse IgGκ BP-HRP (Santa Cruz Biotechnology Inc.; dilution of 1:25) was added to reveal specific site

by 3,3-diaminobenzidine (DAB) colorimetric reaction. Immunofluorescence protocol was applied to investigate the distribution of adhesion protein.

Briefly slides were incubated overnight at 4°C with primary antibody against Claudin-1 (monoclonal antibody raised in mouse, Alexa Fluor 488, Invitrogen; dilution of 1:100), Claudin-4 (monoclonal antibody raised in mouse, Alexa Fluor 594, Invitrogen; dilution of 1:100), Occludin (monoclonal antibody raised in mouse, Alexa Fluor 594, Invitrogen; dilution of 1:100), Connexin- 43 (polyclonal antibody raised in rabbit, Invitrogen; dilution of 1:200) and the Sex Hormone Binding Globulin (SHBG; polyclonal antibody raised in rabbit, Santa Cruz Biotechnology Inc.; dilution of 1:50). After washing in PBS 1X, a second layer of fluoresceine-isothiocyanate conjugated gamma-globulins, goat anti-mouse (dilution of 1:100; Sigma-Aldrich) or goat anti-rabbit (dilution of 1:100; Sigma-Aldrich) following the source of the primary antisera was applied for 30 min in moist chamber at room temperature. Sections were rinsed in PBS 1X, mounted with glycerol-PBS 1X (1:9) and examined under a Leica epifluorescence microscope. The specificity of the immunostaining (both colorimetric and fluorescent) was verified by omitting primary antibody or by replacing the primary antiserum with nonimmune, in both cases no immunostaining was detected.

RT-qPCR

RNA from frozen samples was isolated by the acid phenol-chloroform procedure using the Trizol reagent (Sigma). Quality of isolated RNA was checked by electrophoresis on 1.5% agarose gel. Concentrations and purities of the isolated RNA were assessed by absorption spectroscopy. Aliquots of 1.5 mg RNA were reverse-transcribed into cDNA using 200 units RevertAid H Minus M-MuLV Reverse Transcriptase (Fermentas, MMedical, Milan, Italy), in presence of 200 pmol of poly-T18mer (TIB Mol Biol, Italia), 1 mM dNTPs (Fermentas) at 42°C for 60 min in a reaction volume of 20 ml. The cDNA was used to amplify the genes of interest using a Chromo 4TM System real-time PCR apparatus (Biorad Italy, Milan). Proper aliquots of the RT mixture were diluted to a final volume of 20 ml in presence of iTaq SYBR Green Supermix with Rox (Biorad) and 0.25 mM of each specific primer pairs (TibMolBiol, Genoa, Italy). The primer pairs used are shown in Table 1. Thermal protocol consisted of 3-min initial denaturation at 95°C followed by 40 cycles: 5 s at 95°C and 20 s at 60°C. A melting curve of PCR products (55–94°C) was also performed to rule out the presence of artefacts. Relative quantification of each gene expression was calculated according to comparative Ct method using the Biorad software tool Genex-Gene Expression

MacroTM. Expression of the genes of interest was normalised using the expression levels of GAPDH as housekeeping gene and the normalised expression was then expressed as relative quantity of mRNA (relative expression) with respect to laboratory and ground control samples.

Table 1. Primer sequences used in RT-qPCR analysis

AR	*Forward*	5' — GCAGCTTGTGCATGTGGTCA
	Reverse	5' — AATACCATCAGTCCCATCCAGGAA
LHR	*Forward*	5' — CAGGAATTTGCCGAAGAAAGAACAGAATT
	Reverse	5' — CAGAAGTCATAATCGTAATCCCAGCCA
FSHR	*Forward*	5' — CCTCTGCCAAGATAGCAAGGTA
	Reverse	5' — CTCCAGGTCCCCAAATCCAGA
IL-1β	*Forward*	5' — CAGGCAGGCAGTATCACTCA
	Reverse	5' — GGTGCTCATGTCCTCATCCT

TUNEL

Apoptosis was detected using an in situ TdT technique (In situ Cell Death Detenction Kit, fluorescien; Roche, Applied-Science). Three sections for each sample were incubated with permeabilization solution (0,1% Triton X-100, 0,1% sodium citrate) freshly prepared for 10 minutes at room temperature, washed with PBS 1X (pH 7.2–7.4) and incubated at 37°C for one hour with the TUNEL reaction mixture. At the end of incubation slides were washed twice in PBS 1x, mounted with PBS 1x and analyzed under fluorescence microscope (excitation wavelength 488 nm and detection 515-565 nm).

RESULTS

One out of six mice exposed to hyper-gravity deceased. The other five mice exposed to hyper- gravity environment resulted alive at the end of experiments; they presented weight loss (about 15%), probably due to higher energy expenditure during hyper-gravity period. Any evident suffering status was observed. No weight loss or suffering status was observed in mice used as control. The morphological, immunohistochemical and molecular analysis performed on control and naïve group rats showed similar evidence and results. No more concerns were detailed about comparison between control and naïve group rats.

Histomorphology.

The physiological microanatomy of testis showed oval elongated tubules in the bottom part of each testicular lodge. Here the widely convoluted seminiferous tubules show a

limited interstitial tissue in which can be observed the presence of endocrine Lyedig cells groups (Fig. 1A,C). In the upper part of the testicular lodge, the reduced convoluted form of seminiferous tubules displays a more roundish profile with large part of interstitial tissue, where can be observed Lyedig cell group (Fig. 1E,G). In both part of seminiferous tubules, the stratified epithelium showed well evident the composing two main cell types: spermatogenic cells and Sertoli cells (Fig. 1C,G). The spermatogenic cells appeared intact, regularly roundish and stacked along the epithelium thickness. The germinal layer was represented by cell line located immediately above the basal lamina appeared formed by small roundish cells showing a hypochromatic nucleus (spermatogonia cells) (Fig. 1C,G). The maturating spermatocytes appeared as large round cells with large nuclei and rounded outlines. The last layer of the epithelium was represented by small cells close to the lumen (spermatid cells) where tails of maturating spermatozoa were well visible. The Sertoli cells were visible between the spermatogenic cells, showing a large, round and well chromatic nucleus located

mainly above the germinal line of the epithelium (Fig. 1C,G). Following exposure of mice to hypergravity (3*g*-mice), testicular morphology showed some changes. The seminiferous tubules in the bottom part of testicular lodge appear more convoluted and the interstitial tissue is extremely reduced, similarly the endocrine Lyedig cells groups appeared reduced (Fig. 1B,D). In the upper part tubules appear roundish and smaller, here more interstitial tissue can be observed, where smaller Lyedig cells groups can be noted (Fig. 1F,H). The epithelium of 3*g*-mice showed a reduction in the thickness of seminiferous tubules, spermatocytes showed separation between them and layering disorganization showing small cells adjacent to large cells. A reduced number of tails of maturating spermatozoa were visible (Fig. 1D,H).

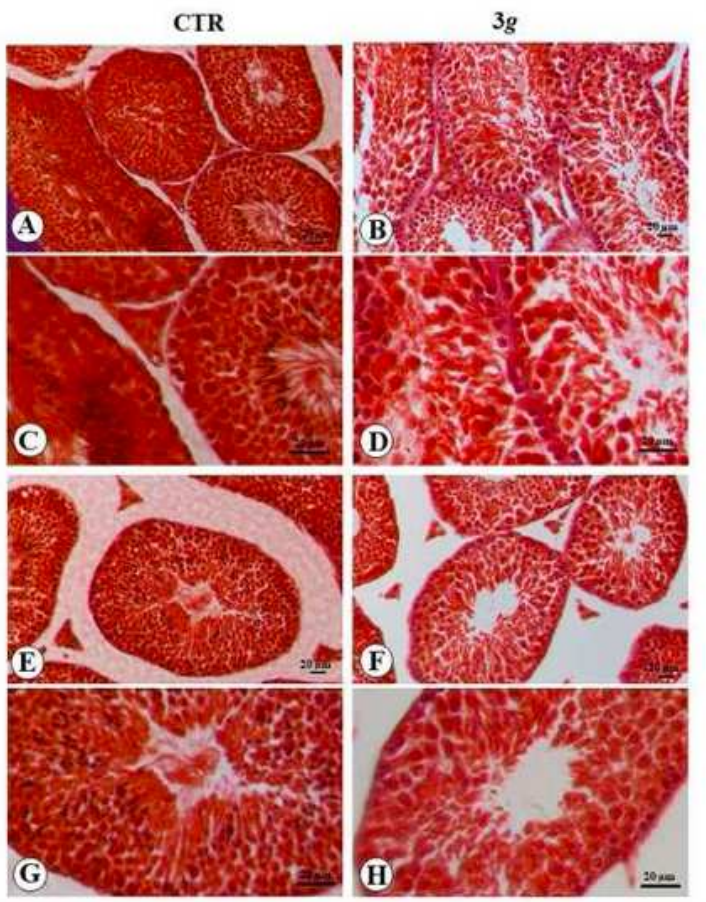

Fig. 1. Microphotograph panel illustrating the microanatomy of testis seminiferous tubules in normogravity (A,C,E,G) and following 3g exposure (B,D,F,H). The tubules presented are detailed in the bottom part (A-D) and the upper part (E-H) of testis seminiferous tubules. Note the irregular disposition of spermatogonia cells and Sertoli cells, and the reduction of tubules thickness following 3g exposure. CTR: normogravity; 3g: hypergravity. Scale bar: 20µm

Immunohistochemistry and Immunofluorescence

Claudin-1, -4, and occludin are structural protein belonging to cell-cell tight junction. In seminiferous tubules these proteins are located in Sertoli cells, where they contribute to maintain the haemato-testis barrier and associative coherence of these cells disposed along all tubular thickness. The claudin-1 immuno-fluorescence in control mice was observed at basis and along all

tubular thickness (Fig. 2A), indicating its localization along the cellular body of Sertoli cells, instead in 3*g*-mice, the claudin-1 signals have been observed only at basis of the tubules (Fig. 2B). The claudin-4 immuno-fluorescence in control mice was observed located at basis and apex of seminiferous tubules (Fig. 2C), while in the 3*g*-mice the fluorescence was observed disposed along all tubules thickness (Fig. 2D). Occludin

immune-fluorescence in normal mice was observed located in the basal layer of seminiferous tubules (Fig. 2E), while in 3*g*-mice immune-fluorescence was evident in intermediate zone of tubules (Fig. 2F). Connexin is a protein that mediate the specific cell-cell contact characterising the gap junction. In seminiferous tubules connexin realises the molecular connection that support the functional syncytium of Sertoli cells. In normal mice connexin is detected along the thickness of tubules, because widely it diffuses along the cell body of Sertoli cells (Fig. 2G). In 3*g*-mice the expression of connexin is reduced to basal part of tubules, indicating a probably functional disconnection of apical part of Sertoli cells (Fig. 2H). Negative immune-fluorescence control slides resulted completely blank (Fig. 2I,L).

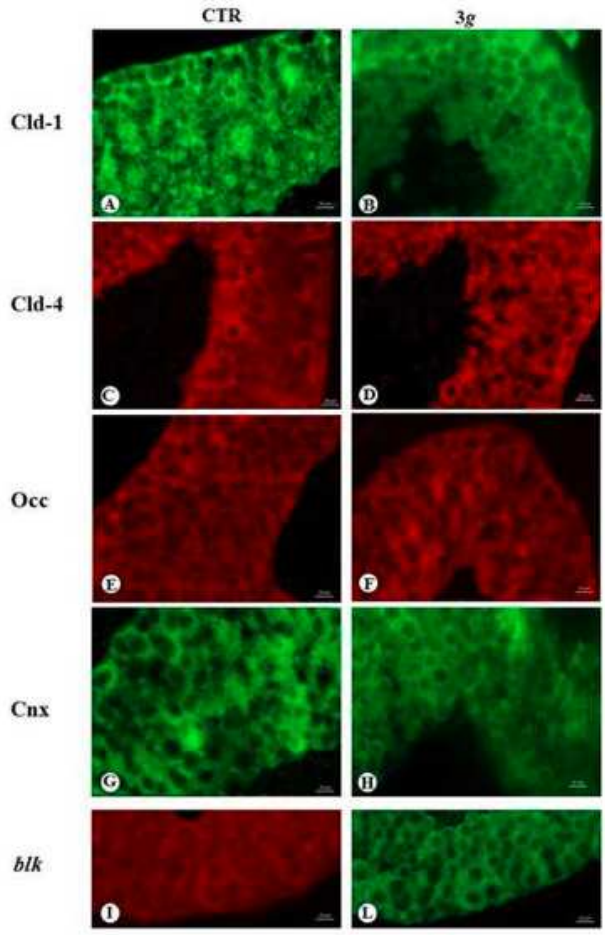

Fig. 2. Microphotograph panel illustrating the immunofluorescence signals of cell-cell junctional complex proteins occurring in the testis seminiferous tubules. A,B: Claudin-1 (Cld-1); C,D: Claudin-4 (Cld-4); E,F: Occludin (Occ); G,H: Connexin (Cnx). I,L; control immunofluorescence images, Blank (blk). Note that the analysed proteins are localised along the Sertoli cells profile. The localization pattern of analysed proteins changes following 3G exposure. Scale bar: 20µm
CTR: normogravity; 3g: hypergravity.

The detection of apoptotic cells in seminiferous tubules of control mice by TUNEL technique showed no evidence (Fig. 3A), instead in 3*g*-mice several TUNEL signal was detected along the basal portion of the tubules, where the large dimension of TUNEL-positive nuclei indicates the occurrence of apoptosis in the Sertoli cells rather than in spermatogonia cells (Fig. 3B).

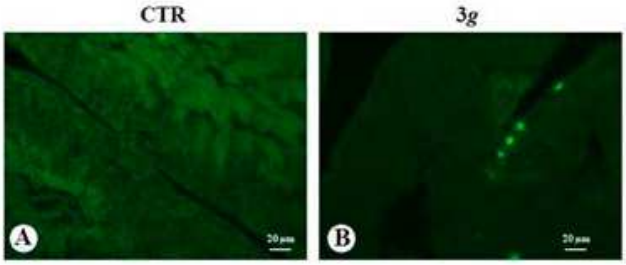

Fig. 3. Microphotograph panel illustrating the immunofluorescence TUNEL signals occurring in the testis seminiferous tubules. Bote that positive signals are selectively localised on basal round and well evident nuclei, compatible with the localization of Sertoli cells nuclei. CTR: normogravity; 3g: hypergravity. Scale bar: 20 μm

Specific immunohistochemistry for 3β-HSD and 17β-HSD showed in either case exclusive localization in Lyedig cells and in control group mice (Fig. 4 A,B). In 3*g*-mice the 3β-HSD immunohistochemistry appeared widely reduced, whereas the 17β-HSD immunohistochemistry was completely lacking (Fig. 4C,D). Negative immunohistochemistry control slides resulted completely blank (Fig. 4E,F).

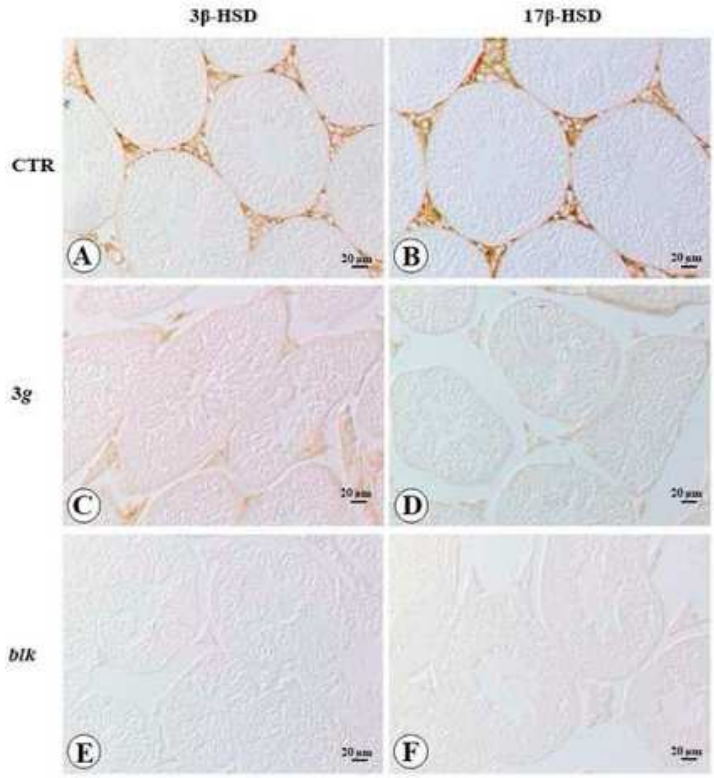

Fig. 4 Microphotograph panel illustrating the immunohistochemistry localization and expression of 3β-HSD (A,B) and 17β-HSD (C,D), in testis of mice exposed to normogravity (A,C) or Hypergravity (B,D). E,F: control immunohistochemistry images, Blank (blk). Note the specific localization of the factor in the endocrine Lyedig cells of the organ and the abrupt of reaction in mice exposed to hypergravity. CTR: normogravity; 3g: hypergravity. Scale bar: 20 μm

SHBG is a testosterone binding protein which function is to reduce the availability of free circulating and active testosterone; it is present in the basal portion of Sertoli cells. The immunofluorescence for SHBG was faintly visible along the basal profile of Sertoli cells in normal mice (Fig. 5A), whereas an evident increase of immunofluorescence was observed along the basal profile of Sertoli cells in 3*g*-mice (Fig. 5B). SHBG immunofluorescence can be observed fully expressed also in endocrine Leydig cells; in this case, no difference between control and 3*g*-mice was detected (Fig. 5A,B). Negative immunohistochemistry control slides resulted completely blank (Fig. 5C,D).

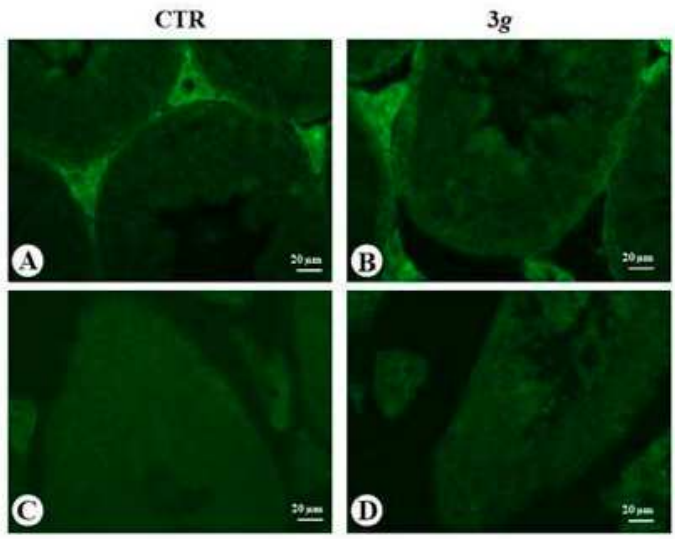

Fig. 5. Microphotograph panel illustrating the immunofluorescence localization and expression of testosterone binding protein (SHBG) in mice testis following normogravity (A) or hypergravity (B). C,D: control immunofluorescence images, Blank. Note the extended localization of immune SHBG on basal profile of Sertoli cells following hypergravity. CTR: normogravity; 3G: hypergravity. Scale bar: 20 µm

RT-Q-PCR

The effects of exposure to hypergravity on the expression of IL1β, FSHR, Androgen Receptor and, LHR were evaluated analysing mRNA expression of these factors. The exposure to hypergravity induces in mice testes no significative changes for IL1β and FSHR (Fig. 6A,B), whereas a reduction of mRNA transcript levels was detected for AR and LHR (Fig. 6C,D).

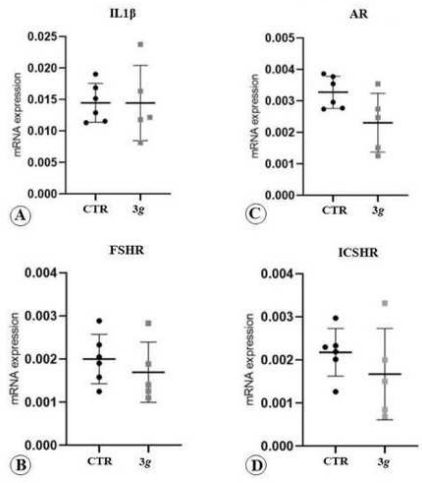

Fig. 6. Dot blot graph illustrating the mRNA expression in testis seminiferous tubules of several receptors involving in the physiological response of the testis. A: IL1β; B: FSHR; C: AR; D: ICSHR.

DISCUSSION

Into the seminiferous tubules, spermatogenic cells are designed to evolve in mature spermatozoa. Many cycles for spermatozoa differentiation occur sequentially along the convoluted seminiferous tubules of the testis, resulting in pulses of sperm release that ensure the continuous production. Sertoli cells (SC) are constitutive non spermatogonia cells that have supportive and trophic functions for the spermatogonia cells of the seminiferous epithelium. SC facilitate transport of mature spermatids towards the lumen of the tubules, provide secretion of androgen binding protein and molecules with endocrine or paracrine action for spermatogenesis. They are responsible to assure the function of the blood-testis barrier. Further, they interact with intertubular endocrine Leydig cells secreting testosterone. Overall, these tasks make SC elements of primary importance for the testicular function. In our study first evidence of hypergravity disturbance into testis environment has been obtained observing the morphology of germinative epithelium. We have observed that hypergravity affects the thickness and the general organization of germinative epithelium of seminiferous tubules, consisting in SC with small nuclei, presence of immature spermatogonia cells with large nuclear profile in the upper layer of germinative epithelium, where in control mice only cells with small hyperchromatic nuclei and differentiative cellular profile can be observed. Consequently, the maturation and production of spermatozoa can be supposed defective, in fact rarely spermatozoa were observable in the lumen of seminiferous tubules in rats exposed to hypergravity. The good physiological performance of SC embedded in the spermatogenic layer is widely dependent on cell-cell tight junctions which are made of proteins called occludins and claudin, which interact forming a branching network between the two opposite cells resulting in a tighter seal and mechanical stability. These proteins are linked to elements of cellular cytoskeleton, being able to transduce mechanical cues in intracellular signals. Proteins of tight junctions are involved in keeping polarity, in establishing organ-specific apical domains and participate into SC assisting function during proliferation, differentiation, and migration of spermatogenic cells and realise the blood-testis barrier to control metabolic access to seminiferous tubules environment (Heiskala et al., 2001; Mruk and Cheng, 2010). Hypergravity was found to alter the expression pattern of claudins and occludin. We hypothesise that a rearrangement of tight junction among SC has occurred, resulting in an efficiency loss of SC cells in supporting the steps of germ cells differentiation. Further, this alteration in the mechanical arrangement can be cause of

the visible disassembly of the spermatogenic cells disposition with larger spaces between cells and smaller cells closer to larger ones.

Besides the tight junction complex, which allow stable linkage between adjacent cells, SC layer exhibit several gap junctions, specialised membrane areas which allow cells to communicate each other exchanging small solutes and ions. The gap junction is made up of two hemichannels, one for each cell, formed by assemblies of six channel proteins called Connexins. This type of junction offers a pivotal advantage in cell-cell communication because it makes the SC layer working as a functional syncytium, able to make all the together SC cells responsive, optimising in such a way the physiological behaviour of each tubule. Following hypergravity treatment the connexin expression was markedly reduced suggesting a probable decrease in cell-cell communication, reflecting a severe trouble in coordinating cellular response aimed to spermatozoa production. Thus, the occurrence of this kind of alterations has an important negative effect on germ cells differentiation culminating in a limited reproduction rate of spermatozoa. Although we do not have any direct evidence, we can suppose that that other epithelial layers or tissues may be subjected to intimate alterations of cell-cell junctions shattering the physiological performances under hypergravity conditions. Blood-brain barrier (BBE) destabilisation has been proved in mice following centrifugation treatment at 2*g* showing altered permeability characteristics which represent the main topic of the endothelial lining of the BBE to control exchanges between blood and brain parenchyma (Dubayle et al., 2020). Similarly, we expect that in the seminiferous tubules the alteration of cell-cell contact among Sertoli cells could induce an alteration in the blood-testis barrier, compromising the regular surveillance of metabolic traffic between blood and germinative epithelium.

Another important compartment in the testis anatomo-physiology is represented by Leydig cells inside the interstitial stroma representing the glandular compartment producing the bulk quantity of testosterone.

Testosterone biosynthesis is powered by different enzymes being the 3β-hydroxysteroid dehydrogenase (3β-HSD) and the 17β-hydroxysteroid dehydrogenase (17β-HSD) the main ones involved (O'Shaughnessy et al. 2000). Our data have shown that hypergravity exposition reduce widely the expression of these two enzymes, suggesting a loss of function of the glandular compartment of the testis. Testosterone is a powerful hormone involved not only in spermatogenesis physiology, but in upper brain cognitive functions (Celec et al., 2015), bone metabolism (Sinnesael et al., 2011), cardiovascular parameters (Oskui et al., 2013), glucose homeostasis (Grossmann and

Wu, 2014). Therefore, a lack in this hormone synthesis can affects multiple physiological pathways. In similar case the adrenal gland can compensate for testis function by producing another font of testosterone.

At the present we don't have any evidence concerning a direct effect of hypergravity on other endocrine glands, however, the scientific literature reports following hypergravity exposure, the alteration of the adrenal gland zona reticularis representing the secondary font of production of testosterone (Moroz et al., 2018). Following these evidence hypergravity seems to decrease widely the testosterone production, and the hypothesis of a wider involvement of hormonal balance may be advanced. Indeed, recent data show that hypergravity conditions might remodel thyrocytes cell membrane by increasing thyrotropin-receptor (TSHR) surface protein (Albi et al., 2014), but further data concerning the hypergravity effects on hormone receptor expression is still lacking. In this view, we have analysed the receptor pattern expression for key hormones regulating the physiological function of the testis. We focused on androgen receptor (AR), interstitial cell stimulating hormone receptor (ISCHR), follicle-stimulating hormone receptor (FSHR) and we also detected the expression level of interleukin-1β. AR is a nuclear receptor which reflects the cellular response to testosterone and, in general to androgen hormones, in supporting the normal testis physiology and maintaining the male sexual phenotype. ICSHR is mainly expressed in Leydig cell where it drives testosterone production under hypothalamic-hypophysis axis control. FSHR regulates spermatogenesis and its main function is, upon binding of FSH, to increase the number of Sertoli cells by stimulation of their mitotic activity. It is also essential for tight junctions' formation (Sluka et al., 2006). IL1β is a pleiotropic cytokine that contributes to the specific immune environment of mammalian testis and in regulating cell differentiation. Our data show only a significant reduction in AR and ICSHR expression, without changes in FSHR and IL-1β levels. These findings further could confirm the occurrence of a diminished release of testosterone from Leydig cells with the consequent reduction of AR and ICSHR expression. SC provide key signals to support germ cell survival proceeding through spermatogenesis, and the withdrawal of ICSH and/or testosterone results in the induction of apoptosis at particular stages of germ cell development reducing spermatogenic efficiency (Walker, 2021). Lacking the effects on FSHR and IL-1β, together the specific increasing of SHBG expression on SC, could suggest the falling down of physiological function of SC toward a quiescent phase, that evolve in a loss of some SC as evidenced by apoptotic signals, leading to an altered homeostasis of the organ and reduced formation of spermatozoa.

CONCLUSIONS

The present research aimed to investigate morphological and physiological alterations induced by hypergravity in the testis, used as putative model of endocrine gland deregulation. Preliminary results show a disassembly in SC lining organization and in hormone responsiveness pattern pointing towards severe consequences for the reproductive axis. We need to perform experiments with longer time exposure in order to detect slower effects of hypergravity on other possible tissue targets. Further, we want evaluate deregulation patterns on other glands and organs which could reveal even strong side effects due to modified gravity conditions.

REFERENCES

Afshinnekoo, E., Scott, R.T., MacKay, M.J., Pariset, E., Cekanaviciute, E., Barker, R., Gilroy, S., Hassane, D., Smith, S.M., Zwart, S.R., et al: Fundamental Biological Features of Spaceflight: Advancing the Field to Enable Deep-Space Exploration. Cell 183, 1162–1184 (2020).

Albi, E., Curcio, F., Lazzarini, A., Floridi A., Cataldi S., Lazzarini, R., Loreti E., Ferri I., Ambesi- Impiombato F.: A firmer understanding of the effect of hypergravity on thyroid tissue: cholesterol and thyrotropin receptor. PLoS One 9, e98250 (2014).

Albi, E., Curcio, F., Spelat, R., Lazzarini, A., Lazzarini, R., Cataldi, S., Loreti, E., Ferri, I., Ambesi- Impiombato, F.S.: Loss of parafollicular cells during gravitational changes (microgravity, hypergravity) and the secret effect of pleiotrophin. PLoS One 7, e48518 (2012).

Bonfiglio, T., Biggi, F., Bassi, A.B., Ferrando, S., Gallus, L., Loiacono, L., Ravera, S., Rottigni, M., Scarfì, S., Strollo, F., et al.: Simulated microgravity induces nuclear translocation of Bax and BCL-2 in glial cultured C6 cells. Heliyon 5, e01798 (2019).

Casey, T, Zakrzewska, E.I., Maple, RL., Lintault, L., Wade, C.E., Baer, L.A., Ronca, A.E., Plaut K.: Hypergravity disruption of homeorhetic adaptations to lactation in rat dams include changes in circadian clocks. Biol. Open 1, 570–581 (2012).

Celec, P., Ostatníková, D., Hodosy, J.: On the effects of testosterone on brain behavioural functions. Front. Neurosci. 9, 12 (2015).

Clement, G., Boyle, R., and Gunga H.C.: Editorial: The Effects of Altered Gravity on Physiology. Front. Physiol. 10, Article 1447 (2019).

Dubayle, D., Vanden-Bossche, A., Beraneck, M., Vico, L., Morel, J.-L.: Effects of centrifugation and whole-body vibrations on blood-brain barrier permeability in mice. N.P.J. Microgravity 6, 1 (2020).

Frett, T., Petrat, G., van Loon, J., Hemmersbach, R., Anken, R.H.: Hypergravity Facilities in the ESA Ground-Based Facility Program – Current Research Activities and Future Tasks. Micrograv. Sci. Techn. 28, 205–214 (2016).

Genchi, G.G., Cialdai, F., Monici, M., Mazzolai, B., Mattoli, V., Ciofani, G.: Hypergravity stimulation enhances PC12 neuron-like cell differentiation. Biomed. Res. Int. 2015, 748121 (2015) .

Grossmann, M. and Wu, F.C.: Male androgen deficiency: a multisystem syndrome. Asian J. Androl. 16: 159–160 (2014).

Heer, M. and Paloski, W.: Space motion sickness: Incidence, etiology, and countermeasures. Autonom. Neurosci. 129, 77–9 (2006).

Heiskala, M., Peterson, P.A., Yang, Y.: The roles of claudin superfamily proteins in paracellular transport. Traffic. 2, 93–98 (2001).

McLachlan, R.I., O'Donnell, L., Meachem, S.J., Stanton, P.G., de Kretser, D.M., Pratis, K., Robertson, D.M.: Hormonal Regulation of Spermatogenesis in Primates and Man: Insights for Development of the Male Hormonal Contraceptive. J. Androl. 23, 149–162 (2002).

Mishra, B. and Luderer, U.: Reproductive hazards of space travel in women and men. Nature Rev. Endocrinol. 15, 713–730 (2019).

Morita, H., Obata, K., Abe, C., Shiba, D., Shirakawa, M., Kudo, T., Takahashi, S.: Feasibility of a Short-Arm Centrifuge for Mouse Hypergravity Experiments. PlosOne 10, e0133981 (2015).

Moroz, G.A., Kriventsov, M.A., Kutia S.A.: Morphofunctional changes in the adrenal glands of juvenile rats systematically exposed to hypergravity. Russian Open Med. J. 7, Article e0401 (2018).

Mruk, D.D. and Cheng, C.Y. Tight junctions in the testis: new perspectives. Phil. Trans. R. Soc. B. 365, 1621–1635 (2010).

O'Shaughnessy, P.J., Baker, P.J., Heikkilä, M., Vainio S., McMahon A.P.: Localization of 17 β - Hydroxysteroid Dehydrogenase/17-Ketosteroid Reductase Isoform Expression in the Developing Mouse Testis—Androstenedione Is the Major Androgen Secreted by Fetal/Neonatal Leydig Cells. Endocrinology 141, 2631–2637 (2000).

Oskui, P.M., French, W.J., Herring, M.J., Mayeda, G.S., Burstein, S., Kloner, R.A.: Testosterone and the cardiovascular system: a comprehensive review of the clinical literature. J. Am. Heart Assoc. 2, e000272 (2013).

Sapp, W.J., Philpott, D.E., Williams, C.S., Kato, K., Stevenson, J., Vasquez, M., Serova, L.V.: Effects of spaceflight on the spermatogonial population of rat seminiferous epithelium. FASEB J. 4, 101–104 (1990).

Sharma, C.S., Sarkar S., Periyakaruppan A., Ravichandran P., Sadanandan B., Ramesh, V., Thomas, R., Hall, J.C., Wilson, B.L. and Ramesh G.T.: Simulated microgravity activates apoptosis and NF-kappaB in mice testis. Mol. Cell Biochem. 313, 71–78 (2008)

Sinnesael, M., Boonen, S., Claessens, .F, Gielen, E., Vanderschueren, D.: Testosterone and the male skeleton: a dual mode of action. J. Osteoporos. 2011, 240328 (2011).

Sluka, P., O'Donnell, L., Bartles, J.R., Stanton, P.G.: FSH regulates the formation of adherens junctions and ectoplasmic specialisations between rat Sertoli cells in vitro and in vivo. J. Endocrinol. 189, 381–395 (2006).

Uva, B.M., Masini, M.A., Sturla, M., Prato, P., Passalacqua, M., Giuliani, M., Tagliaferro, G., Strollo, F.: Clinorotation-induced weightlessness influences the cytoskeleton of glial cells in culture. Brain Res. 934, 132–139 (2002).

Van Loon, J.J.W.A., Krausse, J., Cunha, H., Goncalves, J., Almeida, H., Schiller, P.: The Large Diameter Centrifuge, LDC, for life and physical sciences and technology. In: L. Ouwehand (eds)

Life in Space for Life on Earth, ESA-SP Vol. 553. Proceedings of the conference held 22-27 June, 2008 at Angers, France (2008).

Wade, C.: Responses across the Gravity Continuum: Hypergravity to Microgravity. Adv. Space Biol. Med. 10, 225–245 (2005).

Walker, W.H.: Androgen Actions in the Tests and the Regulation of Spermatogenesis. Adv. Exp. Med. Biol. 1288, 175-203 (2021).

Chapter 2

Morphofunctional, viability and antioxidant system alterations on rat primary testicular cells exposed to simulated microgravity

Morphofunctional, viability and antioxidant system alterations on rat primary testicular cells exposed to simulated microgravity

Valentina Bonetto,[1] Linda Scarabelli,[2] Maria Angela Masini[1]

[1]DISIT, University of Eastern Piedmont, Alessandria; [2]DIMES, University of Genoa, Genova, Italy

Abstract

This study focused on effects induced by Short-term Simulated Microgravity (SMG) condition on primary cell culture from pre-pubertal Wistar rats testis. Cells were analyzed for cytoskeletal and Sex Hormone Binding Globulin (SHBG/ABP) changes by immunofluorescence technique, for antioxidant system exploiting RT-PCR and cell viability. Cells were cultured for 6 and 24h on a three-dimensional clinostat, Random Positioning Machine (RPM). At the end of each experiment, once stopped the RPM rotation, cells were either fixed in paraformaldehyde or lysed and RNA extracted. In cells exposed to SMG the cytoskeleton became disorganized, microtubules fragmented and SHBG was already undetectable after 6h of treatment. Moreover, various antioxidant systems significantly increased after 24h of SMG exposure. Initially, SMG seemed to disturb antioxidant protection strategies allowing the testes to support sperm production, thus generating an aging-like state of oxidative stress. Studies on changes induced by short-term altered gravity conditions, carried out in real microgravity, could give more information on steroidogenesis and germ cell differentiation within the testis exposed to this condition and confirm the validity of simulation approach.

Correspondence: Valentina Bonetto, DISIT, University of Eastern Piedmont, Via T. Michel 11, 15121 Alessandria, Italy.
Tel.: +39.0131.360274 Fax: +39.0131.360390
E-mail: valentina.bonetto@uniupo.it

Key words: Testicular primary culture; simulated microgravity; cytoskeleton; oxidative stress.

Acknowledgements: This work was supported by the Italian Space Agency (ASI).

Contributions: VB: histology, immunohistochemistry, mitocapture, data analysis; LS: PCR; MAM: design of the research, data analysis.

Conflict of interest: The authors have no conflict of interest to declare.

Received for publication: 24 May 2021.
Revision received: 9 October 2021.
Accepted for publication: 16 October 2021.

Journal of Biological Research 2021; 94:9875
doi:10.4081/jbr.2021.9875

Introduction

Since the advent of space flights more than 530 men and women have travelled to space, introducing the problem concerning the effects of microgravity on human physiology.[1] Nowadays it is well known that any alteration of the gravitational force causes relevant physiological changes in organisms, and it may affect their reproductive physiology and fertility.[2-4] During spaceflight, the astronauts experiment not only microgravity, but also hypergravity, which occurs during launch and re-entry phases, that is another interesting topic investigated by several researchers.[2,5,6]

In the present study, testis has been chosen because of its relevance as an endocrine organ and because of its key role in the reproductive system. The investigation of reproductive health requires extensive studies using animals and cell culture models, in order to fill gaps regarding the effect of long duration space missions on mammalian reproduction, starting from changes induced by short-term altered gravity conditions.

Due to the limited possibilities to perform experiments in real microgravity, several methods have been developed to Simulate Microgravity (SMG) such as the randomization of the direction of gravity force using a 3D-clinostat, as Random Positioning Machine (RPM).[2,7] Studies on the effect of weightlessness on the reproductive system of rodent models, conducted in real and Simulated Microgravity (SMG), showed similar morpho-functional testicular alterations.[8,9] The results obtained in rodent studies and experiments, made by others researchers and our group, showed an increase of physiological and morphological changes on reproductive system using different gravity vectors (0g, through 1g to 2g).[10-12] Moreover, such findings are consistent with the results of cell biology studies using SMG, which show morphological and functional changes to occur in testicular cells exposed to RPM. More in detail, these studies demonstrates that SMG causes changes in the seminiferous tubules, with altered tubular architecture and reduction in the number of spermatogenic cells, in addition microgravity induce hypogonadism directly rather than through stress-induced gonadal inhibition.[12] On the other hand, rats under SMG showing variation in testosterone levels demonstrated complete protection of both muscle and bone using a combination of bisphosphonate and testosterone, suggesting that androgen deficiency contributes at least partially to the pathophysiology of space flight-related muscle and bone atrophy.[10] As regard to humans, a decrease in testosterone secretion was also observed in astronauts during space flights.[13]

At cellular level, both real and simulated microgravity has proved to be one of the stress environmental factors that results in severe damages to the cytoskeleton of cells kept in culture.[14-16] Results of different studies shown damages to the cytoskeleton of Sertoli cell line and the lymphocytes' cytoskeleton both during spaceflight and in SMG.[12,14,17,18] Spermatogonial cell differentiation into mature spermatozoa requires Sertoli cells, which play a crucial role in the development of germ cells and in the regulation of spermatogenesis. In addition to its nursing function, Sertoli cells produce a large number of proteins essential for germ cell survival and development.[12]

The aim of this study was to evaluate the influence on a primary cell culture from rat testis, at first stages of exposure to SMG; cells were exposed for 6 and 24h to the treatment and analyzed by immunohistochemistry, molecular biology and general chemistry techniques, in order to evaluate the cell functionality after short-term SMG treatment. The intervals of time were chosen according to previous works that demonstrate alterations in cellular structure and functionality already after 6h and important changes at 24h.[19,20,21]

Materials and Methods

Preparation of cell culture

Cells were isolated from pre-pubertal (8 days old) Wistar rats and grown in DMEM (Sigma, St. Louis, Missouri) with the addition of 10% Fetal Bovine Serum, 1% L-glutamine, 1% gentamicin, streptamicin and amphotericin, at 34°C in a 5% CO_2 incubator. The cells were seeded at 20,000 cells/mL using "flasks on a slide" (flasks located onto a removable slide, 9.0 cm^2, Thermo Scientific Nunc). The flasks were positioned as close as possible to the center of the platform on the RPM (Dutch Space, Leiden, The Netherlands) and kept under rotation at 56 deg/sec, using the real random mode of the instrument, for 6h and 24h (SMG, 10^{-6} g) (Figure 1). Static controls (ground controls, 1g), were cultured for 24h under normal gravity conditions onto the supporting frame of the instrument in order to get cells to the same vibration stress conditions.

At the end of the experiment, once stopped the RPM rotation, some flasks were fixed with Phosphate Buffered Saline (PBS) containing 4% paraformaldehyde. Fixed cells were submitted to immunohistochemical techniques and to detect apoptotic cells with Mitocapture Mitochondrial Apoptosis detection kit (Biovision, Milpitas, CA), whereas other flasks were used to obtain cells for RT-PCR.

Microgravity conditions were simulated using an RPM connected to a control console through standard electrical cables. The apparatus is a 3D clinostat consisting of two independently rotating frames. One frame is positioned inside the other, exerting a complex net change in orientation on a biological sample mounted in the center of the RPM platform.[22] The rotation of the sample induces centripetal acceleration but placing the sample in the center of the RPM platform this effect will be negligible. Moreover, culture flasks were completely filled with medium without gas bubbles, avoiding loss of liquid during rotation. Gas bubbles result in unwanted fluid motion and associated shear stress to the sample.[22] This device does not actually eliminate gravity, but the RPM is a micro-weight simulator based on the principle of "gravity-vector averaging": it allows a 1 g stimulus to be applied omnidirectionally, and the sum of the gravitational force vectors tends to equal zero. The effects generated by the RPM are comparable to the effects of real microgravity, provided that the direction changes are faster than the response time of the system to the gravity field. The desktop RPM used was positioned within an incubator set at 34 °C, value close to the physiological testicular temperature, and 5% CO_2 to match physiologic conditions and to maintain a constant pH.[22]

Immunohistochemical techniques

The slides removed from the flasks, containing the cell cultures, were submitted to the indirect immunofluorescence technique.[23] After permeabilization with Triton X-100 (Sigma, St. Louis, Missouri) 01% in phosphate buffered saline (PBS, 0.01 M, pH 7.4), PBS washing and exposure to Normal Goat Serum (diluted 1:50 in PBS; Sigma, St. Louis, Missouri) in a moist chamber at 20°C, the cells were incubated overnight at 4°C with the antisera to α-tubulin (raised in mouse, diluted 1:500 in PBS, Sigma, St. Louis, Missouri) or to Sex Hormones Binding Globulin (SHBG/ABP, raised in rabbit against aminoacids 197-403 mapping at the C-terminus of SHBG of mouse origin, diluted 1:100, Santa Cruz Biotechnology, Inc). After PBS washing, a second layer of fluoresceine-isothiocyanate conjugated γ-globulins (FITC), goat anti-mouse (diluted 1:100 in PBS, Sigma, St. Louis, Missouri) and goat anti-rabbit (diluted 1:100 in PBS, Sigma, St. Louis, Missouri) following the specificity of the antisera for 30 min into a moist chamber, at 20°C. The slides were rinsed in PBS, mounted with gel-mount (Biomeda Corp., Foster City, CA). The specificity of the immunostainings was verified by omitting one of the steps of the

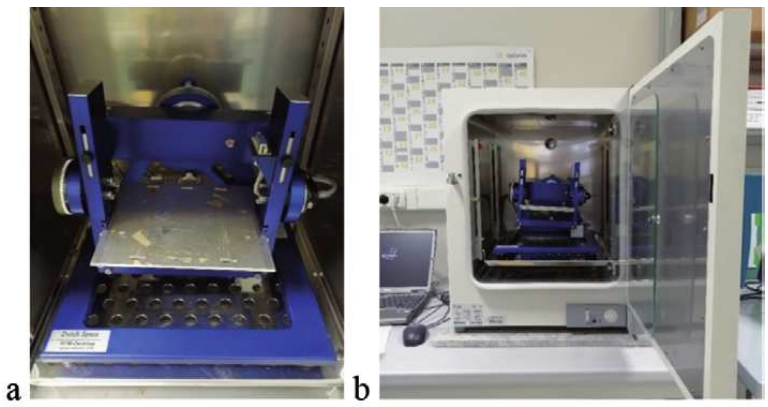

Figure 1. Random Positioning Machine (RPM).The RPM (Dutch Space, Leiden, Netherlands) (a) was run in a commercially available incubator at 34°C and 5% CO_2 (b).

immunohistochemical procedure, or by replacing the primary antisera with non-immune rabbit serum or PBS. Immunoreactions were visualized using a conventional epifluorescence microscope (Leica Axiovert).

RNA isolation and real-time RT-PCR

Since cytoskeleton alterations, we investigated the level of oxidative stress after 24h of SMG by measuring the expression level of genes involved in ROS metabolism or antioxidant defense mechanism. Total RNA was isolated by the acid phenol-chloroform procedure using the Trizol reagent (Sigma, St. Louis, Missouri) according to the manufacturers' instructions.[24] The purity of RNA was checked via absorption spectroscopy by measuring the 260/280 ratio. Only high purity samples ($OD_{260}/_{280}$> 1.8) were subjected to further manipulation. The quality of isolated RNA was assessed by electrophoresis on 1.5% formaldehyde-agarose gel to verify the integrity of the 18S and 28S rRNA bands. First strand cDNA was synthesized from 1 µg of total RNA using 200 ng oligo(dT)18-primer (TIB MolBiol, Italia), 200 units RevertAid H-Minus M-MuLV reverse transcriptase (Fermentas, Hannover MD, USA), 40 units RNAsin and 1 mM dNTPs (Promega, Milan, Italy) in a final volume of 20 µL. The reaction was performed in a Master-cycler apparatus (Eppendorf, Milan Italy) at 42°C for 1 h after an initial denaturation step at 70 °C for 5 min. The expression levels of genes were quantified in 96-well optical reaction by using a Chromo 4™ System real-time PCR apparatus (Biorad, Milan, Italy). Real-time PCR reactions were performed in quadruplicate in a final volume of 20 µL containing 10 ng cDNA, 10 µL of iTaq SYBR Green Supermix with ROX (Biorad, Milan, Italy), and 0.25 µM of each primer pair (TibMolBiol, Genoa, Italy). The glyceraldehyde 3-phosphate dehydrogenase (GAPDH) was used as a housekeeping gene to normalize the expression data. The accession numbers of the genes used in the study and the primer sequences are given in Table 1. The thermal protocol included an enzymatic activation step at 95°C (3 min) and 40 cycles of 95°C (15s), 60°C (30s) and 72°C (20s). The melting curve of the PCR products (55–94 °C) was also recorded to check the reaction specificity. The relative gene expression of target genes in comparison of the GAPDH reference gene was conducted following the comparative C_T threshold method using the Biorad software tool Genex-Gene Expression Macro™.[25,26] The normalized expression was then expressed as the relative quantity of mRNA (fold induction) with respect to the control sample. Data are the mean ±SD for three experiments in quadruplicate.

Cell viability assays

Cell death was assessed by staining with MitoCapture (Biovision, Milpitas, CA), a fluorescent lipophilic cationic reagent that assesses mitochondrial membrane permeability, according to the supplier's instructions. Briefly, cells were incubated with the MitoCapture reagent for 15 min at 37°C and observed by fluorescence microscopy using a wide band pass filter. Cells with intact mitochondria exhibited focal red cytosolic fluorescence, whereas cells with permeabilized mitochondria exhibited diffuse green cytosolic fluorescence. Cells lacking red fluorescence and having green fluorescence were scored positive. Cell death was evaluated in each experiment from control and treated cultures. Data were expressed as Integrated Density and the corrected total cell fluorescence (CTCF) calculated from three fields chosen at random in two slide preparations for each sample.

Statistical analysis

Statistical analysis was performed by using ANOVA followed by Bonferroni ad hoc post test, values were expressed as mean± standard deviation (SD; INSTAT software,GraphPad Software, Inc., San Diego, CA 92130 USA).

Results

Effect of modeled microgravity on cytoskeleton and Sex Hormone Binding Globulin

After 6h in modeled microgravity (Figure 2b), cells didn't show relevant morphological differences as compared with the cells maintained at 1g (Figure 2a). The cytoskeleton, identified with a specific antibody directed against α-tubulin, was well organized, with microtubules radiating in discrete filaments from the nucleus to the plasma membrane. When the rotation was prolonged to 24 h, the microtubular array was more disorganized and microtubules appeared fragmented; as a consequence, the cells lost their shape after 24h of SMG (Figure 2c).

An immunoreactive signal for Sex Hormone Binding Globulin (SHBG/ABP) was detected in the control cells, whereas is totally absent in cells exposed to SMG (Figure 3).

Cell viability assays: MitoCapture

In healthy cells, the MitoCapture reagent remains in the mitochondria in form of polymers and gives off a red fluorescence; however, in case of mitochondrial damage, the reagent leaks out into cytoplasm as monomers that generate a green signal. As

Table 1. Name and accession numbers of the target genes are listed together with the primer sequences used for RT-PCR analysis in the study.

Gene name	Accession number	Forward primer (5'-3')	Reverse primer (3'-5')
MT-1	NM_013602	CTGCTCCACCGGCGG	GCCCTGGGCACATTTGG
MT-2	NM_008630	TCCTGTGCCACAGATGGATC	GTCCGAAGCCTCTTTGCAGA
p53	NM_030989	GGCTCCTCCCCAACATCTTATC	TACCACCACGCTGTGCCGAAAA
PARP-1	NM_013063	TGCAGTCACCCATGTTCGATGG	AGAGGAGGCTAAAGCCTTG
GST	NM_013541	GTGCCCGGCCCAAGAT	TTGATGGGACGGTTCACATG
CAT	NM_009804	CCTGAGAGAGTGGTACATGC	CACTGCAAACCCACGAGGG
Mn-SOD	NM_013671	GGCTCCCGGCACAACACAGCC	CCTCGTGGTACTTCTCCTCGGTG
GAPDH	NM_008084	GACCCCTTCATTGACCTCAAC	CGCTCCTGGAAGATGGTGATGGG

demonstrated in Figure 4 the red fluorescence in the control cells (Figure 3a) was replaced by green fluorescence under SMG treatment. After 6h (Figure 4b) and 24h treatments (Figure 4c) the red signal decreased and there is a significant difference in CTCF value related to the red signal in samples cultured under SMG (Figure 4d). This indicates that increasing the time of exposure to SMG increases mitochondrial transmembrane permeability.

Effect of microgravity on the antioxidant system

In order to investigate the role of SMG on the enzymatic constituents of the antioxidant system in testis primary cells culture, Superoxide Dismutase (SOD), Catalase (CAT) and Glutathione S-Trasferase (GST) activities were evaluated. Metallothionein-1 (MT-1) and metallothionein-2 (MT-2) expression was also investigated, as part of the array of protective stress responses. Moreover,

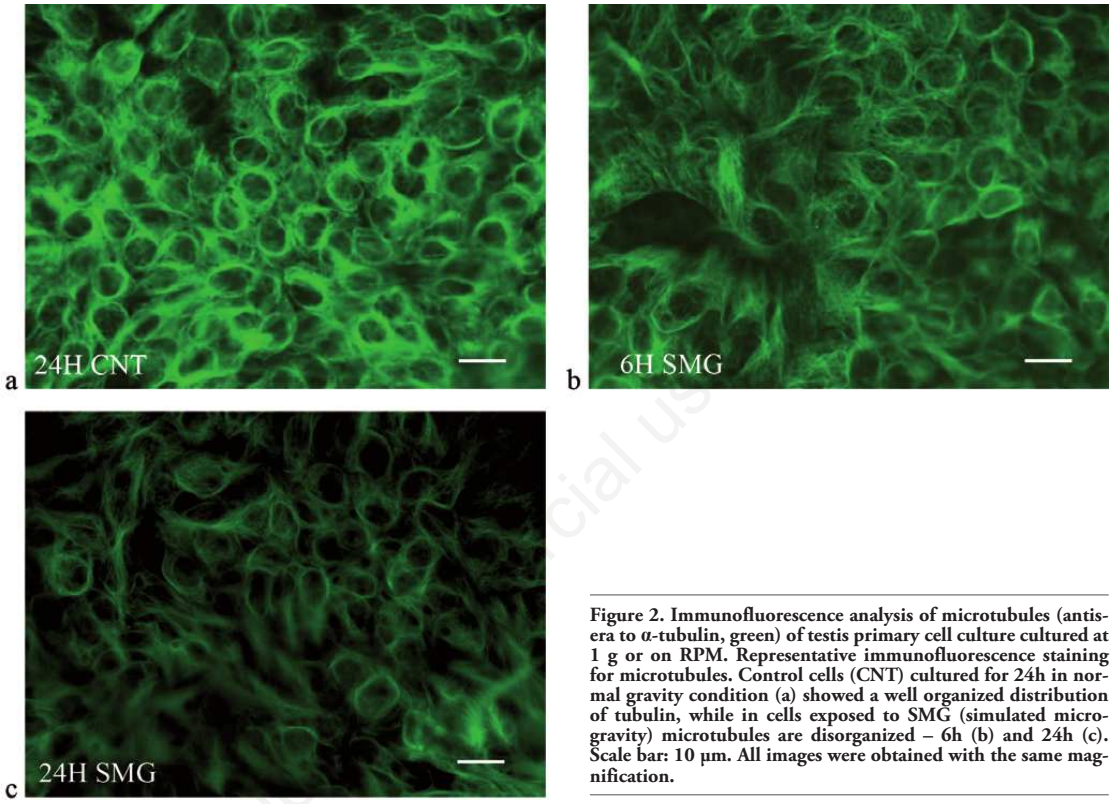

Figure 2. Immunofluorescence analysis of microtubules (antisera to α-tubulin, green) of testis primary cell culture cultured at 1 g or on RPM. Representative immunofluorescence staining for microtubules. Control cells (CNT) cultured for 24h in normal gravity condition (a) showed a well organized distribution of tubulin, while in cells exposed to SMG (simulated microgravity) microtubules are disorganized – 6h (b) and 24h (c). Scale bar: 10 µm. All images were obtained with the same magnification.

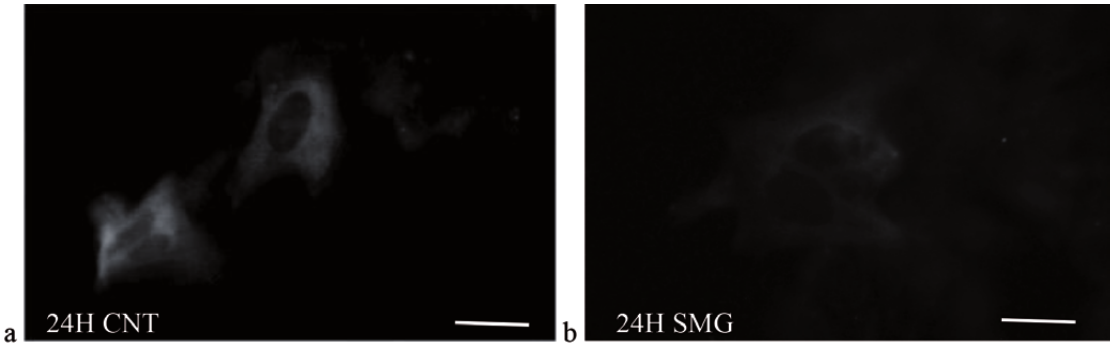

Figure 3. Immunofluorescence analysis for Sex Hormone Binding Globulin/Androgen-Binding Protein (SHBG/ABP). Representative immunofluorescence staining for SHBG/ABP detected in the control cells (CNT) growth for 24h in normal gravity condition (a). In cells exposed for 24 h to simulated microgravity (SMG) the immunostaining is very weak (b). Scale bar: 10 µm.

the expression of poly [ADP-ribose] polymerase 1 (PARP-1), an enzyme normally activated by oxidative stress, and the protective role of the oncosuppressor gene p53 were also evaluated. After 24 h of rotation the expression of MT-1, p53, PARP and GST showed a significant increase with respect to controls (Figure 5).

Discussion

Colonization of deep space poses a lot of hazards to human reproduction, one of these is the exposure to weightlessness. Experiments carried out with different organisms exposed to microgravity and space flight conditions showed subtle abnormalities in fertilization. Only a few studies concerned mammals, making difficult to fill gaps in knowledge regarding the effect of space mission on mammalian reproduction.[12]

Spermatogenesis is a complex, highly ordered process of cell division and differentiation by which spermatogonia become mature spermatozoa. The understanding of this process in microgravity condition needs to be investigated starting from firsts responses of testes system, in order to evaluate the effects on male fertility. Spermatogenesis depends from intratesticular and extratesticular hormonal regulatory processes and functions of the intertubular microvasculature, the Leydig cells and other cellular components of the intertubular space. These signals are integrated, thus allowing the secretion of products that control germ cell development and modulate the function of the other testicular cells, including their own.[9]

After 6h in modeled microgravity testis cells (obtained from pre-pubertal 8 days old Wistar rat) showed firsts signs of cytoskeleton alterations, as reported in previous studies and in other cell types (glial, endothelial, thyroid cells or lymphocytes), and that increases over time.[14-16,18-20] Moreover, gravity vector variation influenced the androgen binding protein (SHBG/ABP) expression, absent in treated testis cells. Considering the role of SHBG/ABP as androgen carrier, the absence of this protein, at 6h and 24h, could significantly compromise the efficiency of spermatogenesis.

During spaceflight most of physiological changes are related to microgravity,[1,3,4] additionally this condition has been reported to cause cellular oxidative stress that leads to the production of Reactive Oxygen Species (ROS) linked to cellular senescence.[27] However, the study of microgravity induced oxidative stress is not yet completely understood.

The testes have developed a sophisticated array of antioxidant systems which includes both enzymatic and non-enzymatic constituents.[28] Our results showed a significant up-regulation of glu-

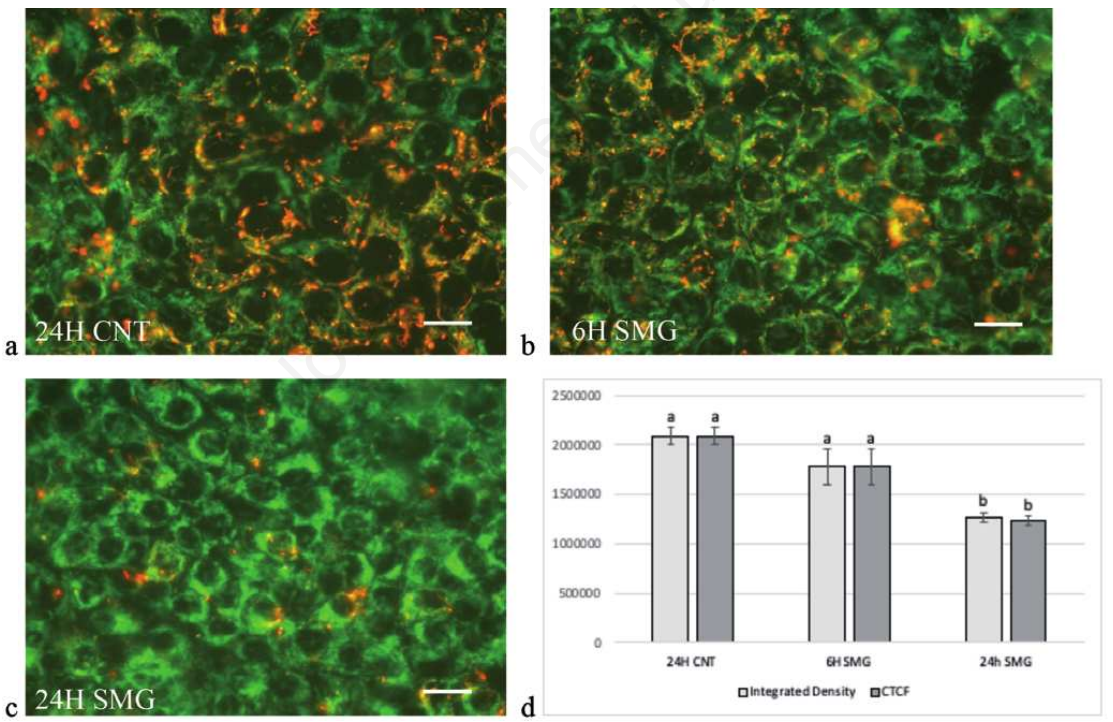

Figure 4. Analysis of cell viability and mitochondrial integrity. Cells were incubated with the MitoCapture reagent to detect mitochondrial membrane integrity after microgravity treatment. The figures show representative images of cells with intact (punctate red fluorescence) or permeabilized (diffuse green fluorescence) mitochondria. Control cells (CNT) cultured for 24h in normal gravity condition (a); cells after 6h under SMG (b); cells after 24h under SMG (c). Integrated Density and correct total cell fluorescence (CTCF) related to red signal (healthy cells) graph (d). Differences among means were assessed using ANOVA test followed by Bonferroni ad hoc post test. p≤ 0.05 was considered statistically significant. Scale bar: 10 µm. All images were obtained with the same magnification.

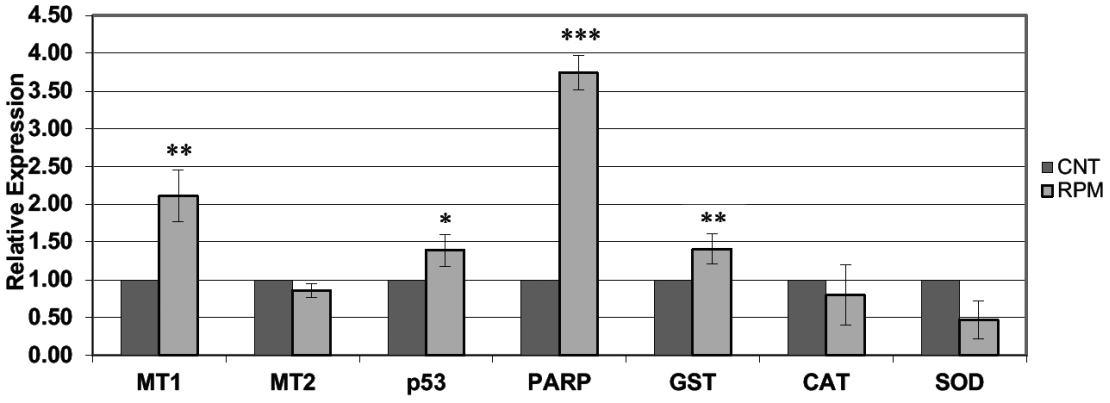

Figure 5. Effects of simulated microgravity on the expression of antioxidant enzymes, p53 and PARP-1 by testis primary cell culture. Relative expression of Metallothioneins (MT-1 and MT-2), p53, PARP-1, Glutathione Transferase (GST), Catalase (CAT) and Superoxide Dismutase (SOD) were quantified in testis cells after 24 h of Simulated Microgravity (SMG) by real-time RT-PCR. Values represent the fold induction as compared to the Respective Controls (CNT) after normalization for GA3PDH mRNA, used as reference gene. Data are expressed as means ± SD of three independent experiments. Differences among means were assessed using ANOVA test followed by Bonferroni ad hoc post test. ***p<0.0001, **p < 0.001, *p<0.01 as compared to the respective controls.

tathione S-transferase, GST, active in oxidative and xenobiotic response, that support the hypothesis of a ROS increase at intracellular levels after 24h of SMG. Moreover, higher MT-1 expression level observed could reflect a defensive response or adaptation to the microgravity stress, suggesting an interaction with ROS scavenging enzymes, which agrees with the fundamental role of MTs as maintainers of zinc pool, restoring zinc to antioxidant zinc-dependent enzymes and proteins.[27,28]

Compared to control, the expression of both p53 and PARP-1, also named "guardians of the genome" due to their function in maintaining genome integrity, could represent a complementary and additional way by which testes cells may face the negative effects of ROS accumulation.[29]

PARP-1 is a zinc-finger DNA-binding enzyme able to recognize DNA damages, DNA nicks and double stranded breaks, and once activated catalyzes the synthesis of branched poly(ADP-ribose) polymers that stabilize the surrounding chromatin and converts DNA damages into intracellular signals which activate DNA repair programs.[29] In this regard, a similar function of PARP could be also assumed in rat testes' cells in response to SMG-induced oxidative stress. By the same token, the up-regulation in p53 expression, observed in the present work, is probably due to its pivotal role in regulating cell response to multiple stress signals, including the oxidative stress.

Moreover, we observed mitochondrial dysregulation in treated cells. Similar effects, although occurring in different species, suggests that mitochondria changes could be a stress adaptive response to ensure cell energy. Considering that mitochondria are the major targets of ROS negative effects, an increase of free radicals and other reactive oxygen species is able to induce a mitochondrial membrane permeabilization, a process that could leads to mitopsosis and mitophagy, in order to eliminate dysfunctional mitochondria and protect cells.[30]

Taking the current data together, it seems that short-term SMG exposure induced morphofunctional alteration and an increase in oxidative stress response in rat primary testis culture, in agreement with results obtained in other works.[19,20,28]

Conclusions

In this study, we validated our hypothesis that short-term SMG induces oxidative cellular stress in rat testes primary culture cells, as demonstrated by the response of the antioxidant system and impaired mitochondrial function. We hypothesized that the significant expression level increase of oxidative stress-induced gene, as GST and MT1, PARP and p53 could be related to an increase in ROS production. ROS level the observed morpho-functional, in cytoskeleton, SHBG/ABP production, cell viability, could have a significant inhibitory effect on germ cell differentiation which may result in male infertility.

Our data ought to provide important insight in this topic concerning the effect of short-term SMG exposure, but also in 1g condition, because of male infertility is also a social concern, considering the increase of life expectancy. These findings could lead the way to evaluate steroidogenesis, spermatogenesis and cell senescence via oxidant stress mechanisms induced by microgravity, performing further investigation during simulated or actual spaceflights.

References

1. Mishra B, Luderer U. Reproductive hazards of space travel in women and men. Nat Rev Endocrinol 2019;15:713–30.
2. Tou J, Ronca A, Grindeland R, Wade C. Models to study gravitational biology of mammalian reproduction. Biol Reprod 2002;67:1681–87.
3. Zhu H, Wang H, Liu Z. Effects of real and simulated weightlessness on the cardiac and peripheral vascular functions of humans: a review. Int J Occup Med Environ Health 2015;28:793–802.
4. Tanaka K, Nishimura N, Kawai Y. Adaptation to microgravity deconditioning and countermeasures. J Physiol Sci 2017;67:271–81.

5. Sominsky L, Hodgson DM, McLaughlin EA, et al. Linking stress and infertility: a novel role for ghrelin. Endocr Rev 2017;38:432–67.
6. Nargund VH. Effects of psychological stress on male fertility. Nat Rev Urol 2015;12:373–82.
7. Herranz R, Anken R, Boonstra J, et al. Ground-based facilities for simulation of microgravity: organism-specific recommendations for their use and recommended terminology. Astrobiology 2013;13:1–17.
8. Grindeland RE, Popova IA, Vasques M, Arnaud SB. Cosmos 1887 mission overview: effects of microgravity on rat body and adrenal weights and plasma constituents. FASEB J 1990;4:105–9.
9. Hadley JA, Hall JC, O'Brien A, Ball R. Effects of a simulated microgravity model on cell structure and function in rat testis and epididymis. J Appl Physiol 1992;72:748–59
10. Vasques M, Lang C, Grindeland RE, et al. Comparison of hyper- and microgravity on rat muscle organ weights and selected plasma constituents. Aerosp Med Hum Perform 1998;69:2–8.
11. Strollo F, Barger L, Fuller C. Testosterone urinary excretion rate increases during hypergravity in male monkeys. J Gravit Physiol 2000;7:181–82.
12. Masini MA, Albi E, Barmo C, et al. Impact of long-term exposure to space environment on adult mammalian organisms: a study on mouse thyroid and testis. Plos one 2012;7:e35418.
13. Smith SM, Heer M, Wang Z, et al. Long-duration space flight and bed rest effect on testosterone and other steroids. J Clin Endocrinol Metab 2012;97:270–78.
14. Uva BM, Masini MA, Sturla M, et al. Clinorotation-induced weightlessness influences the cytoskeleton of glial cells in culture. Brain Res 2002;934:132–39.
15. Sciola L, Cogoli-Greuter M, Cogoli A, et al. Influence of microgravity on mitogen binding and cytoskeleton in Jurkat cells. Adv Space Res 1999;24:801–5.
16. Infanger M, Kossmehl P, Shakibaei M, et al. Simulated weightlessness changes the cytoskeleton and extracellular matrix proteins in papillary thyroid carcinoma cells. Cell Tissue Res 2006;324:267–77.
17. Tauber S, Hauschild S, Paulsen K, et al. Signal transduction in primary human T lymphocytes in altered gravity during parabolic flight and clinostat experiments. Cell Physiol Biochem 2015;35:1034–51.
18. Gmunder FH, Kiess M, Sonnefeld G, et al. A ground-based model to study the effects of weightlessness in lymphocytes. Biol Cell 1990;70:33–38.
19. Uva BM, Strollo F, Ricci F, et al. Effect of conditions of three dimensional clinostating on testicular cell machinery. Acta astronautica 2007;60:391–96.
20. Masini M, Prato P. Effects of a simulated microgravity model on cell structure and function in mouse testis. J Biol Res 2010;83:29–32.
21. Aleshcheva G, Sahana J, Ma X, et al. Changes in morphology, gene expression and protein content in chondrocytes cultured on a random positioning machine. Plos One 2013;8:e79057.
22. Van Borst AG, van Loon JJWA. Technology and development for the random positioning machine, rpm. Micorgravity Sci Technol 2009;21:287.
23. Coons AH, Leduc EH, Connolly JM. Studies on antibody I A method for the histochemical demonstration of specific antibody and its application to a study of the hyperimmune rabbit. J Exper Med 1955;102:49–59.
24. Chomczynski P, Sacchi N. Single-step method of RNA isolation by acid guanidinium thiocyanate–phenol–chloroform extraction. Anal Biochem 1978;162:156–59.
25. Pfaffl MW, Horgan GW, Dempfle L. Relative expression software tool (REST) for group-wise comparison and statistical analysis of relative expression results in real-time PCR. Nucleic Acids Res 2002;30-6.
26. Vandesompele J, De Preter K, Pattyn F, et al. Accurate normalization of real-time quantitative RT-PCR data by geometric averaging of multiple internal control. Genome Biol 2002;3:1–12.
27. Morabito C, Guarnieri S, Catizone A, et al. Transient increases in intracellular calcium and reactive oxygen species levels in TCam-2 cells exposed to microgravity. Sci Rep 2017; 7:148-56.
28. Aitken RJ, Roman SD. Antioxidant systems and oxidative stress in the testes. Oxid Med Cell Longev 2008;1:15–24.
29. Elkholi R, Chipuk JE. How do I kill thee? Let me count the ways: p53 regulates PARP-1 dependent necrosis. Bio Essays 2014;36:46-51.
30. Venditti P, Di Meo S. The role of reactive oxygen species in the life cycle of the mitochondrion. Int J Mol Sci 2020;21:21-73.

Chapter 3

Prolonged exposure to simulated microgravity promotes stemness impairing morphological, metabolic and migratory profile of pancreatic cancer cells: a comprehensive proteomic, lipidomic and transcriptomic analysis

Cellular and Molecular Life Sciences (2022) 79:226
https://doi.org/10.1007/s00018-022-04243-z

ORIGINAL ARTICLE

Prolonged exposure to simulated microgravity promotes stemness impairing morphological, metabolic and migratory profile of pancreatic cancer cells: a comprehensive proteomic, lipidomic and transcriptomic analysis

Maria Angela Masini[1] · Valentina Bonetto[1] · Marcello Manfredi[2,8,9] · Anna Pastò[10] · Elettra Barberis[2,8,9] · Sara Timo[1] · Virginia Vita Vanella[2] · Elisa Robotti[1] · Francesca Masetto[4] · Francesca Andreoli[3] · Alessandra Fiore[4] · Sara Tavella[5,7] · Antonio Sica[3,6] · Massimo Donadelli[4] · Emilio Marengo[1,8,9]

Received: 28 October 2021 / Revised: 21 February 2022 / Accepted: 10 March 2022

Abstract

Background The impact of the absence of gravity on cancer cells is of great interest, especially today that space is more accessible than ever. Despite advances, few and contradictory data are available mainly due to different setup, experimental design and time point analyzed.

Methods Exploiting a Random Positioning Machine, we dissected the effects of long-term exposure to simulated microgravity (SMG) on pancreatic cancer cells performing proteomic, lipidomic and transcriptomic analysis at 1, 7 and 9 days.

Results Our results indicated that SMG affects cellular morphology through a time-dependent activation of Actin-based motility via Rho and Cdc42 pathways leading to actin rearrangement, formation of 3D spheroids and enhancement of epithelial-to-mesenchymal transition. Bioinformatic analysis reveals that SMG may activates ERK5/NF-κB/IL-8 axis that triggers the expansion of cancer stem cells with an increased migratory capability. These cells, to remediate energy stress and apoptosis activation, undergo a metabolic reprogramming orchestrated by HIF-1α and PI3K/Akt pathways that upregulate glycolysis and impair β-oxidation, suggesting a de novo synthesis of triglycerides for the membrane lipid bilayer formation.

Conclusions SMG revolutionizes tumor cell behavior and metabolism leading to the acquisition of an aggressive and metastatic stem cell-like phenotype. These results dissect the time-dependent cellular alterations induced by SMG and pave the base for altered gravity conditions as new anti-cancer technology.

Keywords Microgravity · Cancer stem cells · Metabolism · Proteomic · Lipidomic

Abbreviations

AA	Arachidonic acid
CSC	Cancer stem cell
EMT	Epithelial-to-mesenchymal transition

Maria Angela Masini, Valentina Bonetto, Marcello Manfredi and Anna Pastò contributed equally to the work.

✉ Anna Pastò
annapasto.phd@gmail.com

[1] Department of Sciences and Innovation Technologies (DISIT), University of Eastern Piedmont, Alessandria, Italy

[2] Department of Translational Medicine (DIMET), University of Eastern Piedmont, Novara, Italy

[3] Humanitas Clinical and Research Center, IRCCS, Rozzano, Milan, Italy

[4] Department of Neurosciences, Biomedicine and Movement Sciences (DNBM), University of Verona, Verona, Italy

[5] Department of Experimental Medicine (DIMES), University of Genova, Genova, Italy

[6] Department of Pharmaceutical Sciences (DSF), University of Eastern Piedmont 'A. Avogadro', Novara, Italy

[7] IRCCS Ospedale Policlinico San Martino, Genova, Italy

[8] ISALIT, Novara, Italy

[9] CAAD, Center for Autoimmune and Allergic Disease, University of Eastern Piedmont, Novara, Italy

[10] School of Cancer & Pharmaceutical Sciences New Hunt's House, Guy's Campus, King's College London, SE1 UL London, United Kingdom

Published online: 07 April 2022

FA	Fatty acid
PC	Phosphatidylcholine
PDAC	Pancreatic ductal adenocarcinoma
PE	Phosphatidylethanolamine
LPC	Lysophosphatidylcholine
LPE	Lysophosphatidylethanolamine
ROS	Reactive oxygen species
RPM	Random Positioning Machine
SMG	Simulated microgravity
TCA	Tricarboxylic acid
TG	Triglyceride/triacylglycerol

Introduction

The force of gravity affects all living beings on Earth. From 1969, when men stepped on the moon, the importance of gravity was clear. During their stay in space, astronauts showed many physiological changes mainly impairing the musculoskeletal and cardiovascular system [1], due to the impact of reduced gravity on cellular properties including morphology, metabolism, and proliferation. In the last years, it has grown a huge interest in the effects of the absence of gravity on tumor cells in order to exploit microgravity for the development of novel anti-cancer therapies. In gravity-altered conditions, cancer cells behave differently from healthy ones: some processes, including apoptosis, adhesion, proliferation, and migration, are differently activated in cancer cells [2, 3]. Indeed, it was demonstrated that microgravity induces apoptosis [3] through the up-regulation of the pro-apoptotic factors Bax, PARP and p53, and inhibition of proliferation of cancer cells, but not of healthy cells. In addition, tumor cells are subjected to profound morphological rearrangement, linked to F-actin accumulation [4]. We and others [5, 6] proved that cytoskeleton, in particular the microfilamentous and microtubular components, became disorganized after a very short time of exposure to microgravity. This alteration affected many genes involved in the regulation of cancer cell proliferation, susceptibility to drugs [7], DNA repair (e.g. PARP), cell damage and invasion [2, 8]. However, to date the results of microgravity effects on cancer cells are contradictory mainly due to different setups, experimental designs and time points analyzed.

Given the difficulty of exposing cells and organisms to the real absence of gravity, many experiments are conducted on Earth, using tools that simulate the reduction of the gravity vector. The 3-Dimensional clinostat, Random Positioning Machine (RPM) is one of the most useful devices in this perspective. It simulates some of the physical effects of spaceflight by providing a gravity vector average reduction (down to 10^{-6} g) of the apparent force of gravity, without generating significant shear forces [9].

Exploiting the RPM tool, we decided to perform a comprehensive analysis of the long-term effects of simulated microgravity (SMG) on pancreatic ductal adenocarcinoma (PDAC) cells. Despite its incisiveness, PDAC has not been examined so far in microgravity conditions. This neoplasia is one of the most severe malignancies, representing the 4^{th}-5^{th} cause of death from cancer in the western world. The therapeutic option currently available for PDAC is surgery, alone or in combination with radio or chemotherapy; however, only 8% of patients remain alive 5 years after diagnosis due to late diagnosis and/or resistance to the treatments. It is largely accepted that resistance to conventional anti-cancer treatments is due to a small cell subset called cancer stem cells (CSCs). CSCs are the main orchestrators of tumor establishment, metastatic progression and relapse. Already identified in most of the neoplastic tissues, differently from other tumor cells, CSCs are endowed with great plasticity, capability to enter quiescence and survive to microenvironment changes adapting metabolism, energy machinery and proliferation.

Performing a comprehensive transcriptomic, proteomic and lipidomic analysis in PDAC cells exposed for different time points to SMG, we demonstrated that microgravity induces cell transformation towards the acquisition of cancer stem cell-like features, leading to a more aggressive and metastatic phenotype.

Materials and methods

Cell cultures

Human ductal pancreatic adenocarcinoma cell lines PaCa-44 and CFPAC-1 were grown in RPMI-1640 medium supplemented with 10% fetal bovine serum (FBS), 1% penicillin and streptomycin (PS). Human ductal pancreatic adenocarcinoma cell line AsPC-1 was grown in DMEM medium supplemented with 10% fetal bovine serum (FBS), 1% penicillin and streptomycin (PS). Cells were plated at the final concentration of 5×10^5 cells/ml on flask, Petri dish or flask on slide, according to the experimental design, and maintained at 37 °C with 5% CO_2.

For simulated microgravity (SMG) cell culture 5×10^5 cells/ml were seeded in slide flasks and subsequently fitted onto a Random Positioning Machine (RPM, Dutch Space, NL), where they were kept under continuous rotation at 56 deg/s and at the temperature of 37 °C, for 1, 7 or 9 days. To avoid air bubbles formation and to ensure a minimization of turbulence and shear stress, flasks were completely filled with medium [9]. Flasks were placed close to the support center to minimize any centrifugal acceleration, using "real random mode". In this manner, speed and

direction of the two rotating frames, changed randomly under the control of a software [10].

For 3D culture, PaCa-44 cells were seeded onto U-bottom low adhesion 96 well-plates (Greiner Bio-One) at a concentration of 5×10^4 cells/well in 100 µl RPMI-1640 complete medium supplemented with 0,5% methyl-cellulose (spheroid-forming medium). Spheroids were grown at 37 °C and 5% CO_2. Cells subjected to SMG were compared to two different control groups: frame controls and ground controls. Frame control cells (F, 1xg) were placed on the frame supporting the RPM in order to expose them to any vibration eventually produced and transmitted by the rotating machinery to the supporting structure. Ground control cells (1 g) both in spheroid-forming culture condition (Spheroid 1 g) and normal adhesion (Adhesion) were kept in an incubator at 37 °C and 5% CO_2. Controls were analyzed at the same time points of SMG-cells.

Spheroid staining and immunofluorescence

Spheroids were fixed in 4% PFA, dehydrated and embedded in London Resin White. Spheroids' Sects. (1 µm thickness) were stained with toluidine blue and morphologically analyzed using an optic microscope (Zeiss Axiovert 100 M, Oberkochen, Germany).

For Calcein/PI staining, unfixed spheroids were stained with Calcein-AM (1 mM) for 20 min, followed by staining with PI (0.4 mg/ml) for 5 min. Then, spheroids were washed twice in PBS solution (0.1 M, pH 7.2) and observed at a fluorescent microscope (Axiovert 100 M, Zeiss). Fluorescent images were captured using AxioObserver Z2 inverted microscope (Zeiss), with Apotome2 system (Zeiss) and ZEN Blue 2.6 image acquisition software (Zeiss).

Proteomic analysis

At different time points (according to the experimental setting), the cells were collected, washed in PBS and resuspended in RIPA buffer (Thermo Fisher Scientific, Waltham, MA, USA) supplemented with protease inhibitors cocktail 1X (Roche, Basilea, Switzerland). To increase yields, cells were sonicated twice for 10 min; the lysate was gently mixed for 15 min on ice and then centrifuge at 14,000×*g* for 15 min at 4 °C to pellet the cell debris. Protein concentration was measured with BCA Protein Assay (Thermo Fisher Scientific) using bovine serum albumin as a standard. The cell lysates were reduced using 2.5 µL of dithiothreitol (200 mM DTT stock solution) (Sigma-Aldrich, St.Louis, MO, USA) at 90 °C for 20 min, and alkylated with 10 µl of Cysteine Blocking Reagent (Iodoacetamide, IAM, 200 mM Sigma-Aldrich) for 1 h at room temperature in the dark. Trypsin (Promega, Sequence Grade) was added and digestion was performed overnight at 37 °C. Then, the peptides digests were desalinated on the Discovery® DSC-18 solid phase extraction (SPE) 96-well Plate (25 mg/well) (Sigma-Aldrich) and the samples were ready for the analysis.

LC–MS/MS analyses were performed using a micro-LC Eksigent Technologies (Dublin, CA, USA) system with a stationary phase of a Halo Fused C18 column (0.5 × 100 mm, 2.7 µm; Eksigent Technologies). The mobile phase was a mixture of 0.1% (v/v) formic acid in water (A) and 0.1% (v/v) formic acid in acetonitrile (B), eluting at a flow-rate of 15.0µL min − 1 at an increasing concentration of solvent B from 2 to 40% in 30 min. The samples used to generate the SWATH-MS (Sequential window acquisition of all theoretical mass spectra) spectral library were subjected to the traditional data-dependent acquisition (DDA): the mass spectrometer analysis was performed using a mass range of 100–1500 Da (TOF scan with an accumulation time of 0.25 s), followed by a MS/MS product ion scan from 200 to 1250 Da (accumulation time of 5.0 ms) with the abundance threshold set at 30 cps (35 candidate ions can be monitored during every cycle). Samples were then subjected to cyclic data independent analysis (DIA) of the mass spectra, using a 25-Da window. A 50-ms survey scan (TOF–MS) was performed, followed by MS/MS experiments on all precursors. These MS/MS experiments were performed in a cyclic manner using an accumulation time of 40 ms per 25-Da swath (36 swaths in total) for a total cycle time of 1.5408 s. The ions were fragmented for each MS/MS experiment in the collision cell using the rolling collision energy. The MS data were acquired with Analyst TF 1.7 (AB SCIEX, Concord, Canada). Three instrumental replicates for each sample were subjected to the DIA analysis.

The mass spectrometry files were searched using Protein Pilot (AB SCIEX) and Mascot (Matrix Science Inc., Boston, USA). Samples were input in the Protein Pilot software v. 4.2 (AB SCIEX), with the following parameters: cysteine alkylation, digestion by trypsin, no special factors and False Discovery Rate at 1%. The UniProt Swiss-Prot reviewed database containing human proteins (version 12/10/2018, containing 48,561 sequence entries). The Mascot search was performed on Mascot v. 2.4, the digestion enzyme selected was trypsin, with 2 missed cleavages and a search tolerance of 50 ppm was specified for the peptide mass tolerance, and 0.1 Da for the MS/MS tolerance. The charges of the peptides to search for were set to 2 + , 3 + and 4 + , and the search was set on monoisotopic mass. The instrument was set to ESI-QUAD-TOF and the following modifications were specified for the search: carbamidomethyl cysteine as fixed modification and oxidized methionine as variable modification [11, 12].

The quantification was performed by integrating the extracted ion chromatogram of all the unique ions for a given peptide. The quantification was carried out with PeakView 2.0 and MarkerView 1.2. (AB SCIEX). Six peptides per

protein and six transitions per peptide were extracted from the SWATH files. Shared peptides were excluded as well as peptides with modifications. Peptides with FDR lower than 1.0% were exported in MarkerView for the t-test.

Ingenuity Pathways Analysis (IPA) software (Qiagen, Redwood City, CA, USA) and STRING software (www.stringdb.org), were used for bioinformatics analysis [13].

Lipidomic analysis

Cells were extracted using a solution 75:15 IPA/H_2O, after the addition of 100µL of MeOH 5% deuterated standard (Splash Lipidomix®). Then the samples were vortexed for 30 s, sonicated for 2 min and vortexed again for 30 s and then they were incubated for 30 min at 4 °C, under a gentle, constant shaking. Another 30 min were used to keep the sample rest in ice. To remove debris and other impurities, the samples were centrifuged for 10 min at 3500*g* at 4 °C. 1 mL of supernatant was collected and dried using a SpeedVac. The dried samples were reconstituted in 100µL of MeOH containing the internal standard CUDA (12.5 ng/mL).

For the analysis of the reconstituted lipids a UHPLC Vanquish system (Thermo Scientific, Rodano, Italy) coupled with an Orbitrap Q-Exactive Plus (Thermo Scientific) was used. A reverse phase column was used for the separation of lipids (Hypersil Gold™ 150 × 2.1 mm, particle size 1.9 µm), the column was maintained at 45 °C at a flow rate of 0.260 mL/min. Mobile phase A for the ESI positive mode consisted of acetonitrile/water 60:40 (v/v) while B was isopropanol/acetonitrile 90:10 (v/v) both modified with ammonium formate (10 mM) and 0.1% formic acid while in the negative ESI mode the same organic solvents and same proportioning were used, except for the use of ammonium acetate (10 mM) as mobile-phase modifier instead of ammonium formate. The gradient used was as follows: 0–2 min from 30 to 43% B, 2–2.1 min from 43 to 55% B, 2.1–12 min from 55 to 65% B, 12–18 min from 65 to 85% B, 18–20 min from 85 to 100% B; 100% B was kept for 5 min and then the column was allowed to re-equilibrate at 30% B for another 5 min. The total run time was 30 min.

Mass spectrometry analysis was performed in both positive and negative ion mode. The source voltage was maintained at 3.5 kV in the positive ion mode and 2.8 kV in the negative ion mode. All other interface settings were identical for the two types of analysis. The capillary temperature, sheath gas flow, and auxiliary gas flow were set at 320 °C, 40 arb, and 3 arb respectively. S-lens was settled at 50 rf. Data were collected in a data-dependent (ddMS2) top 10 scan mode. Survey full-scan MS spectra (mass range m/z 80 to 1200) were acquired with resolution $R = 70{,}000$ and AGC target 1×106. MS/MS fragmentation was performed using high-energy c-trap dissociation (HCD) with resolution $R = 17{,}500$ and AGC target 1×105. The stepped normalized collision energy (NCE) was set to 15, 30, and 45, respectively. The injection volume was 3µL. Lockmass and regular inter-run calibrations were used for accurate mass-based analysis. An exclusion list for background ions was generated analysing the same procedural blank sample, both for the positive and negative ESI mode.

The acquired raw data from the untargeted analysis were processed using MSDIAL software (Yokohama City, Kanagawa, Japan), version 4.24. This included the detection of peaks, MS2 data deconvolution, compound identification, and the alignment of peaks through all the samples.

For identification a cut off value of 85% was selected: this value is based on 6 different similarity scores: 1 for retention time, 1 for m/z 1 for isotopic pattern, and 3 for MS/MS (dot product, dot product reversed and presence). The dataset containing m/z values, retention time, peak area, and annotation from the aligned files were exported as an Excel file and manually checked in order to eliminate signals from blanks or wrong records.

For quantification, the peak area for different detected molecular species for each particular lipid was combined (e.g., [M + NH4] + & [M + Na] + for TG) followed by normalization using the deuterated internal standard for each lipid class. In order to obtain an estimated concentration expressed in ug/mL the normalized areas were multiplied by the concentration of the internal standard. An in-house library of standards was also used for lipids identification. MetaboAnalyst 4.0 software (www.metaboanalyst.org) was used for statistical analysis [14].

Spheroid migration assay

96-well flat-bottomed plates were coated with 50ul/well of gelatin 0.1% (v/v) in sterile ddH2O. The plate was incubated at room temperature for 2 h; then the residual of gelatin was aspirated. The wells were washed twice with PBS and 100ul of 1% (w/v) BSA (Sigma Aldrich) in PBS was added for 1 h at room temperature. Residual BSA was aspirate and one single spheroid was plated in each well in 200ul of complete culture medium (RPMI-1640). The plate was then transferred for 30 min in the incubator to allow spheroids to adhere to the coated surface before imaging for the $t = 0$ time point. Pictures were analyzed using Image-Pro premier software and the migration capability was evaluated as the delta volume compared to the spheroid at T0.

FACS sorting

PaCa-44 cells were stained with Live/Dead fixable dye (1:1000; ThermoFisher) and anti-human EpCAM (1:100, BD, Franklin Lakes, NJ, USA) for 30 min at + 4 °C. After washed in MACS buffer, cells were FACS-sorted with a

MoFlo Astrios Cell Sorter (Beckman Coulter, Brea, CA); the purity of the sorted populations always exceeded 90%.

Lactate dehydrogenase (LDH) assay

To evaluate LDH enzyme activity the CyQUANT™ LDH cytotoxicity assay kit (Invitrogen, Thermo Fisher Scientific) was used according to the manufacturer's instructions. 50 µL of supernatant was collected from cells cultured in the different culture conditions (normal adhesion, spheroid at 1 g and simulated microgravity, SMG) at the end of each experiment and dispensed into a new 96-well plate (Thermo Fisher Scientific). LDH activity was quantified with Tecan Infinite F200Pro plate reader (Tecan, Austria) at 490 nm absorption.

Cell proliferation MTT assay

10^5 cells were seeded in 100ul of complete culture medium (RPMI-1640) in 96 well flat-bottomed plates. For proliferation analysis in PaCa-44 cells grown in adhesion culture condition, the cells were allowed to adhere to the plate o/n in the incubator. 10 µl of MTT solution (final concentration 0.5 mg/ml) was added to each well and the plate transferred for 4 h in the incubator. The reaction was then stopped adding 100 µl/well of solubilization solution (12 M HCl, isopropanol and TritonX 10%). After 15 min in the incubator, the absorbance of the samples was measured using a microplate reader at the wavelength of 570 nm. Results were presented as delta absorbance between the samples and the blank condition.

TUNEL assay

Apoptosis was evaluated using the In Situ Cell Death Detection Kit, Fluorescein (Roche, Lewes, UK) in the spheroids obtained in SMG. Spheroids were fixed in PFA 4%, embedded in Technovit 8100 resin (BioOptica, Milan, Italy) and sectioned. Sections were permeabilized with 0.1% Triton X-100 in 0.1% sodium citrate and exposed to TUNEL reaction mixture for 1 h at 37 °C, in a humidified atmosphere, protected from light. After PBS washes, sections were analyzed with AxioObserver Z2 inverted microscope (Zeiss), with Apotome2 system (Zeiss) and ZEN Blue 2.6 image acquisition software (Zeiss).

Western Blot analysis

After 9 days of maintenance in the different culture conditions (adhesion, spheroid at 1 g and simulated microgravity), cells were collected and lysed with RIPA buffer supplemented with protease and phosphatase inhibitors (PPC1010, Sigma-Aldrich, Milan, Italy). The protein concentration was determined using BCA protein assay (71,285, Sigma-Aldrich, Milan, Italy) and equal amounts of protein were loaded on NuPAGE™ 4–12% Bis–Tris protein precast polyacrylamide gels (Invitrogen, Thermo Fisher Scientific) in denaturing and reducing conditions. After transfection into nitrocellulose membranes (Perkin Elmer), membranes were saturated with 5% non-fat milk in TBS- 0.1% Tween 20 buffer, and hybridized overnight at 4 °C with the following primary anti-human antibodies: rabbit anti-N-cadherin (1:3000**,** Genetex, Irvine, CA), rabbit anti-E-cadherin (1:3000**,** Genetex), rabbit anti-NF-kB p50 (1:1000, Santa Cruz), rabbit anti-NF-kB p65 (1:1000, Santa Cruz), rabbit anti-phopsho-NF-kB p65 (Ser536, 1:1000, Cell Signaling, Boston, MD), mouse anti-Epcam (1:1000, Cell Signaling), mouse anti-GAPDH (1:1000, Santa Cruz), mouse anti-α-Tubulin (1:1000, Merckmillipore), mouse anti-β-Actin (1:1000, Cell Signaling), rabbit anti-LDHA (1:2000, Cell signaling) and mouse anti-Nanog (1:1000, Biorbyt, Cambridge, UK). Membranes were then washed and probed for 1 h at room temperature with HRP-conjugated secondary antibodies and developed using chemiluminescence reagents (SuperSignal™ West Pico PLUS Chemiluminescent Substrate, 34,580, Thermo Fisher Scientific). Membranes were scanned using a ChemiDoc™ XRS Imaging System (Bio-Rad, Hercules, CA) and bands were quantified using NIH Image J software (Version 1.53f51, National Institutes of Health (NIH), Bethesda, MA, USA).

RNA extraction and qRT-PCR

Total RNA was extracted, using TRIzol Reagent (Thermo Fisher Scientific), from PaCa-44 cells cultured under all the different culture conditions. 1 µg of RNA was reverse transcribed using first-strand cDNA synthesis. Real-time qPCR quantification was performed in triplicate samples by SYBR-Green detection chemistry with GoTaq qPCR Master Mix (Promega, Madison, WI, USA) with a QuantStudio 3 Real-Time PCR System (Thermo Fisher Scientific, USA). The primers used are listed in Table 1. The cycling conditions used were: 95 °C for 10 min, 40 cycles at 95 °C for 15 s, 60 °C for 1 min, 95 °C for 15 s, and 60 °C for 15 s. The average of the cycle threshold of each triplicate was analyzed according to the $2^{-\Delta\Delta Ct}$ method. 18S gene expression was used as endogenous control to standardize mRNA expression.

Statistical analysis

Values were expressed as mean ± s.e.m. Either one-way ANOVA or two-tailed, unpaired Student's *t*-test was used to compare unmatched groups with Gaussian distribution. A Mann–Whitney *U*-test was used in cases of non-Gaussian distribution. Two-way ANOVA corrected for multiple comparison tests was used to take into account multiple

Table 1 Sequences of primers used for qPCR analysis

GENES	FORWARD PRIMER SEQUENCE	REVERSE PRIMER SEQUENCE
CDH1	5′-GACACCAACGATAATCCTCCGA-3′	5’-GGCACCTGACCCTTGTACGT-3’
ZEB1	5′-GTTACCAGGGAGGAGCAGTGAAA-3′	5′-GACAGCAGTGTCTTGTTGTTGTAGAAA-3′
EpCAM	5'-CCGCTGCGAGGACGTAGA-3'	5'-TGTTGGCTGCGTCTCATCAAACC-3'
CASP 3	5’-CTGGTTTTCGGTGGGTGT-3’	5’-CACTGAGTTTTCAGTGTTCTCCA-3’
CASP 8	5’-CAGCAGCCTTGAAGGAAGTC-3’	5’-CGAGATTGTCATTACCCCACA-3’
CASP 9	5’-CCCAAGCTCTTTTTCATCCA-3’	5’-AGTGGAGGCCACCTCAAAC-3’
BAD	5’-ACCAGCAGCAGCCATCAT-3’	5’-GGTAGGAGCTGTGGCGACT-3’
TRAIL	5’-CCTCAGAGAGTAGCAGCTCACA-3’	5’-CAGAGCCTTTTCATTCTTGGA-3’
BAX	5’-CAAGACCAGGGTGGTTGG-3’	5’-CACTCCCGCCACAAAGAT-3’
N-CDH	5’-CCTCCAGAGTTTACTGCCATGAC-3’	5’-GTAGGATCTCCGCCACTGATTC-3’
OCT4	5′-GACAG GGGGAGGGGAGGAGCTAGG-3′	5′-CTTCCCTCCAACCAGTTGCCCCAAAC-3
NANOG	5′-AGTCCCAAAGGCAAACAACCCACTTC-3′	5′-TGCTGGAGGCTGAGGTATTTCTGTCTC-3′
SOX2	5′-GGGAAATGGGAGGGGTGCAAAAGAGG-3′	5′-TTGCGTGAGTGTGGATGGGATTGGTG-3′
18S	5’-ACTTTCGATGGTAGTCGCCGT-3’	5’-CCTTGGATGTGGTAGCCGTTT-3’
GAPDH	5′-ATCAGCAATGCCTCCTGCAC-3′	5′-TGGTCATGAGTCCTTCCACG-3′

comparisons. $P \leq 0.05$ was considered statistically significant. Statistical analyses were performed with GraphPad Prism v.7 GraphPad Software.

Results

Simulated microgravity alters the proteomic profile of PaCa-44 cells in a time-dependent manner

To investigate the effects of microgravity on PDAC, PaCa-44 cells were plated in complete medium in uncoated flasks and cultured at 1 g (as control, Adhesion) or in RPM (SMG); in parallel some cells were plated in spheroid-forming medium in u-bottom low adhesion 96 well-plates at 1 g (Spheroids 1 g, Fig. 1A). While in Adhesion the cells maintained their shape along all the evaluated time points, after 24 h (T1), both in 1 g spheroid-forming and SMG conditions, the cells underwent spontaneous aggregation forming small and loose tridimensional structures (Fig. 1A). These aggregates began to form spherical-like structures with a diameter around 100 µm that grew over 1 mm from the 7th to the 9th day (T7 and T9 respectively; Fig. 1A) in SMG, whereas in normal gravity they remained around 100 µm of diameter over time (Fig. 1A). When stained with Calcein-PI, spheroids obtained from SMG culture condition revealed an inner necrotic core of dead cells surrounded by vital cells accumulated in the outer layer (Fig. 1B). Similar results were obtained in other two pancreatic cancer cell lines, CFPAC-1 and AsPC-1, maintained in the same culture conditions: 9 days of SMG exposure was associated with a morphological rearrangement of the cells that grown as compact and large 3D spheres (Suppl. Fig S1, panel A and D).

To investigate the biological alterations induced by SMG exposure, PaCa-44 cells were cultured in RPM or in normal culture conditions (Adhesion 1 g, as control) in the same plastic supports, same medium, and at the same concentration (as detailed in the Methods section). At different time points (1, 7 and 9 days) a large proteomic analysis was performed with SWATH-MS using a statistical cut-off of p-value < 0.05 and fold change > 1.3. Results showed that 24 h of SMG induced the modulation of 360 proteins (206 up and 154 downregulated, compared to control culture condition). On the 7th day in SMG condition, cells upregulated 128 proteins and downregulated 111 (for a total of 239 proteins), whereas on the 9th day in SMG 335 proteins were modulated, of whom 208 upregulated and 127 downregulated.

The proteomic data set, including UniProt code and fold changes, was then uploaded to Ingenuity Pathway Analysis (IPA) bioinformatics tool, to identify the canonical pathways significantly modulated. After 24 h in SMG, 34 canonical pathways were upregulated (z-score > 0) and 21 downregulated (z-score < 0; Fig. 1C, T1 SMG); 10 pathways, instead, presented a modulation of protein expression but the final z-score was 0. After 7 days, 27 pathways were upregulated (z-score > 0), 18 downregulated (z-score < 0) and 5 presented z-score $= 0$ (Fig. 1C, T7 SMG). On the day 9 in SMG, 59 pathways were upregulated (z-score > 0), 14 downregulated (z-score < 0) and 6 presented a z-score $= 0$ (Fig. 1C, T9 SMG). Evaluating only the pathways enriched at all the three time points, we discovered that most of the upregulated pathways were involved in cell cytoskeletal modification such as *Integrin signaling*, *ILK signaling*, *Regulation of actin-based motility by Rho*, *RhoA signaling*, *Signaling by Rho Family GTPase* and *Actin cytoskeleton signaling* (Fig. 1D).

These results clearly support the effect of SMG in cellular reorganization.

Exposure to simulated microgravity is associated with cytoskeletal reorganization and increased migration capability

One of the protein pathways most altered by SMG exposure is the "*Regulation of actin-based motility by Rho*". RhoA signaling is involved in cytoskeleton reorganization, which induces actin migration toward the external plasma membrane where it participates in the formation of membrane blebs, thus promoting cell migration [15]. Proteomic analysis indicated a time-dependent upregulation of the pathway, from 24 h up to 9 days in SMG (Fig. 2A). Cdc42 signaling, which belongs to the Rho family of GTPase, contributes to the cytoskeletal organization throughout the perturbation of actin polymerization, as well as in the formation of actin bundle-containing filopodia at the cellular surface. Our results indicated that, as for RhoA, Cdc42 pathway was upregulated by SMG at all the 3 time points evaluated (Fig. 2B).

After 24 h in SMG, tubulin expression was upregulated (Fig. 2C); actin upregulation, instead, was evident only at longer exposure time, from 7 up to 9 days, when keratin's upregulation was massive (Fig. 2D, E). Interestingly, lamin A and B (LMNA and LMNB2, respectively), involved in oxidative stress resistance [16], were downregulated by SMG already after 24 h up to 9 days (Fig. 2C–E). In addition, 9 days of SMG exposure was associated with upregulation of E-cadherin (CDH1) and integrins (ITGA3, ITGB1 and ITGA6) that play a key role in cell adhesion to the extracellular matrix (substrate). In line, at the same time point (T9), we observed an increment of cell migration from the spheroidal structures to the flask where cells adhere to the surface (data not shown). The over time upregulation of keratins and integrins could be associated with increased cell aggregation and spheroid formation. Indeed, while after 24 h cells were mainly organized in weakened aggregates, after 7 days in SMG cells formed spheroidal structures already compact that progressively grew (up to 9 days) as demonstrated by blue toluidine staining (Fig. 2F). The spheroids appeared to be constituted by an outer shell of cells exhibiting extensive cell-to-cell adhesion, and an inner necrotic core (Fig. 2F). Such morphological changes are crucial for cell migration and metastatic potential. In line, "*Leukocytes extravasation signaling*" was altered in all the evaluated time points. Interestingly, on the 1st day in SMG the pathway was inhibited (Fig. 2G, T1 SMG) while after 7 days it was activated and remained active up to the 9th day (Fig. 2G). The upregulation of *"Actin-based motility by RhoA signaling"*, "*Leukocytes extravasation signaling*" and "*ILK signaling"* at all the analyzed time points (Fig. 2H) suggests the capability of PaCa-44 cells to adhere to the endothelium and migrate in SMG conditions. To confirm the impact of SMG on cell migration, we analyzed the expression levels of genes regulating the epithelial-to-mesenchymal transition (EMT) process at 1, 7 and 9 days of SMG exposure. EMT regulates morphological changes in tumor cells inducing the acquisition of a mesenchymal phenotype, rather than epithelial, thus supporting migration and spreading of cancer cells. qRT-PCR analysis indicated increased expression of N-cadherin (N-CDH), Vimentin and Zeb1 (mesenchymal markers), and matrix-metallopeptidase-7 (MMP-7) in PaCa-44 cells under SMG, particularly evident on the 9th day (Fig. 2I), compared to cells maintained in normal gravity adhesion condition. Modulation of E-cadherin (CDH-1) and N-CDH1 expression in PaCA-44 cells after 9 days of exposure to SMG was also confirmed by Western blot analysis (Fig. 2L). Similar results were obtained in CFPAC-1 and AsPC-1 cells: both lines showed downregulation of CDH-1 (Suppl. Fig. S1, panel B and E) and upregulation of Zeb-1 and N-CDH after 9 days in SMG (Suppl. Fig. S1, panel B, C, E, F). In addition, we performed a spheroid-migration assay comparing spheroids obtained from PaCa-44 cells maintained in SMG or spheroid-culture condition at 1 g (Spheroid 1 g) for 9 days. The results showed higher migration capability of tumor cells exposed to SMG (Fig. 2M) confirming the regulation of cell mobilization mediated by altered gravity.

Simulated microgravity triggers cancer stem cell selection

It has been largely demonstrated that the ability to form spheroids and migrate is related to the acquisition of a stemness phenotype. To further confirm that SMG exposure induces stemness enrichment, we evaluated the expression of specific stemness-related master genes (Nanog, Sox2 and Oct4) in PaCa-44 cells maintained in the different culture conditions. As shown in Fig. 3A, 9 days in SMG induced a significantly increased expression of all the evaluated genes. These results suggest a key role of microgravity in time-dependent stemness regulation. In support, proteomic analysis indicated that IL-8 signaling, which is involved in stemness, neo-angiogenesis and EMT process regulation [17], was upregulated after 9 days in SMG (Fig. 3B). ERK5 signaling, instead, was upregulated already after 24 h in SMG (Fig. 3C). Interestingly, it has been reported that the activation of ERK5 pathway triggers the upregulation of IL-8 signaling and NF-κB transcriptional activity, suggesting an ERK5/NF-κB/IL-8 signaling axis involved in the regulation of stem cell malignancy [18]. Proteomic analysis indicated that NF-κB signaling was upregulated on the 9th day in SMG (whereas after 1 and 7 days in SMG the pathway has a z -score = 0; Fig. 3D). In line, western blot evaluation of p50 and p65 NF-kB family members in PaCa-44

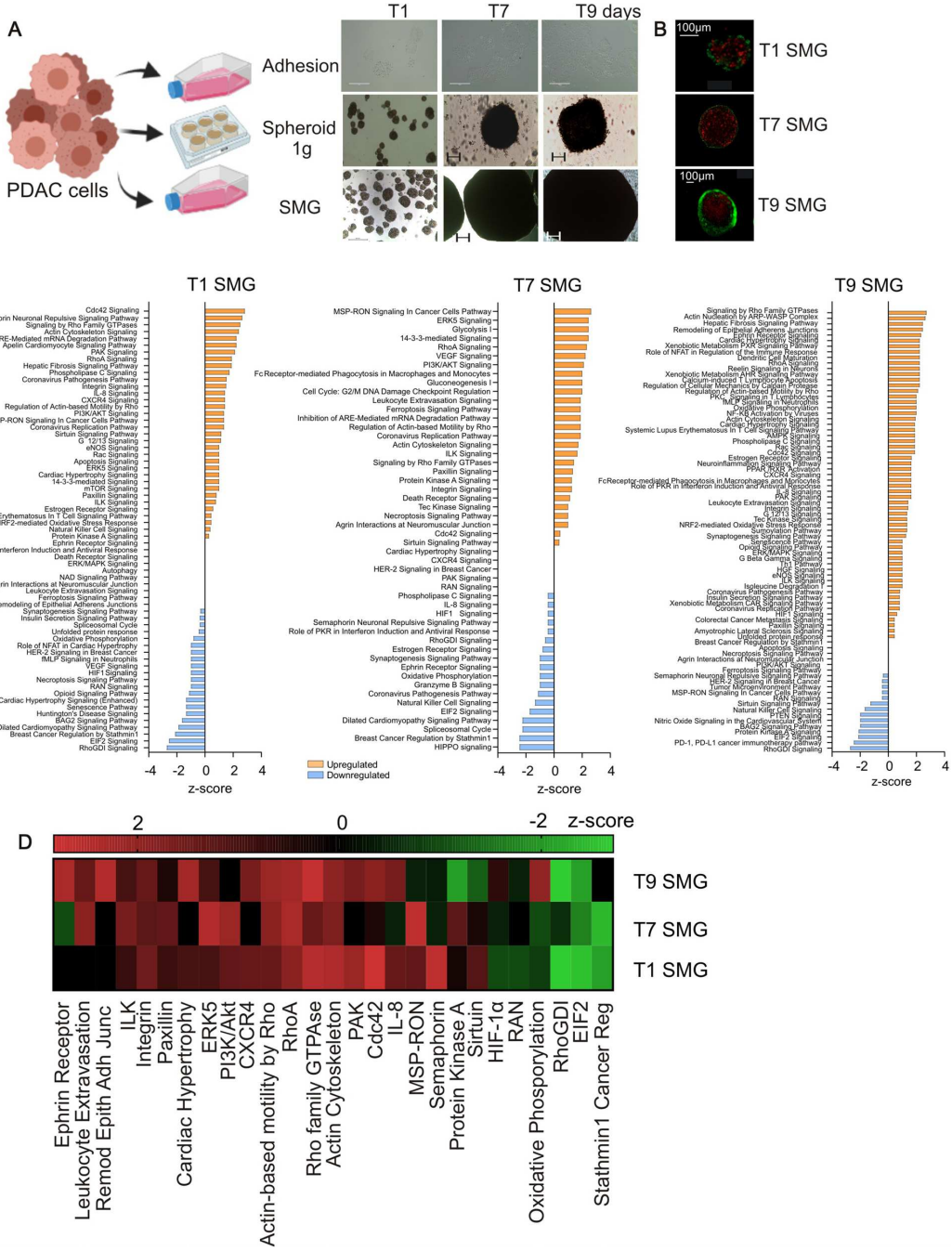
A
PDAC cells
T1
T7
T9 days
Adhesion
Spheroid 1g
SMG
B
100µm
T1 SMG
T7 SMG
T9 SMG
C
T1 SMG
T7 SMG
T9 SMG
z-score
Upregulated
Downregulated
D
2
0
-2 z-score
T9 SMG
T7 SMG
T1 SMG
Ephrin Receptor
Leukocyte Extravasation
Remod Epith Adh Junc
ILK
Integrin
Paxillin
Cardiac Hypertrophy
ERK5
PI3K/Akt
CXCR4
Actin-based motility by Rho
RhoA
Rho family GTPAse
Actin Cytoskeleton
PAK
Cdc42
IL-8
MSP-RON
Semaphorin
Protein Kinase A
Sirtuin
HIF-1α
RAN
Oxidative Phosporylation
RhoGDI
EIF2
Stathmin1 Cancer Reg

◂**Fig. 1** Simulated microgravity (SMG) alters the proteomic profile of PaCa-44 cells in a time-dependent manner. **A** PaCa-44 cells were cultured in adhesion condition at 1 g (Adhesion) or in SMG, and in spheroid-forming culture condition at normal gravity (Spheroid 1 g). Representative pictures acquired at 1, 7 and 9 days of culture (T1, T7 and T9, respectively); scale bar 400 µm for Adhesion, 200 µm for Spheroids 1 g and SMG pictures. **B** Calcein/PI staining on spheroids obtained after 1, 7 and 9 days in SMG culture conditions (T1, T7 and T9 SMG, respectively). Scale bar 100 µm. **C** Canonical pathways modulated by differentially expressed proteins after 1, 7 or 9 days of SMG (T1, T7 and T9 SMG respectively). The pathways are indicated in the y-axis. On the x-axis, the z-score for each pathway calculated in comparison to the adhesion culture condition. Orange bars predict an overall increase in the pathway activity, while blue bars predict a decrease. **D** Heat-map of z-score of the canonical pathways modulated in all of the three different time points presented in panel C (1, 7 and 9 days in SMG)

cells showed an evident induction of p65 expression and a concomitant inhibition of p50 expression after 9 days SMG, compared to cells maintained in normal adhesion culture condition (Adhesion) or spheroid-forming culture condition (Suppl. Fig. S2).

At this time point (T9) stemness-related proteins such as EpCAM, ALDH1A3, ALDHA3A2, S100A4, ROHA, and ITGA3 (Fig. 3F) were upregulated, indicating a cellular reprogramming towards a more stem and aggressive phenotype. It has been demonstrated [19] that EpCAM is a reliable marker for the identification of CSCs in various tumor types including pancreatic cancer. Indeed, when PaCa-44 cells were FACS sorted according to the expression of EpCAM, we observed a significantly higher expression of stemness-associated master genes (Nanog, Sox2 and Oct4) in $EpCAM^{pos}$ compared to $EpCAM^{neg}$ cells (Fig. 3G). Analysis of expression levels of EpCAM in PaCa-44 cells subjected to SMG indicated an over time increase of this marker, supporting our findings of a CSC enrichment mediated by altered gravity force (Fig. 3H).

Simulated microgravity strongly edits cell metabolism

The morphological rearrangement (3D spheroids) induced by SMG also affected cellular nutrition and metabolism. From the proteomic analysis, it has emerged that eIF2 signaling was the most enriched pathway modulated by SMG (Fig. 4A-C). Compared to the control, the pathway was inhibited already after 24 h (Fig. 4A) and it was maintained downregulated up to 9 days in SMG (Fig. 4B, C). eIF2 is a component of the translational machinery and plays a key role in the orchestration of protein synthesis. Repression of global protein synthesis (as in the case of eIF2 signaling inhibition) allows cells to conserve nutrients and energy for stress remediation. Indeed, it has been demonstrated that eIF2 signaling regulates autophagy and metabolism in order to maintain an energy balance in cancer cells. In line, our proteomic data revealed that glycolysis was downregulated after 24 h in SMG (as indicated by negative logFC of SLC2A1, LDH and ENO1; Fig. 4D, T1 SMG), but after 7 days was upregulated (positive logFC of ENO1, GAPDH, ALDOA, PGAM1, TPI1 and PKMI proteins; Fig. 4D, T7 SMG). The pathway remained upregulated on the 9th day (positive logFC of LDHA, GAPDH, PKM and SLC2A1 proteins; Fig. 4D, T9 SMG). In parallel, the analysis of extracellular lactate dehydrogenase (LDH) indicated a reduction of LDH levels after 1 day in SMG (compared to normal adhesion culture condition) and an increase on the 7th and 9th day in SMG (Fig. 4E) suggesting a metabolic switch of PaCa-44 cells under reduced gravity culture condition. Similar results were obtained in CFPAC-1 and AsPC-1 cells exposed to SMG. After 9 days both cell lines presented an upregulation of GAPDH and LDHA at mRNA and protein level compared to the same cells maintained in normal adhesion or spheroid-forming culturing condition in normal gravity (Suppl. Fig. S1, panel B, C, E and F).

HIF-1α, is a key regulator of cancer-related metabolic pathways, including glycolysis, gluconeogenesis, the Tricarboxylic acid (TCA) cycle, as well as metabolism of nucleotides, amino acids and lipids. According to oxygen availability, HIF-1α dynamically regulates glucose metabolism in order to reduce reactive oxygen species (ROS) accumulation, maintain redox homeostasis and sustain cell survival. Proteomic analysis indicated an inhibition of the HIF-1α signaling at 24 h and 7 days in SMG (Fig. 4F); at 9 days instead, the pathway was upregulated, in line with the over time increased dimension (and necrotic core) of spheroids. HIF activation regulates the fate of pyruvate produced by glycolysis, triggering the production of Acetyl-CoA to provide cells with substrates involved in the membrane biogenesis, orchestrated by fatty acid (FA) and phospholipids synthesis, energy production by TCA cycle and post-translational modification, such as protein acetylation. To better clarify the alteration in lipid catabolism and synthesis, lipidomic analysis was performed at the three time points of SMG exposure. 447 lipids belonging to 18 different lipid classes were identified in PaCa-44 cells (Fig. 4G), with Triacylglycerols (TGs) as the most abundant lipid class. Monoacylglycerols were not identified whereas only few diacylglycerols were detected, most likely for their re-esterification in TGs (Jones et al., 2019). The hierarchical clustering heat-map analysis (Fig. 4H) highlighted specific SMG-induced lipidomic profiles for each time point. Total TG levels decreased at 1 and 7 days in SMG, while increased at 9 days (Fig. 4I). On the contrary, both total lysophosphatidylcholines (LPCs), lysophosphatidylethanolamine (LPEs) and polyunsaturated FAs increased at 1 and 7 days in SMG to then shrank at 9 days (Fig. 4I). Interestingly, almost all the modulated FAs (FA 20:3, FA 20:4, FA 20:5, FA22:5 and FA 22:6) were polyunsaturated (Fig. 4L) that

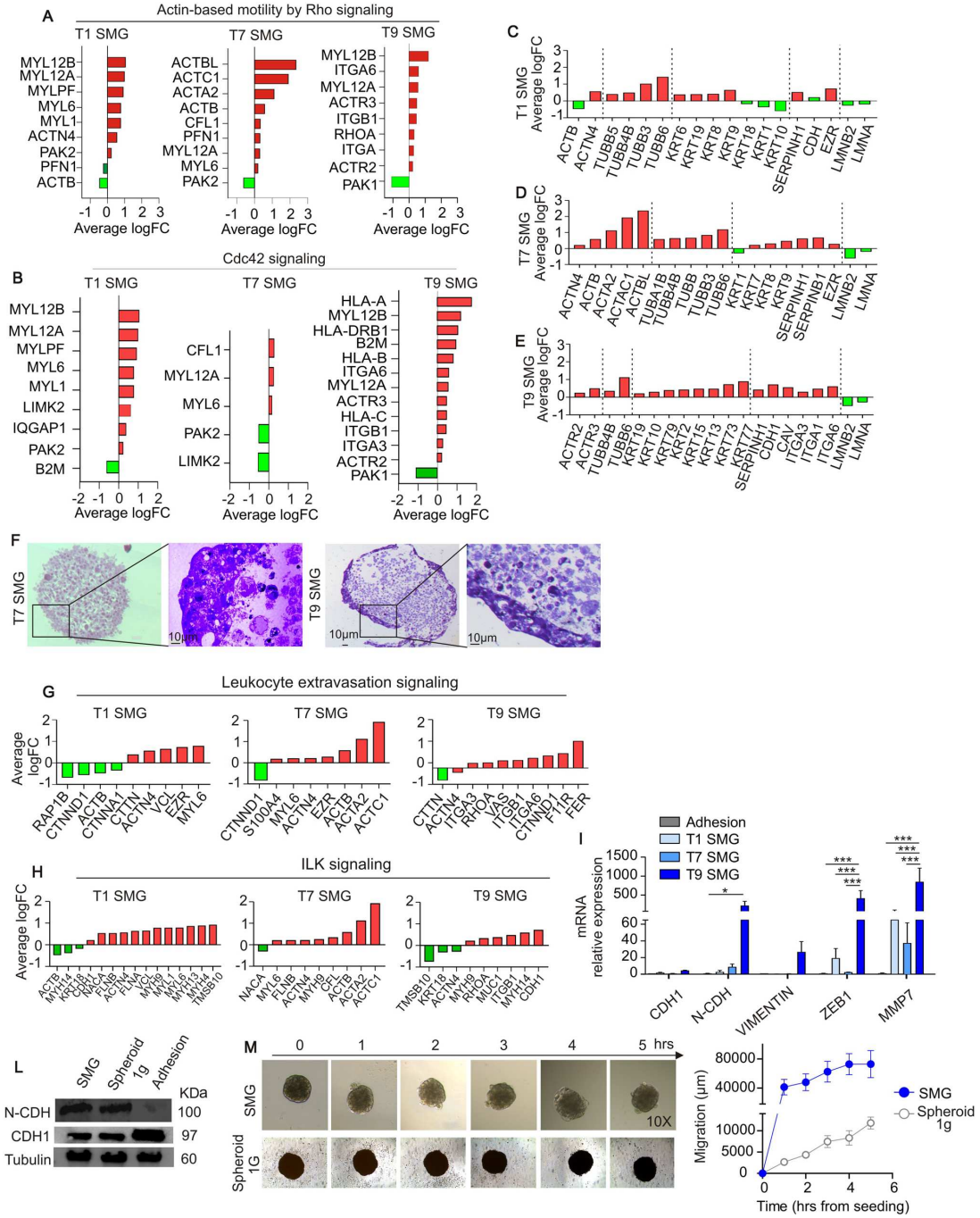
A
Actin-based motility by Rho signaling
T1 SMG
T7 SMG
T9 SMG
MYL12B
MYL12A
MYLPF
MYL6
MYL1
ACTN4
PAK2
PFN1
ACTB
ACTBL
ACTC1
ACTA2
CFL1
MYL12A
ITGB1
RHOA
ITGA
ACTR2
PAK1
Average logFC
B
Cdc42 signaling
LIMK2
IQGAP1
B2M
HLA-A
HLA-DRB1
HLA-B
HLA-C
C
D
E
T1 SMG Average logFC
T7 SMG Average logFC
T9 SMG Average logFC
F
10µm
G
Leukocyte extravasation signaling
Average logFC
H
ILK signaling
I
Adhesion
mRNA relative expression
CDH1
N-CDH
VIMENTIN
ZEB1
MMP7
L
SMG
Spheroid 1g
Adhesion
KDa
N-CDH
CDH1
Tubulin
100
97
60
M
0 1 2 3 4 5 hrs
10X
Migration (µm)
Time (hrs from seeding)

◂**Fig. 2** Exposure to simulated microgravity (SMG) is associated with cytoskeletal reorganization and increased migration capability. **A–B** Average logarithmic fold change of proteins involved in the Actin-based motility by Rho signaling (**A**) and Cdc42 signaling (B) evaluated in PaCa-44 cells maintained in SMG for 1, 7 or 9 days (T1, T7 and T9 SMG, respectively); in green proteins downregulated while in red proteins upregulated compared to adhesion culture conditions. **C–E** Average logarithmic fold change of proteins involved in the cytoskeletal and nuclear reorganization, evaluated in PaCa-44 cells maintained in SMG for 1 (**C**), 7 (**D**) or 9 (**E**) days; in green proteins downregulated while in red proteins upregulated compared to adhesion culture conditions at 1 g. **F** Representative pictures of Toluidine blue staining in semithin sections of spheroids obtained after 7 or 9 days in simulated microgravity (SMG); scale bar 10 µm. **G–H** Average logarithmic fold change of proteins involved in the leukocyte extravasation (**G**) and ILK (**H**) signaling evaluated in PaCa-44 cells maintained in SMG for 1 (**A**), 7 (**B**) or 9 (**C**) days (T1, T7 and T9 SMG, respectively); in green proteins downregulated while in red proteins upregulated compared to adhesion culture conditions. **I** qRT-PCR analysis of EMT-associated markers in PaCa-44 cells maintained in normal culture condition (Adhesion) or in simulated microgravity (SMG) for 1, 7 or 9 days (T1, T7 and T9 SMG, respectively). Data are expressed as mean ± sem of n = 3 replicates. *0.05, ***0.0002 and **** < 0.0001. **L** Western blot analysis of CDH-1 and N-CDH1 on PaCa-44 cells maintained in normal culture condition (Adhesion), spheroid-forming condition at 1 g (Spheroid 1 g) or in simulated microgravity (SMG) for 9 days; Tubulin is used as housekeeping. **M** Migration capability of spheroids collected on the 9th day from SMG culture or 1 g spheroid culture (Spheroid 1 g). On the left representative pictures of spheres at the different time points after seeding; on the right the graph with the mean ± sem migration calculated as spheres' circumference at each time point compared to T0 (Delta)

may potentially be used as signaling molecules or as substrates for obtaining energy through β-oxidation. Concomitantly, the lysophospholipids increase, at 7 days, may sustain a deep membrane phospholipid remodeling as revealed by the increment of TGs together with the reduction of LPCs, LPsE and FAs (on the 9th day). These results suggest the synthesis of novel TGs and phosphatidylcholines (PCs) at prolonged exposure to SMG (9 days), probably to sustain the request of membrane lipids. In particular, we observed an increase of PC 18:1_20:4; PC 18:0_20:4, PC O-18:1_20:4 and PE 16:0_18:0 (Fig. 4M), supporting the hypothesis of a remodeling of the cellular membrane. Furthermore, at the same time point (9 days) the marked TG increase may be explained with their packaging into lipid droplets, which have been shown to accumulate in hypoxic conditions and to be associated with higher tumor aggressiveness [20].

Concerning polyunsaturated FAs including arachidonic acid (FA 20:4) released on the 9th day, we speculate a role for arachidonic acid and its bioactive derivatives in inflammation and in local signaling of CSCs. Indeed, the high degree of unsaturation makes these metabolites reactive and susceptible to oxygenation and hydrogenation reactions, suggesting metabolic flexibility that allows cells to adapt their metabolism to survive in hostile conditions, typical of CSCs [21]. Moreover, we investigated whether free FAs may be coupled with CoA to form acyl-CoA moieties that are then transferred to carnitine to generate acylcarnitine, which subsequently enters the mitochondrial matrix via the carnitine shuttle [22]. In order to understand if there is an impairment of the β-oxidation over time, we focused our attention on the acylcarnitine class. The acylcarnitine to L-carnitine ratio is recognized as a marker of carnitine deficiency and is associated with mitochondrial β-oxidation [23]. In addition, the trend of this ratio is also maintained between long-intermediate-chain acylcarnitines (C16-20) compared to short-chain ones (C4). Our data showed an increased (C16-20)/(C4) ratio over time, suggesting an impairment of the β-oxidation (Fig. 4N) [24].

At 9 days of SMG exposure, we observed upregulation of several proteins involved in metabolic-related pathways such as autophagy (LAMP1, SQSTM1), mitochondrial activity (ATP5B, ATP5A1, ATP5P0, VDAC2, ATP6V1A, COX4I1, HSD17B10, HADHA, PRDX5), TCA cycle (DLST) and Pentose phosphate pathway (PGLS, Fig. 5A). Other pathways are involved in the glucose fate decision, including the phosphatidylinositol-3-kinase/Akt (PI3k/Akt) pathway, which is also a key regulator of apoptosis and cell proliferation. In our setting, we observed upregulation of PI3K/Akt signaling already on the 1st and the 7th day of exposure to SMG (Fig. 5B). Interestingly, after 9 days in SMG the pathway was downregulated (Fig. 5B, T9 SMG). These results, together with the upregulation of proteins involved in autophagy, suggest the cell capability of activating alternative survival mechanisms. The crosstalk between apoptosis, which invariably leads to cell death, and autophagy, which has pro-survival functions is complex. To clarify this aspect, we evaluated, at the different time points of SMG exposure, key genes of the apoptotic signaling. qRT-PCR analysis indicated a higher expression after 9 days of all the pro-apoptotic genes evaluated (i.e. Caspase 9,8,3, Bax, Bad and Trail, Fig. 5C). Tunel staining on spheroids collected on the 9th day in SMG showed apoptotic signals on the outer membrane of the structure (Fig. 5D) suggesting an external layer of apoptotic cells. Accordingly, MTT assay demonstrated a lower signal on cells maintained for 9 days in spheroid-forming culture condition both at 1 g and in SMG, compared to adhesion condition (Fig. 5E).

Discussion

Understanding the impact of altered gravity on tumor cells represents the starting point for the development of novel anti-cancer therapies. We evaluated the impact of SMG to PDAC cells (PaCa-44) performing a comprehensive proteomic, lipidomic and transcriptomic analysis at different time points (1, 7 and 9 days); the major results have been confirmed in other two PDAC cell lines: CFPAC-1 and

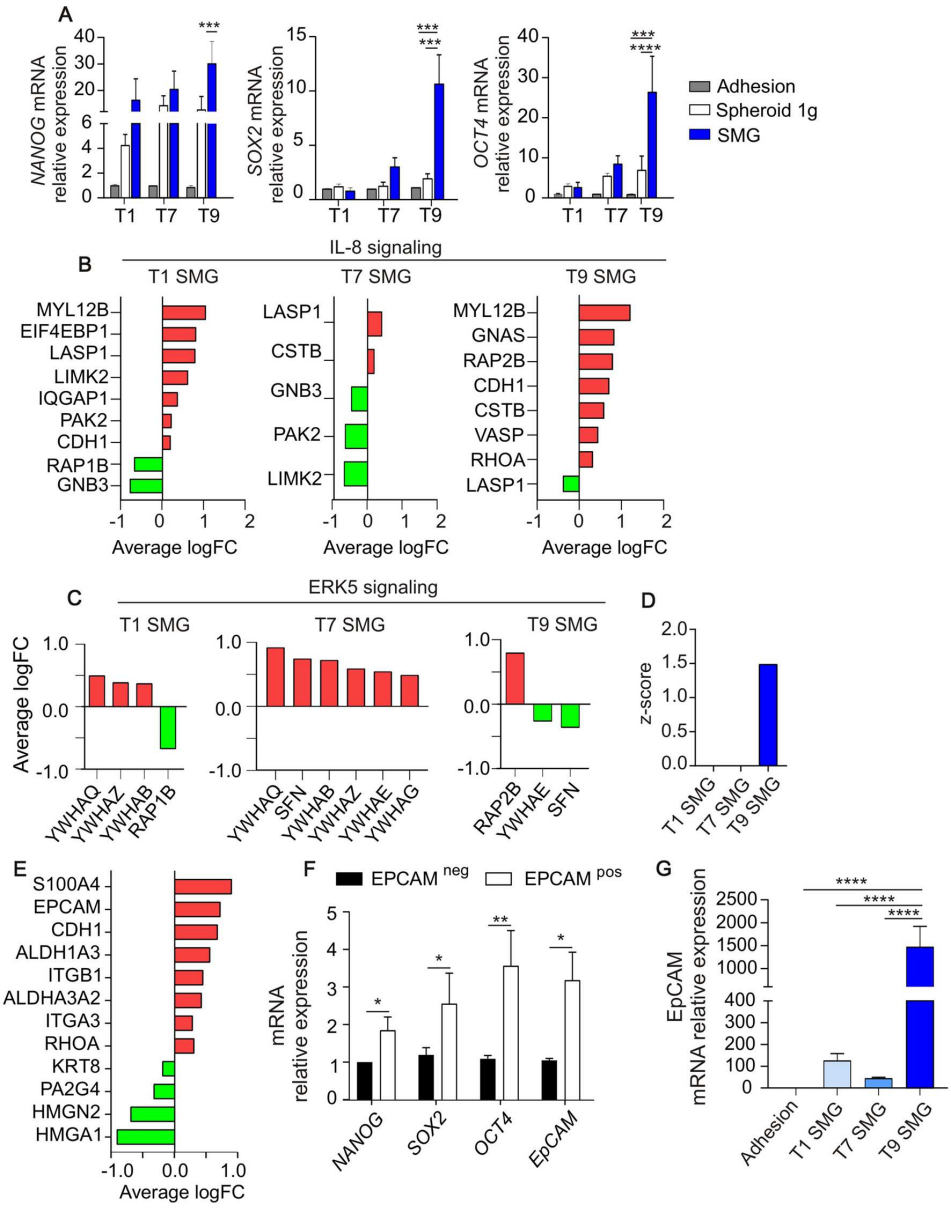

Fig. 3 Simulated microgravity (SMG) triggers cancer stem cell selection. **A** qRT-PCR analysis of stemness-associated genes in PaCa-44 cells maintained in adhesion culture condition at normal gravity (Adhesion), altered gravity (SMG), or in spheroid-forming culture condition at normal gravity (Spheroid 1 g) for 1, 7 or 9 days. Data are expressed as mean ± sem of n = 3 replicates. * 0.05, ***0.0002 and **** < 0.0001. **B–C** Average logarithmic fold change of proteins involved in IL-8 (**B**) and ERK5 signalings (**C**) evaluated in PaCa-44 cells maintained in SMG for 1, 7 or 9 days (T1, T7 and T9 SMG, respectively); in green proteins downregulated while in red proteins upregulated, compared to adhesion culture conditions. **D** Z-score of NF-κB pathway evaluated in PaCa-44 cells exposed to SMG for 1, 7 or 9 days. **E** Average logarithmic fold change of proteins related to stemness and epithelial-to-mesenchymal transition signaling in PaCa-44 cells maintained in SMG for 9 days. **F** qRT-PCR analysis of stemness genes in PaCa-44 cells grown in normal culture condition and FACS separated according to the expression of EpCAM. **G** qRT-PCR analysis of EpCAM expression in PaCa-44 cells maintained in Adhesion culture condition at 1 g or in SMG for 1, 7 or 9 days (T1, T7 and T9 SMG, respectively). Data are expressed as mean ± sem of n = 3 replicates. *0.05; **** < 0.0001

AsPC-1. Our aim was to elucidate the time-dependent modification induced by the alteration of the gravity force. Our data clearly indicated that SMG impacts in a time-dependent manner on the structural, metabolic and migratory profile of tumor cells selecting an aggressive subset endowed with stem-like features.

Dissecting cell alterations induced by SMG, we speculate that in the first 24 h, to survive SMG exposure, cells collect energy in form of ATP activating the degradation of long FAs through β-oxidation in the peroxisome. This is suggested by acylcarnitine decrease and consequent impairment of mitochondrial β-oxidation together with the upregulation of acyl-CoA dehydrogenase very long (ACADV). Altogether these observations, and the fact that FAs may enter the peroxisome via ABC carrier system rather than the carnitine shuttle, suggest that there is involvement of peroxisomes in very long FA degradation rather than the classical mitochondrial β-oxidation pathway in the early days of SMG exposure. In this way, the acetyl-CoA produced by peroxisomes is used by the mitochondrial TCA cycle to support energy consumption due to cell respiration. Indeed, at this time point, the spheroids present small dimensions and are mainly composed of aggregated cells. The upregulation at 1 day of RhoA and Cdc42 signaling contributes to dynamic actin rearrangements required for cell migration which became more evident at longer time points of SMG exposure. Indeed, Cdc42 promotes cell protrusion with formation of a leading edge where a localized actin polymerization moves forward to the membrane in filopodia and lamellipodia, generating the locomotive force. On the other hand, RhoA regulates the assembly of actomyosin filaments whose contractile force induces the retraction of the cell tail [25]. The prolonged exposure (7 days) to SMG triggers actin upregulation, cytoskeleton rearrangement and deep cellular metabolic alterations to overcome the hypoxic-core formation within the spheroidal structure. Cells upregulate glycolytic enzymes (GAPDH, ENO and PKM) in order to use glucose as energy substrate in an anaerobic manner (Fig. 6). The cellular machinery is involved in the synthesis of new phospholipids (as indicated by the increase in total LPCs, LPEs and in particular species of PCs and PEs) and FAs, to sustain the formation of novel membrane lipids. We observed an increase in total FAs, comprising arachidonic acid. It has been demonstrated that PI3K/mTOR/PKC axis induces calcium-dependent phospholipase A2 (cPLA2) involved in the release of arachidonic acid, oleic acid (FA 18:1) and other bioactive lipids (such as eicosanoids) [26]. Remarkably, arachidonic acid and derived eicosanoids may have a role in CSC proliferation and be involved in the aggressive phenotype of CSCs [27, 28]. However, both the pathways sustaining stemness (i.e. IL-8 and NF-κB) and the CSC markers are not upregulated. Only at a longer time point, the selection of a stem-enriched and more aggressive subset of cells is significant. Indeed, after 9 days of SMG exposure we observed upregulation of IL-8 and NF-κB pathways that promoted expression of cell adhesion molecules and proteins involved in the invasion process (e.g. matrix metalloproteinases), characteristic of cancer stemness [29]. Moreover, NF-κB is an upstream modulator of cyclooxygenase-2 (COX-2) acting as a procarcinogenic enzyme. COX-2 can promote tumor growth and progression activating mechanisms including immune evasion and increased invasiveness through EMT processes [29]. Indeed, on the 9th day we observed higher expression of all the evaluated mesenchymal markers and higher cell migration capability, suggesting the complete transformation towards a more stem and aggressive phenotype induced by SMG exposure, as indicated also by upregulation of EpCAM and other stemness-associated markers (Nanog, Sox2 and Oct4). NF-kB regulation is integrated in a very complex network of molecular and metabolic pathways [30, 31]. Indeed, CSCs are endowed with a more active glycolysis that leads to a higher pyruvate production, which in turn fuels ATP synthesis involved in the regulation of metastasizing and aggressiveness. In line, 9 days after SMG exposure, cells undergo a profound membrane remodeling through the synthesis of PCs from LPCs and FAs. It has been shown that PCs work as oncogenic signals [32] triggering cell proliferation and tumor growth. At this time point, we observed a reduction

Fig. 4 Simulated microgravity (SMG) exposure edits tumor cell metabolism. **A–C** Heat map of eiF2-related protein fold change expression, evaluated in PaCa-44 cells maintained in SMG for 1 (**A**), 7 (**B**) or 9 (**C**) days; **D** Average logarithmic fold change of proteins involved in glycolysis evaluated in PaCa-44 cells maintained in SMG for 1, 7 or 9 days; in green proteins downregulated while in red proteins upregulated compared to adhesion culture conditions. **E** Extracellular levels of LDH evaluated at 1, 7 and 9 days (T1, T7 and T9, respectively) in PaCa-44 cells maintained in adhesion or spheroid-forming culture condition at normal gravity (Adhesion or Spheroid 1 g, respectively) and in SMG. **F** Average logarithmic fold change of proteins involved in HIF-1α signaling evaluated in PaCa-44 cells maintained in SMG for 1, 7 or 9 days; in green proteins downregulated while in red proteins upregulated compared to adhesion culture conditions. **G** Donut chart of the number of identified lipids for each class. **H** Hierarchical clustering heat-map of lipid expression evaluated in PaCa-44 cells maintained in Adhesion culture condition at 1 g or in SMG for 1, 7 or 9 days. **I** Total lipid concentration for triacylglycerols (TGs), lysophosphatidylcholine (LPCs), lysophosphatidylethanolamine (LPEs) and fatty acids (FAs) evaluated in PaCa-44 cells maintained in Adhesion culture condition at 1 g or in SMG for 1, 7 or 9 days. **J–K** Lipid concentration of unsaturated fatty acids (Fas, D), phosphatidylcholines (PC) and phosphatidylethanolamines (PE, E) evaluated in PaCa-44 cells maintained in Adhesion culture condition at 1 g or in SMG. **L** Ratio of long-intermediate-chain acylcarnitines (C16-C20) to short-chain ones (C4) evaluated in PaCa-44 cells maintained in Adhesion culture condition at 1 g or in SMG for 1, 7 or 9 days. All data are expressed as mean ± sd of 3 different replicates. * 0.05, ** < 0.005; *** < 0.0005. For all the panels T1, T7 and T9 represent 1, 7 or 9 days in simulated microgravity (SMG, respectively)

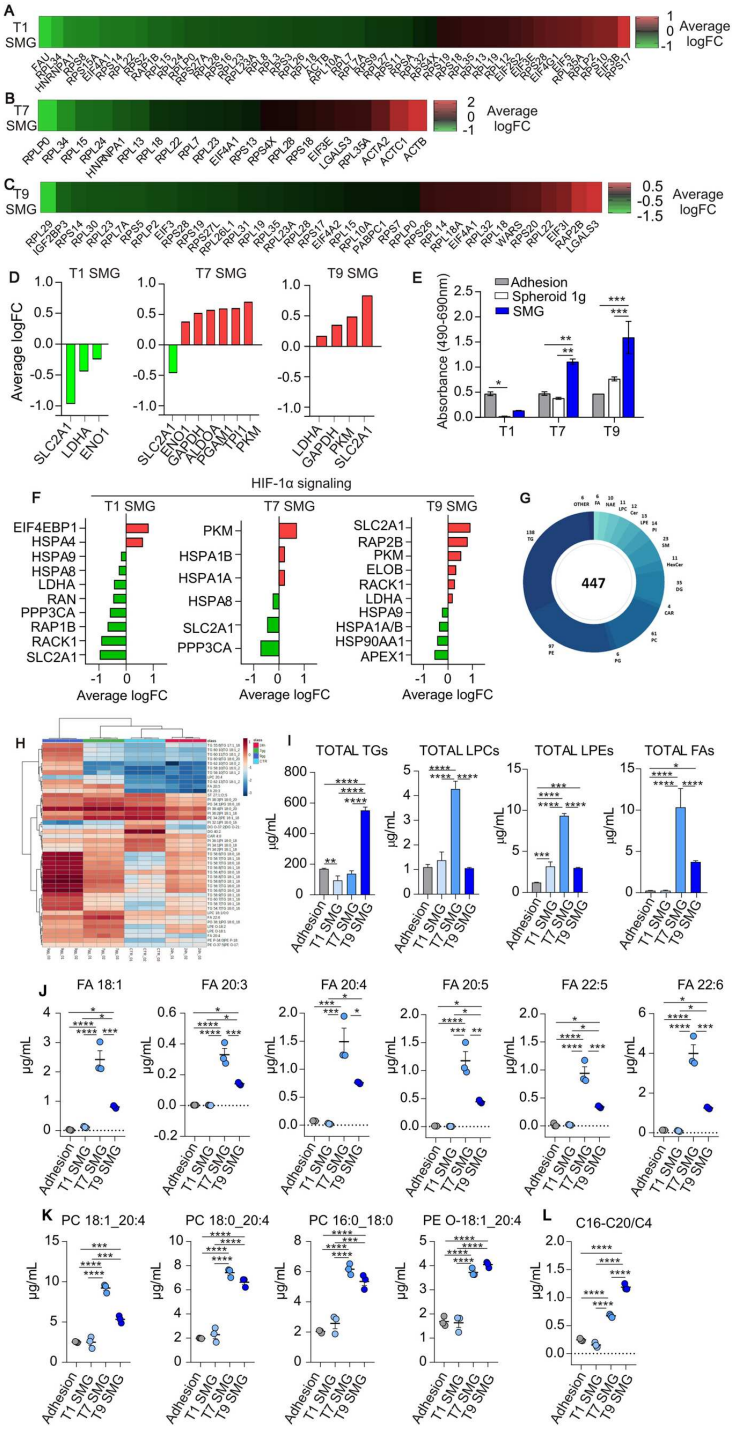
A
T1 SMG
Average logFC
B
T7 SMG
Average logFC
C
T9 SMG
Average logFC
D
T1 SMG
T7 SMG
T9 SMG
Average logFC
SLC2A1
LDHA
ENO1
GAPDH
ALDOA
PGAM1
TPI1
PKM
E
Adhesion
Spheroid 1g
SMG
Absorbance (490-690nm)
T1
T7
T9
F
HIF-1α signaling
T1 SMG
T7 SMG
T9 SMG
EIF4EBP1
HSPA4
HSPA9
HSPA8
LDHA
RAN
PPP3CA
RAP1B
RACK1
SLC2A1
PKM
HSPA1B
HSPA1A
HSPA8
SLC2A1
PPP3CA
SLC2A1
RAP2B
PKM
ELOB
RACK1
LDHA
HSPA9
HSPA1A/B
HSP90AA1
APEX1
Average logFC
G
447
H
I
TOTAL TGs
TOTAL LPCs
TOTAL LPEs
TOTAL FAs
µg/mL
Adhesion
T1 SMG
T7 SMG
T9 SMG
J
FA 18:1
FA 20:3
FA 20:4
FA 20:5
FA 22:5
FA 22:6
K
PC 18:1_20:4
PC 18:0_20:4
PC 16:0_18:0
PE O-18:1_20:4
L
C16-C20/C4

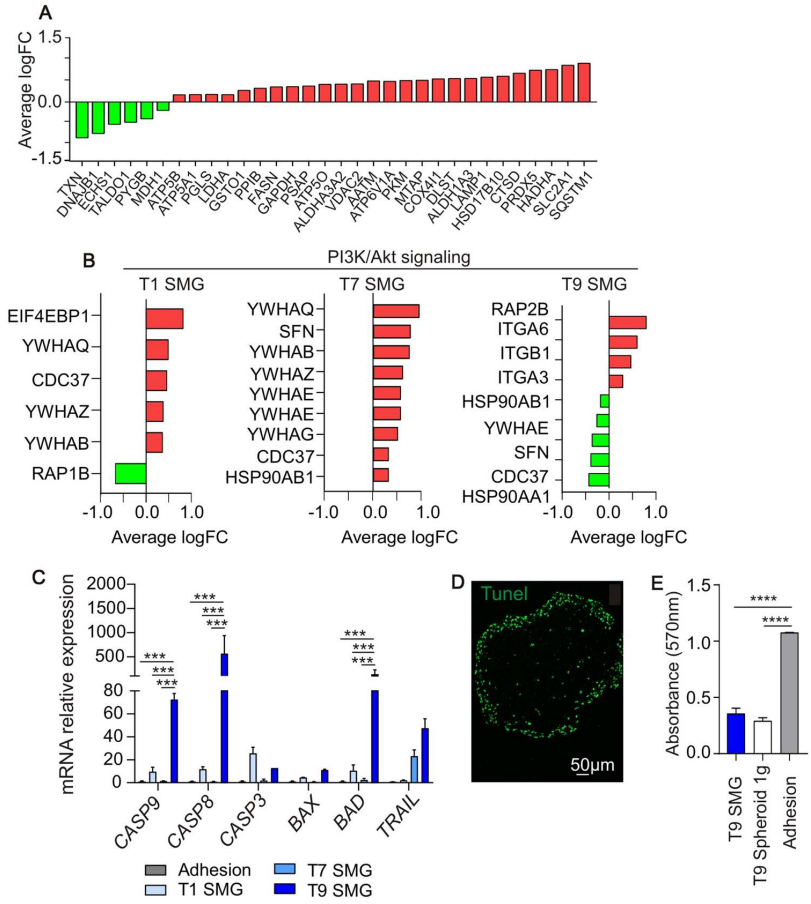

Fig. 5 Simulated microgravity-mediated tumor cell reprogramming. **A** Average logarithmic fold change of proteins involved in metabolic-related pathways evaluated in PaCa-44 cells maintained in SMG for 9 days; in green proteins downregulated while in red proteins upregulated compared to adhesion culture conditions. **B** Average logarithmic fold change of proteins involved in PI3K/Akt signaling evaluated in PaCa-44 cells maintained in SMG for 1, 7 or 9 days (T1, T7 and T9 SMG, respectively); in green proteins downregulated while in red proteins upregulated compared to adhesion culture conditions. **C** qRT-PCR analysis of pro and anti-apoptotic genes in PaCa-44 cells maintained in normal culture condition (Adhesion) or in SMG for 1, 7 or 9 days (T1, T7 and T9 SMG, respectively). Data are expressed as mean ± sem of n = 3 replicates. *0.05; ***0.0002; **** < 0.0001. **D** One representative picture of immunofluorescence analysis for apoptosis (Tunel expression) on spheroids obtained on the 9th day in SMG. Scale bar 50 µm. **E** MTT assay in PaCa-44 cells maintained in normal adhesion culture condition (Adhesion), spheroid-forming condition (T9 Spheroid 1 g) or SMG (T9 SMG) for 9 days. Data are expressed as mean ± sem of $n = 6$ replicates

in total LPCs and LPEs as well as FsA. The LPCs produced at 7 days could be used together with neosynthesized FAs (such as palmitate) as supported by FASN upregulation and ECHS1 downregulation. In addition, to synthetize FAs, cells could use acetyl-CoA produced by glycolysis (GLUT1 and the other glycolytic enzyme are upregulated at this time point) and by glutamine metabolism (upregulation of SLC1A5). The surplus of pyruvate produced by glycolysis is extruded from the cells through LDHA transporter in the form of lactate favoring the acidification of the extracellular milieu, supporting the aggressive and migratory phenotype of the cells. Moreover, enhanced glucose uptake may also sustain the production of NADPH by the pentose phosphate pathway, a glycolytic flux shunt, as indicated by upregulation of PGLS. In turn, NADPH is the essential coenzyme for FAs neosynthesis and consequent formation of TGs, which may

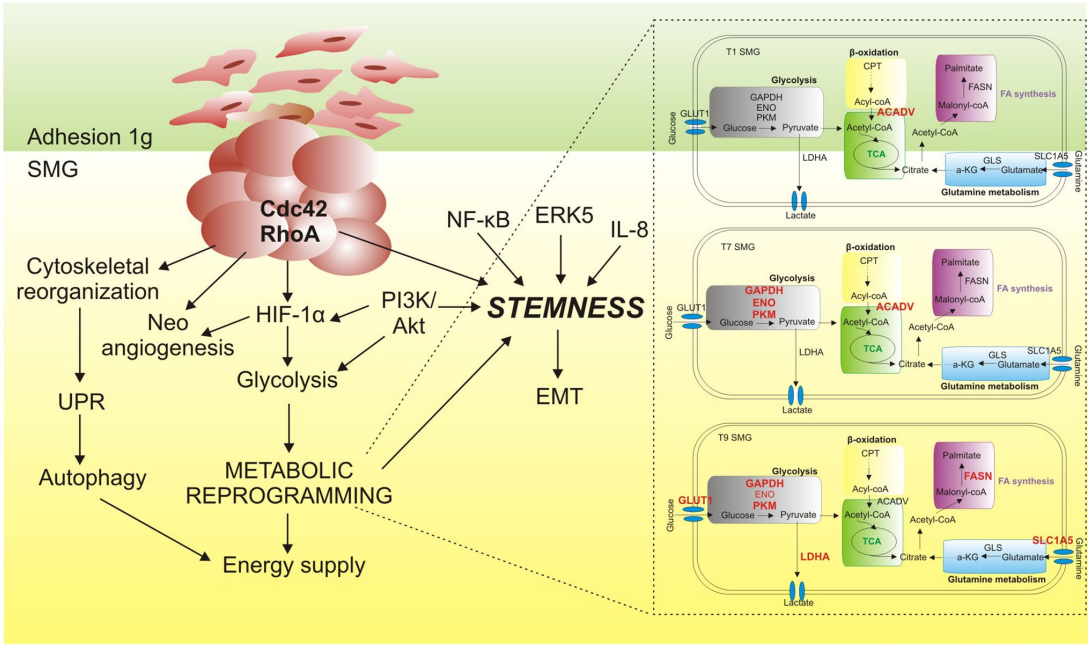

Fig. 6 Schematic illustration of the effects of simulated microgravity (SMG) on PaCa-44 cells. Under SMG, the cells leave their adhesion elongated shape and aggregate in 3D spheroidal structures. Indeed, SMG impacts on cellular morphology through the modulation of proteins involved in Cdc42 and RhoA signaling that in turn affect cytoskeletal organization, neo-angiogenesis and stemness. Cytoskeletal reorganization impairs cell biological processes and induces cancer cells to activate survival mechanisms, among which the unfolded protein response (UPR) pathway, which supports autophagy to prevent cell death. The morphological rearrangement occurring during SMG additionally induces metabolic reprogramming orchestrated by the activation of HIF-1α and PI3K/Akt pathways, which pave the way for glucose metabolism upregulation. A more active glycolysis, compared to adhesion condition, is involved in the regulation of proliferation, metastasization, and aggressiveness. These metabolic changes, together with activation of PI3K/Akt/NF-κB/ERK5/IL-8 signaling axis induce the upregulation of stem-associated proteins and expansion of the CSC subset that supports neoplastic progression through EMT

be used for either energy starvation (lipid droplets) or for membrane biosynthesis.

All together, these results describe time by time cell transformation toward a more stem and aggressive phenotype induced by SMG exposure. This cell rearrangement may also affect tumour cells susceptibility to drugs, thus future works will focus on the evaluation of pancreatic cancer cells response to anti neoplastic drugs under simulated microgravity.

Supplementary Information The online version contains supplementary material available at https://doi.org/10.1007/s00018-022-04243-z.

Acknowledgements Not applicable

Author contributions Conceptualization: MAM, TS, SA, DM, ME; methodology: MAM, BV, MMPA, BE, TS VVV, RE, MF, AF, DM; validation: BV, MM, PA, MF, SA FA; formal analysis: BV, MM, PA, FA, BE, VVV, RE, AF, TS, DM; investigation: MAM, BV, MM, PA, BE, VVV, MF, AF; resources: MAM, MM, TS, SA, DM; data curation: BV, MM, PA, BE, TS, VVV, RE, MF, AF, DM; writing—original draft: MAM, MM, PA, DM, ME; writing—review and editing: MAM, BV, MM, PA, BE, TS, SA, DM, ME; supervision: MAM, MM, PA, SA, DM, ME; Project administration: MAM, ME; funding acquisition: MAMSA, D.M., M.E. All authors read and approved the final manuscript.

Funding This study was supported by the AGING Project—Department of Excellence—DIMET, by "progetto FAR-2017 di Ateneo", Università del Piemonte Orientale; Associazione Italiana per la Ricerca sul Cancro (AIRC) IG no. 19885 to A.S. and AIRC 5×1000 no. 22757; Ministero della Salute RF-2016-02364842 and Ministero Università Ricerca (project no. 2017BA9LM5_001); Associazione "Augusto per la Vita" Novellara (RE); and Associazione "Medicine Rocks", Milano.

Data availability The mass spectrometry proteomics data, dataset identifier PXD028708, have been deposited to the ProteomeXchange Consortium via the PRIDE partner repository (https://www.ebi.ac.uk/pride/archive/). Dataset identifier proteomic analysis: PXD028708. Reviewer account details: Username: reviewer_pxd028708@ebi.ac.uk; Password**:** fId4pe3W.

Declarations

Conflict of interests The authors declare no conflict of interests.

Ethics approval Not applicable.

Consent for publication All authors give consent for the publication of the manuscript on Molecular Cancer.

References

1. Winnard A, Nasser M, Debuse D, Stokes M, Evetts S, Wilkinson M, Hides J, Caplan N (2007) Systematic review of countermeasures to minimise physiological changes and risk of injury to the lumbopelvic area following long-term microgravity. Musculoskelet Sci Pract 1:S5–S14. https://doi.org/10.1016/j.msksp.2016.12.009
2. Kimlin LC, Casagrande G, Virador VM (2013) In vitro three-dimensional (3D) models in cancer research: an update. Mol Carcinog 52(Suppl 3):167–182. https://doi.org/10.1002/mc.21844
3. Vidyasekar P, Shyamsunder P, Arun R, Santhakumar R, Kapadia NK Kumar R, Verma RS (2015) Genome Wide Expression Profiling of Cancer Cell Lines Cultured in Microgravity Reveals Significant Dysregulation of Cell Cycle and MicroRNA Gene Networks. *PLoS One* 10(8):e0135958. https://doi.org/10.1371/journal.pone.0135958
4. Kopp S, Slumstrup L, Corydon TJ, Sahana J, Aleshcheva G, Islam T, Magnusson NE, Wehland M, Bauer J, Infanger M, Grimm D (2016) Identifications of novel mechanisms in breast cancer cells involving duct-like multicellular spheroid formation after exposure to the Random Positioning Machine. Sci Rep 6:268–287. https://doi.org/10.1038/srep26887.
5. Masini MA, Strollo F, Ricci F, Pastorino M, Uva BM (2006) Microtubules disruption and repair phenomena in cultured glial cells under microgravity. Grav Space Biol 19:149–150
6. Ulbrich C, Pietsch J, Grosse J, Wehland M, Schulz H, Saar K, Hübner N, Hauslage J, Hemmersbach R, Braun M et al (2011) Differential gene regulation under altered gravity conditions in follicular thyroid cancer cells: relationship between the extracellular matrix and the cytoskeleton. Cell Physiol Biochem 28:185–198. https://doi.org/10.1159/000331730
7. Mukhopadhyay S, Saha R, Palanisamy A, Ghosh M, Biswas A, Roy S, Pal A, Sarkar K, Bagh S (2016) A systems biology pipeline identifies new immune and disease related molecular signatures and networks in human cells during microgravity exposure. Sci Rep 6:259–275. https://doi.org/10.1038/srep25975
8. Zhao T, Tang X, Umeshappa CS, Ma H, Gao H, Deng Y, Freywald A, Xiang J (2016) Simulated microgravity promotes cell apoptosis through suppressing Uev1A/TICAM/TRAF/NF-kappaB-regulated anti-apoptosis and p53/PCNA- and ATM/ATR-Chk1/2-controlled DNA-damage response pathways. J Cell Biochem 117:2138–2148. https://doi.org/10.1002/jcb.25520
9. Borst AG, van Loon JJWA (2009) Technology and developments for the random positioning machine. RPM Microgravity Sci Technol 21:287–292. https://doi.org/10.1007/s12217-008-9043-2
10. Grimm D, Wehland M, Pietsch J, Aleshcheva G, Wise P, van Loon J (2014) Growing tissues in a real and simulated microgravity: new method for tissue engineering. Tissue Eng Part B Rev 20:555–566. https://doi.org/10.1089/ten.teb.2013.0704
11. Pedrazzi M, Vercellone S, Barberis E, Capraro M, De Tullio R, Cresta F, Casciaro R, Castellani C, Patrone M, Marengo E et al (2021) Identification of potential leukocyte biomarkers related to drug recovery of CFTR: clinical applications in cystic fibrosis. Int J Mol Sci 22:3928. https://doi.org/10.3390/ijms22083928
12. Dalla Pozza E, Manfredi M, Brandi J, Buzzi A, Conte E, Pacchiana R, Cecconi D, Marengo E, Donadelli M (2017) Trichostatin A alters cytoskeleton and energy metabolism of pancreatic adenocarcinoma cells: an in depth proteomic study. J Cell Biochem 119:2696–2707. https://doi.org/10.1002/jcb.26436
13. Manfredi M, Brandi J, Di Carlo C, Vanella VC, Barberis E, Marengo E (2019) Mining cancer biology through bioinformatic analysis of proteomic data. Expert Rev Proteomics 16:733–747. https://doi.org/10.1080/14789450.2019.1654862
14. Barberis E, Joseph S, Amede E, Clavenna MG, La Vecchia M, Sculco M, Aspesi A, Occhipinti P, Robotti E, Boldorini R, Marengo E, Dianzani I, Manfredi M (2021) A new method for investigating microbiota-produced small molecules in adenomatous polyps. Anal Chim Acta 1179:338841. https://doi.org/10.1016/j.aca.2021.338841
15. Yamazaki D, Kurisu S, Takenawa T (2005) Regulation of cancer cell motility through actin reorganization. Cancer Sci 96:379–386. https://doi.org/10.1111/j.1349-7006.2005.00062.x
16. Burke B, Stewart CL (2013) The nuclear lamins: flexibility in function. Nat Rev Mol Cell Biol 14:13–24. https://doi.org/10.1038/nrm3488
17. Singh JK, Simões BM, Howell SJ, Farnie G, Clarke RB (2013) Recent advances reveal IL-8 signaling as a potential key to targeting breast cancer stem cells. Breast Cancer Research: BCR 15:210. https://doi.org/10.1186/bcr3436
18. Pereira DM, Gomes SE, Borralho PM, Rodrigues CMP (2019) MEK5/ERK5 activation regulates colon cancer stem-like cell properties. Cell Death Discov 5:68. https://doi.org/10.1038/s41420-019-0150-1
19. Walcher L, Kistenmacher AK, Suo H, Kitte R, Dluczek S, Strauß A, Blaudszun AR, Yevsa T, Fricke S, Kossatz-Boehlert U (2020) Cancer stem cells-origins and biomarkers: perspectives for targeted personalized therapies. Front Immunol 11:1280. https://doi.org/10.3389/fimmu.2020.01280
20. Jones DT, Valli A, Haider S, Zhang Q, Smethurst EA, Schug ZT, Peck B, Aboagye EO, Critchlow SE, Schulze A et al (2019) 3D growth of cancer cells elicits sensitivity to kinase inhibitors but not lipid metabolism modifiers. Mol Cancer Ther 2:376–388. https://doi.org/10.1158/1535-7163.MCT-17-0857
21. Yanes O, Clark J, Wong DM, Patti GJ, Sánchez-Ruiz A, Benton HP, Trauger SA, Desponts C, Ding S, Siuzdak G (2010) Metabolic oxidation regulates embryonic stem cell differentiation. Nat Chem Biol 6:411–417. https://doi.org/10.1038/nchembio.364
22. Visweswaran M, Arfuso F, Warrier S, Dharmarajan A (2020) Aberrant lipid metabolism as an emerging therapeutic strategy to target cancer stem cells. Stem Cells 38:6–14. https://doi.org/10.1002/stem.3101
23. Yoshihisa A, Watanabe S, Yokokawa T, Misaka T, Sato T, Suzuki S, Oikawa M, Kobayashi A, Takeishi Y (2017) Associations between acylcarnitine to free carnitine ratio and adverse prognosis in heart failure patients with reduced or preserved ejection

fraction. ESC Heart Fail 4:360–364. https://doi.org/10.1002/ehf2.12176
24. Afshinnia F, Rajendiran TM, Soni T, Byun J, Wernisch S, Sas KM, Hawkins J, Bellovich K, Gipson D, Michailidis G et al (2018) Impaired β-oxidation and altered complex lipid fatty acid partitioning with advancing CKD. J Am Soc Nephrol 29:295–306. https://doi.org/10.1681/ASN.2017030350
25. Zegers MM, Friedl P (2014) Rho GTPases in collective cell migration. Small GTPases 5:e28997. https://doi.org/10.4161/sgtp.28997
26. Koundouros N, Karali E, Tripp A, Valle A, Inglese P, Perry NJS, Magee DJ, Anjomani Virmouni S, Elder GA, Tyson AL et al (2020) Metabolic fingerprinting links oncogenic PIK3CA with enhanced arachidonic acid-derived eicosanoids. Cell 181:1596–1611. https://doi.org/10.1016/j.cell.2020.05.053
27. Bennett DT, Deng XS, Yu JA, Bell MT, Mauchley DC, Meng X, Reece TB, Fullerton DA, Weyant MJ (2014) Cancer stem cell phenotype is supported by secretory phospholipase A2 in human lung cancer cells. Ann Thorac Surg 98:439–445. https://doi.org/10.1016/j.athoracsur.2014.04.044
28. Bellamkonda K, Chandrashekar NK, Osman J, Selvanesan BC, Savari S, Sjölander A (2016) The eicosanoids leukotriene D4 and prostaglandin E2 promote the tumorigenicity of colon cancer-initiating cells in a xenograft mouse model. BMC Cancer 16:425. https://doi.org/10.1186/s12885-016-2466-z
29. Hashemi Goradel N, Najafi M, Salehi E, Farhood B, Mortezaee K (2019) Cyclooxygenase-2 in cancer: A review. J Cell Physiol 234:5683–5699. https://doi.org/10.1002/jcp.27411
30. Pastò A, Bellio C, Pilotto G, Ciminale V, Silic-Benussi M, Guzzo G, Rasola A, Frasson C, Nardo G, Zulato E, et al (2010) Cancer stem cells from epithelial ovarian cancer patients privilege oxidative phosphorylation and resist glucose deprivation. *Oncotarget* 5:4305–4319. https://doi.org/10.18632/oncotarget.2010.
31. Pagotto A, Pilotto G, Mazzoldi EL, Nicoletto MO, Frezzini S, Pastò A, Amadori A (2017) Autophagy inhibition reduces chemoresistance and tumorigenic potential of human ovarian cancer stem cells. Cell Death Dis 87:e2943. https://doi.org/10.1038/cddis.2017.327
32. Bi J, Ichu TA, Zanca C, Yang H, Zhang W, Gu Y, Chowdhry S, et al (2019) Oncogene Amplification in Growth Factor Signaling Pathways Renders Cancers Dependent on Membrane Lipid Remodeling. *Cell Metab* 3;30(suppl 3):525–538.e8. https://doi.org/10.1016/j.cmet.2019.06.014.

SUPPLEMENTARY INFORMATION

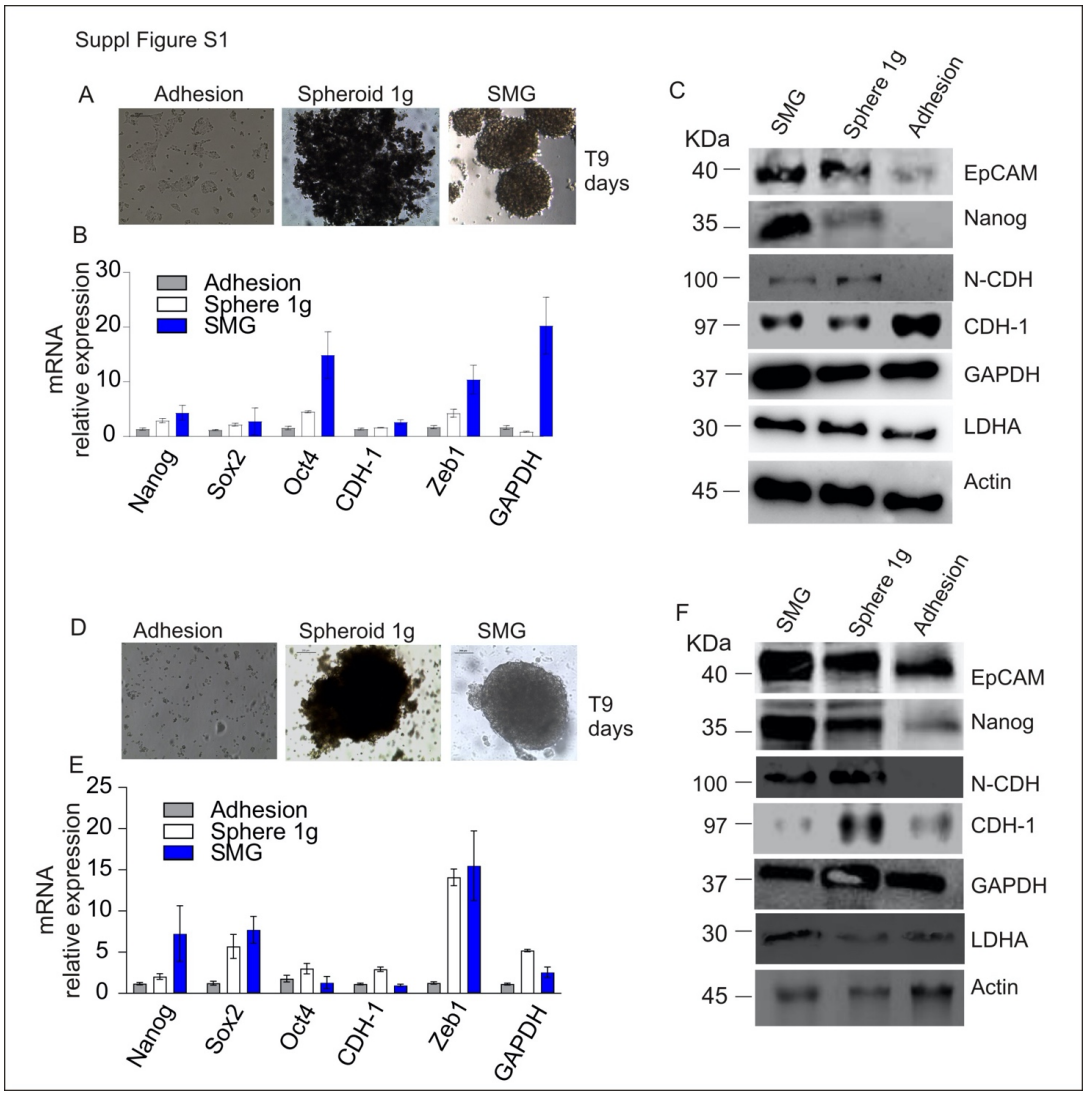

Supplementary Figure S1: Simulated microgravity exposure induces morphological rearrangement, promotes stemness and migratory capability, and impairs cell metabolism in CFPAC-1 and AsPC-1 cells.

A) CFPAC-1 cells were maintained for 9 days in normal adhesion culture condition (Adhesion), spheroid-forming at normal gravity (Spheroid 1 g) or simulated microgravity (SMG). One representative picture for each condition (Magnification 5x). **B)** qRT-PCR analysis of stemness markers (Nanog, Sox2 and Oct4), EMT-associated markers (E-cadherin and Zeb-1) and GAPDH in CFPAC-1 cells maintained in normal culture condition (Adhesion), spheroid-forming at normal gravity (Spheroid 1 g) or in simulated microgravity (SMG) for 9 days. Data are expressed as mean±sd of n=2 replicates. **C)** Western blot analysis of stemness markers (EpCAM and Nanog), EMT-associated markers E-cadherin (CDH-1) and N-cadherin (N-CDH), metabolic components (GAPDH and LDHA) and Actin in CFPAC-1 cells maintained in normal culture condition (Adhesion),

spheroid-forming culture condition at normal gravity (Spheroid 1 g) or in simulated microgravity (SMG) for 9 days.
D) Representative picture of AsPC-1 cells maintained for 9 days in normal adhesion culture condition (Adhesion), spheroid-forming at normal gravity (Spheroid 1 g) or simulated microgravity (SMG). Magnification 5x. **E)** qRT-PCR analysis of stemness markers (Nanog, Sox2 and Oct4), EMT-associated markers (E-cadherin and Zeb-1) and GAPDH in AsPC-1 cells maintained in normal culture condition (Adhesion), spheroid-forming at normal gravity (Spheroid 1 g) or in simulated microgravity (SMG) for 9 days. Data are expressed as mean±sd of n=2 replicates. **F)** Western blot analysis of stemness markers (EpCAM and Nanog), EMT-associated markers E-cadherin (CDH-1) and N-cadherin (N-CDH), metabolic components (GAPDH and LDHA) and Actin in AsPC-1 cells maintained in normal culture condition (Adhesion), spheroid-forming culture condition at normal gravity (Spheroid 1 g) or in simulated microgravity (SMG) for 9 days.

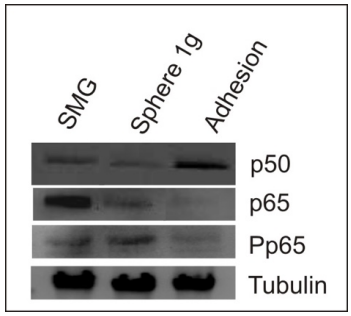

Supplementary Figure S2. Simulated microgravity exposure triggers NF-kB pathway activation.
Western blot analysis of p50, p65 and phospo-p65 in PaCa-44 cells maintained in normal culture condition (Adhesion), spheroid-forming condition at 1g (Spheroid 1g) or in simulated microgravity (SMG) for 9 days; Tubulin is used as housekeeping

Chapter 4

Growth rate and morphology of *Penicillium chrysogenum* exposed to long-term simulated microgravity

Growth rate and morphology of *Penicillium chrysogenum* exposed to long-term simulated microgravity

INTRODUCTION

Fungi exist in all shapes and sizes, contributing to their astounding evolutionary success. Most fungi exist as networks of filamentous cells (hyphae) able to grow indefinitely and in intricate patterns to explore and exploit their territory, a complex task at which they are extremely proficient (Naranjo and Gabaldón, 2020). The structure of this network is typically highly dynamic and responds to fluctuations in environmental parameters and/ or biotic interactions (Simonin et al., 2012). The hypha is a walled cylindrical multinucleated cell that is highly polarised, and cell polarisation is necessary for hyphal growth. The hyphal tip is able to exert physical force, as shown by Kirtzel et al. (2020), on rock particles in which broader and pre-existing cracks might be enlarged due to the effect of fungal turgor pressure. Such pressure reached from 4 to18 bar causing a breaking up of the black slate into smaller pieces. The hyphal tip can grow through solid substrates also by extracellular digestion, using exoenzymes to break down carbohydrates, organic phosphates, protein, or other recalcitrant polymers. At the same time, most microorganisms can access only the surface of such resources. Nutrient transport is performed through cytoplasmic waves and cytoskeleton-based movement, which can also transport cellular components, including new nuclei for growing hyphal tips (Tlalka et al., 2007; Fricker et al., 2008, 2017; Lew, 2011; Simonin et al., 2012). This flexible flux allows fungi to allocate different limiting nutrients from distant sources across heterogeneous environments (Fricker et al., 2008, 2017; Simonin et al., 2012; Boberg et al., 2014). Nowadays, hyphal morphogenesis and tip growth mechanisms are not completely understood as of the environmental factors that rule these processes. The hypha of most filamentous fungi show an organelle called the Spitzenkörper (SPK), involved in the organisation of vesicle traffic for hyphal elongation. The SPK is composed of a collection of vesicles originating in the Golgi apparatus containing the enzymes, lipids, and polysaccharides required to synthesise membranes and cell walls (Fisher and Roberson, 2016). Although the exact function of the SPK has not been completely established, there is a solid reason to believe, because of its position and behaviour, that it also plays a role in gravity perception.

Fungi are ubiquitous organisms and are found both on Earth and on the International Space Station (ISS), where they can survive and reproduce (Novikova et al., 2006). *Penicillium* is one of the main fungal genera detected onboard the Russian Space Station (MIR) and on the ISS, demonstrating its ability to grow on the space stations' surfaces. Moreover, this genus can form biofilms associated with higher tolerance and resistance to adverse conditions (Novikova et al., 2004; Harding et al., 2009; Chechiska et al., 2015). Current studies concerning the responses of microorganisms to real and modelled microgravity are relative to short time (from hours to a few days) exposures to weightlessness (Sathishkumar et al., 2014; Chunmei et al., 2019). To date, little information is available on how fungi are affected and changed due to growth under reduced gravity conditions and, in particular, once returned to Earth.

In the present work, we evaluated the effect of simulated microgravity conditions on fungal and hyphal tip growth from a particular perspective. To verify fungal adaptation capacity, we assessed the behaviour of hyphae developed under simulated microgravity or terrestrial gravity conditions. The conidia collected from colonies constantly kept under simulated microgravity (long-term exposure) were cultured under both gravity conditions. The same has been done for conidia collected from colonies constantly kept under terrestrial gravity.

MATERIALS AND METHODS

Biological Material

Penicillium chrysogenum Thom (P28, isolate from dust in Mycology Laboratory, DiSIT, UPO) inocula were prepared as a spore suspension, collecting spores from the surface of one-week-old Petri dish culture on MEA (Malt Extract Agar, Oxoid) using sterile physiological solution (NaCl, 0,9%). The suspension was adjusted to a concentration of 10^6 spores/ml.

Simulated microgravity condition

Microgravity conditions were simulated using a Random Positioning Machine (RPM) connected to a control console through standard electrical cables (Dutch Space, Leiden, The Netherlands). The apparatus is a 3D clinostat consisting of two independently rotating frames. This device does not eliminate gravity, but the RPM is a micro-weight

simulator based on the principle of "gravity-vector averaging": it allows a 1 g stimulus to be applied omnidirectionally rather than unidirectionally, and the sum of the gravitational force vectors tends to equal zero ($1x10^{-6}$ g). The effects generated by the RPM are comparable to the impact of real microgravity, provided that the direction changes are faster than the system's response time to the gravity field. The desktop RPM used was positioned within an incubator to maintain the temperature.

Simulated Microgravity Experimental Setup

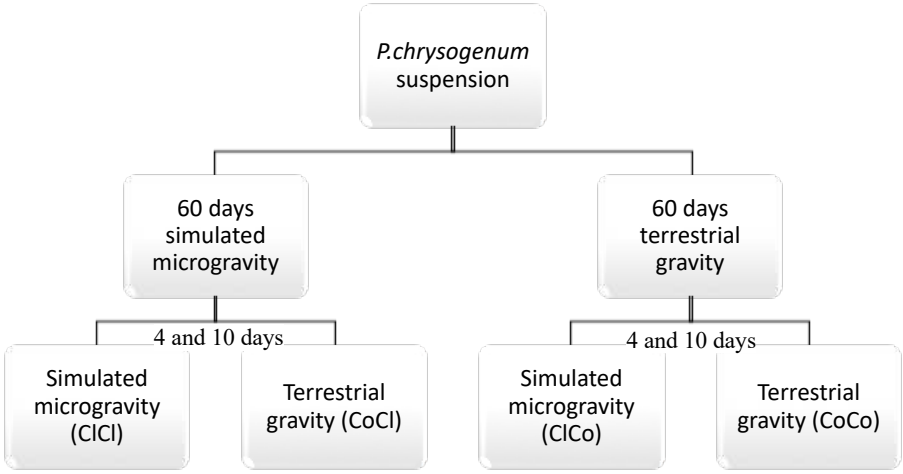

Fig. 1 Workflow of experimental setup. 60-days plates exposure: conidia suspension was inoculated on 5 cm diameter MEA-plates kept for 60-days under simulated or terrestrial gravity conditions. Spore collected from 60-days plates has been used to prepare a spore suspension (10^6 spores/ml) inoculated on MEA-plates and kept for short-time (4 days and 10 days) in different gravity conditions (ClCl, CoCl, ClCo, CoCo).

Inoculated plates were placed on the RPM inner frame for 60 days-culture in simulated microgravity. Controls were cultured in the same conditions without rotation (terrestrial gravity condition). All incubations were carried out at 25°C. The conidia from colonies constantly kept under simulated microgravity (long-term exposure) were collected. The suspension of 10^6 spores/ml was prepared and a 5µl aliquot of spore suspension was inoculated on 5 cm diameter MEA-plates. Plates inoculated were cultured under both gravity conditions, static (CoCl) and simulated microgravity (ClCl) conditions. The same has been done for conidia collected from colonies constantly kept under terrestrial gravity (ClCo and CoCo). These tests were performed in triplicate to evaluate fungal

growth and morphological changes using live imaging techniques at different time points (4 and 10 days; fig.1). Plates were placed on the RPM inner frame for culture in simulated microgravity. Controls for all tests were cultured in the same conditions without rotation. All incubations were carried out at 25°C.

Colony growth

No data have been collected from colonies kept for 60-days under simulated microgravity conditions. For each short-term experiment colonies' diameters were recorded until 10 days, to obtain growth curves, and at 4 and 10 days to evaluate the growth rate. Data were reported as mean ± standard error.

Morphological analysis

Optical Microscopy

Microscopy studies were performed on colonies grown for 4 days under simulated microgravity conditions (Cl) and on 4 days old static control (Co) colonies. Microscopy imaging was performed on samples taken from the margins of the cultures, where growth takes place, using the inverted agar block technique (Lichius et al., 2019) observed with Axiovert 100M inverted optical microscope (Zeiss) with an image acquisition system consisting of a 1.4-megapixel AxioCam high-resolution monochrome digital camera MR3 (Zeiss) connected to a computer equipped with the AxioVision program, version 4.8.2 SP3, used for image processing. All images were acquired with a 40x NA 0.75 objective. All the images obtained were saved in *.tif* format, 1338 x 1040 pixels, in B/W (transmitted light only) and analysed with ImageJ freeware software (Schneider et al., 2012). For each image, measure the hyphal diameters related to the apex of the dominant hypha, the apex of the lateral hyphae (ramifications of the main hypha) and the main hypha before the apical ramifications were acquired.

Live-imaging analysis

Live-cell imaging has been performed to observe morphological variation and vesicle traffic by simulated microgravity by confocal live image. Fluorescent dyes used are FM 4-64 lipophilic styryl dyes (2 mM, Molecular probes) to track plasma membrane, endo-/exocytosis and organelle dynamics, including Spitzenkorper, apical body involved in

fungal tip growth. Samples from fungal colonies were prepared by the inverted agar block method and analysed using a confocal system on an AxioObserver Z1 + LSM 800 (Zeiss) inverted optical microscope with a dual spectral channel, two lasers (488 nm and 561 nm solid-state), managed by the proprietary software ZEN Blue 2.6 (Zeiss). 40x, NA 0.75, and 63x, NA 1.40 Oil objectives were used. The images were saved in *.tif* format, 2048x2048 pixels, in the 488 nm or 561 nm channel or both in multitracking mode.

Germination rate

Penicillium chrysogenum inocula were prepared as previously reported in "Simulated Microgravity Experimental Setup". The suspension was adjusted to a concentration of 10^5 spores/ml and a 100µl aliquot of spore suspension was inoculated on 5 cm diameter MEA-plates. Inoculated plates were placed on the RPM inner frame for culture in simulated microgravity. Controls for all tests were cultured in the same conditions without rotation. All incubations were carried out at 25°C. The germination rate of *P. chrysogenum* conidia was evaluated at 3 different time-points: 8h, 12h, 16h. At least 3 samples with 1 cm^2 area for each plate were collected. Samples were evaluated using the inverted agar block technique (Lichius et al., 2019) and observed with Axiovert 100M inverted optical microscope (Zeiss).

Statistical analysis

Statistical analyses were performed with one-way ANOVA using STATVIEW statistical software. For growth and germination rate results were analysed by one-way ANOVA and Fisher PLSD post-hoc testing (STATVIEW statistical software SAS institute, Inc.) to compare different groups. Differences with $p<0.05$ were considered significant.

RESULTS

Colonies kept for 60-days under simulated microgravity and terrestrial conditions did't show differeces in macroscopic morphology or radial growth beacause all colonies reached plate edge. Data are relative to experiments performed on 4- and 10-days old colonies obtained from 60-days colony conidia.

Colony growth

Colony diameters of *P. chrysogenum* were recorded daily and were plotted in fig. 2a. The growth plot shows that fungal growth slowed down either early on in *P. chrysogenum* plates being in microgravity for two months and returned in static condition (CoCl) compared to static control (CoCo).

Radial growth measures revealed that both time points investigated (4 and 10 days) (fig.2 b, c) have significant differences in growth between colonies cultured in static condition after two months under microgravity (CoCl) compared to control (CoCo). In particular, at ten days, there are significant differences in diameters of colonies constantly kept in simulated microgravity (ClCl and CoCl). The short exposure to simulated microgravity doesn't seem to influence the fungal colony growth that comes from static conditions (ClCo).

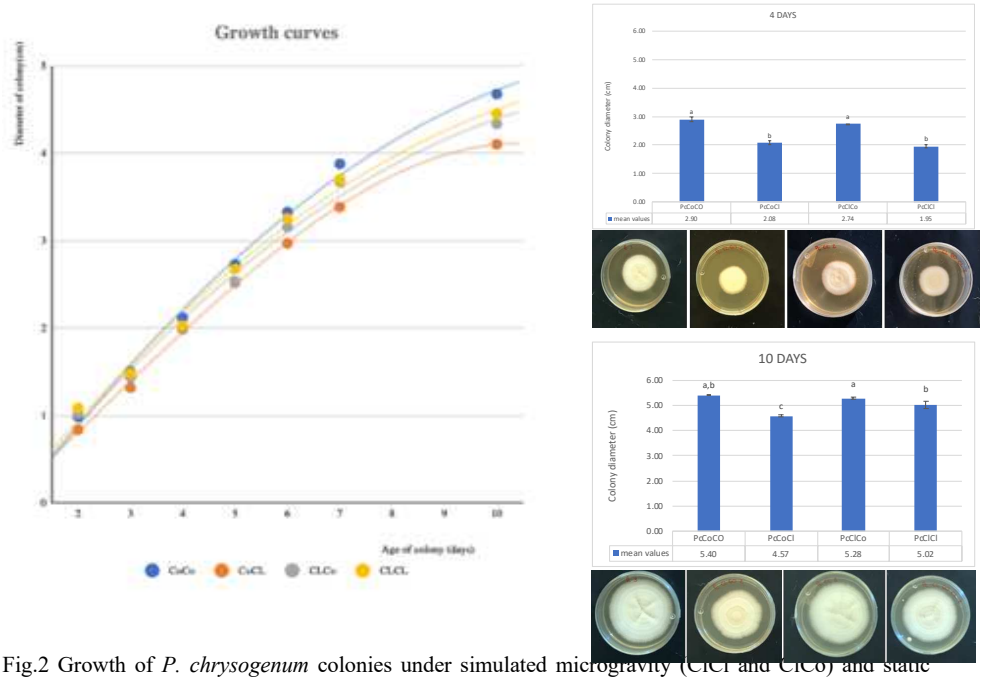

Fig.2 Growth of *P. chrysogenum* colonies under simulated microgravity (ClCl and ClCo) and static conditions (CoCo and CoCl). Growth curves (a); growth rate after 4-days exposure to SMG (b); growth rate after 10-days exposure to SMG (c). Letters indicate statistically significant differences between samples ($p<0.05$); error bars correspond to the standard errors.

The microgravity environment allows the growth of these filamentous fungi; however, the total length of the mycelium is always shorter in colonies that come from conidia

collected from colonies exposed for two months to simulated microgravity conditions (ClCl and CoCl) compared to static control plates (CoCo) at the same time.

Plates inoculated were cultured under both gravity conditions, static (CoCl) and simulated microgravity (ClCl) conditions. The same has been done for conidia collected from colonies constantly kept under terrestrial gravity (ClCo and CoCo).

Colonies cultured in static condition after two months under microgravity (CoCl) compared to control (CoCo). In particular, at ten days, there are significant differences in diameters of colonies constantly kept in simulated microgravity (ClCl and CoCl). The short exposure to simulated microgravity doesn't seem to influence the fungal colony growth that comes from static conditions (ClCo).

Morphology

Hyphae morphologies and apical diameters were evaluated on 4-days colonies from plates kept in static (CoCo) and simulated microgravity (ClCo) conditions. Microscopic analysis showed changes in hyphae morphology, tip shape and lateral hyphae formation (fig.3). Colonies grown under microgravity conditions produced hyphae with irregular diameters and symmetrical enlargements (sausage-like) (fig.3c, d, f).

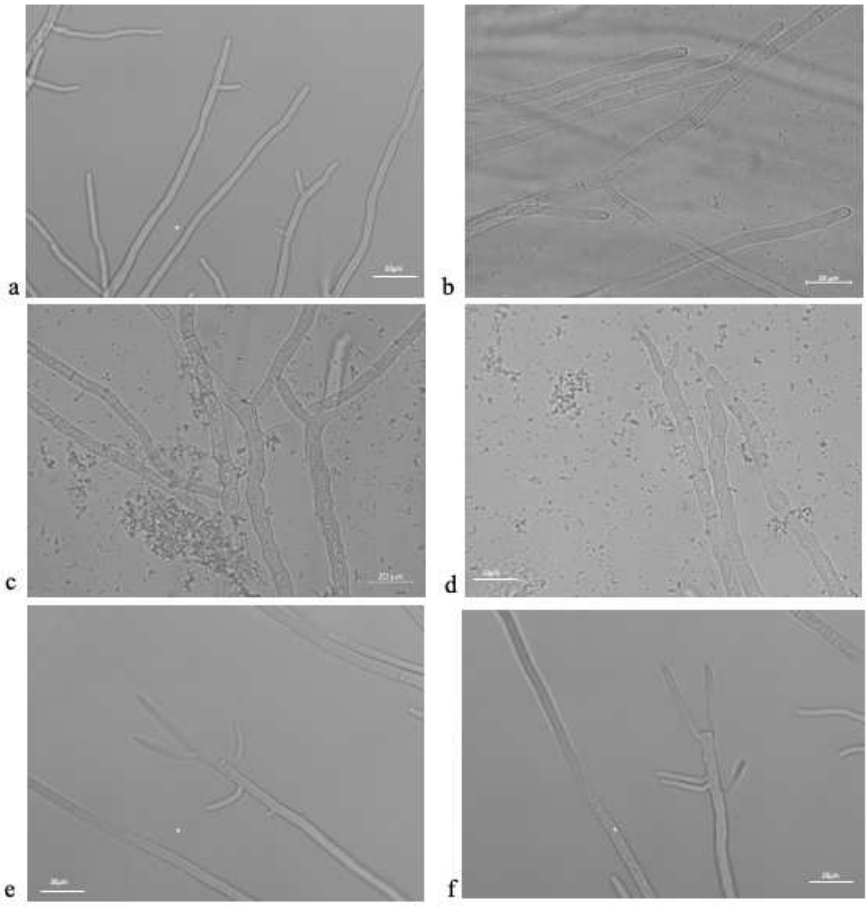

Fig.3 Hyphae morphologies evaluated on 4-days colonies from plates kept in static (CoCo; a, c) and simulated microgravity (ClCo; b, d, e) conditions. Canonical apical branching (a), hyphae with regular septa before branch (b), symmetrical enlargements “sausage-like” (c, d), narrowing of main tip (e) and aberrant branching close to the tip. Scale bar: 20 µm.

The diameter of the hyphal apexes in colonies grown in simulated microgravity conditions is always significantly thinner than those grown in normal gravity. Interestingly, dominant hyphae diameter before apical branches is significantly increased in microgravity conditions than those grown under static conditions (fig.4).

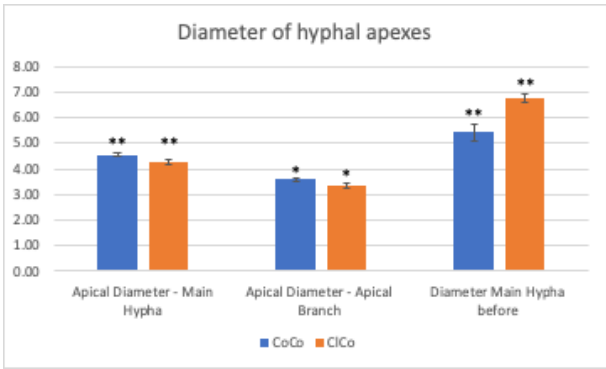

Fig.4 Apical diameters evaluated on 4-days colonies from plates kept in static (CoCo) and simulated microgravity (ClCo) conditions. Asterisks (*) indicate statistically significant differences between samples (*p<0.05, significant differences; **p<0.01, high significant differences); error bars correspond to the standard errors.

On the fourth day, a confocal microscope analysis confirmed morphological changes under microgravity and static conditions. Using laser confocal microscopy, we tracked plasma membrane and apical body with FM4-64 (red). The most conspicuous FM4-64 patches are located predominantly at the hyphal apex, but the patterns changed when the fungus grew in microgravity. In static samples, the patches are mainly concentrated in the apex, where we can find the Spitzenkörper (fig.5a). This type of organisation seems to be lost when the fungus is under microgravity, as shown by the photos obtained analysing samples of colonies that have experienced microgravity, even for a few days (fig.5b, c, d). Besides, in microgravity samples, there is a reorganisation of vesicle traffic in the hyphal tip where we observe a lateral accumulation of vesicles that move up apical branches, or we did not see the collection at all vesicles that had to make up Spitzenkörper (fig.5d).

a 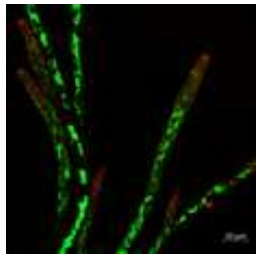 b 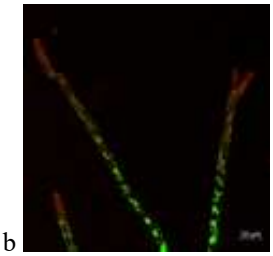

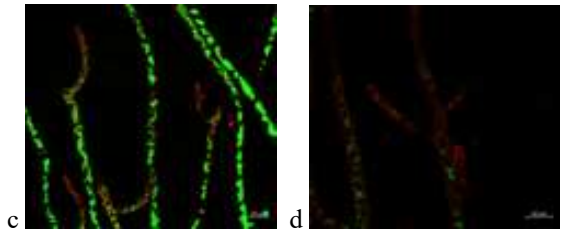

Fig.3 Confocal images of the hyphal tip in *P. chrysogenum* stained with FM4-64 (red, excitation wavelength at 488 nm) and vesicle traffic (green, excitation wavelength at 561 nm). CoCo (a), ClCo (b), CoCl (c) and ClCl (d). The Spitzenkörper is located at the foremost point of the apical dome. Scale bar: 10 μm.

Germination rate

Conidia germination was evaluated at different time points in samples kept under simulated microgravity and static conditions. At 8 hour the germination speed was significant higher in samples always exposed to simulated microgravity (ClCl) than those germinated in static conditions (CoCo and CoCl). Conidia collected from colonies always kept in terrestrial gravity and exposed to simulated microgravity for a few hours (ClCo) showed no significant difference in germination rate (fig.6).

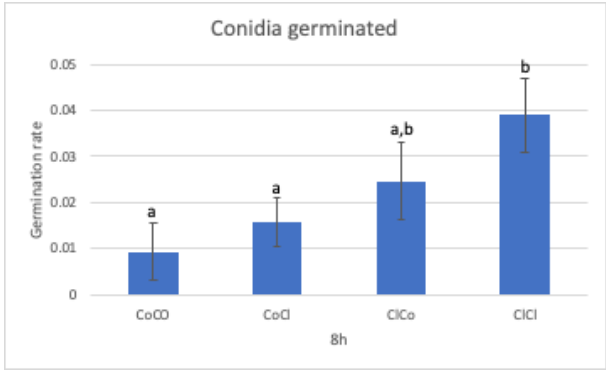

Fig.6 Germination rate at 8h of *P. chrysogenum* conidia exposed to simulated microgravity (ClCl and ClCo) and static conditions (CoCo and CoCl). Letters indicate statistically significant differences between samples ($p<0.05$); error bars correspond to the standard errors.

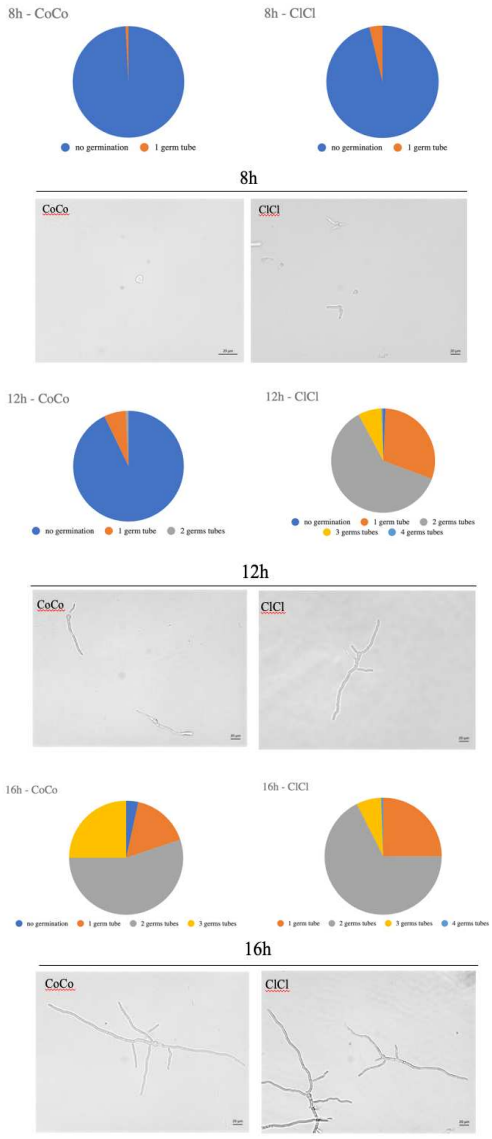

Fig.7 Mean value in % of germination rates (a) and germ tube formation of *P. chrysogenum* conidia never exposed to simulated microgravity for few hours (CoCo) and of conidia exposed to simulated microgravity for two month (ClCl) at different time points (b). Scale bar: 20 µm.

Conidia maintained for long periods in simulated microgravity (ClCl and CoCl) have higher germination rates than those of the spores with terrestrial gravity (CoCo). In tests carried out in simulated microgravity irregular morphologies of germ tubes have been observed with the formation of multiple germinative tubes (double, triple, quadruple).

Already at 12 hours three germ tubes appear in conidia exposed to simulated microgravity over a long time (fig. 7). Moreover, development of four germ tubes has

been noted only in conidia exposed to simulated microgravity over a long time apart from gravity environment where germination takes place (figg. 7 and 8).

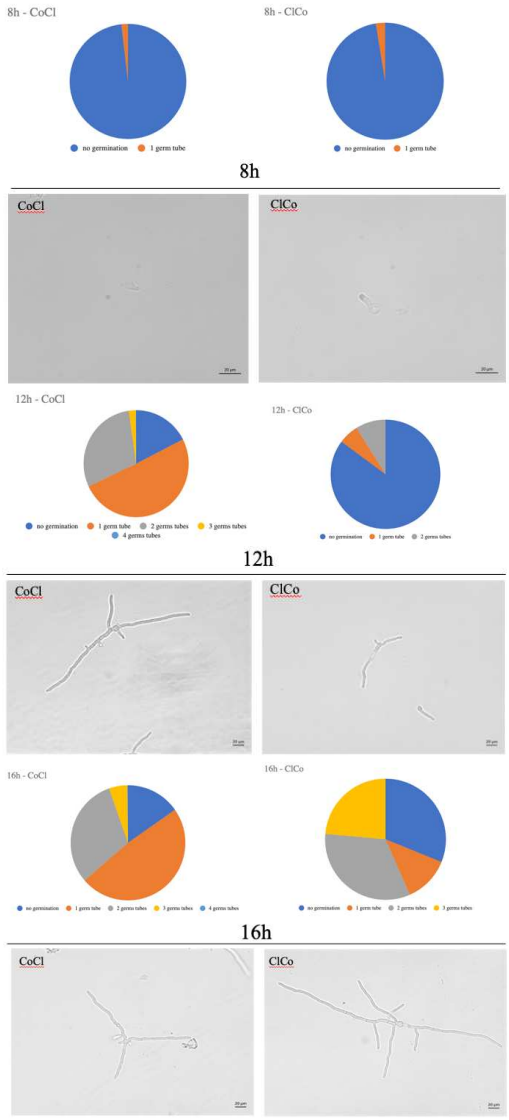

Fig.8 Mean value in % of germination rates and germ tube formation of *P. chrysogenum* conidia exposed to terrestrial gravity after a long-simulated microgravity exposure (CoCl) and of conidia exposed to simulated microgravity for the first time (ClCo) at different time points. Scale bar: 20 µm.

The change in the conditions of gravity implies a slowdown in germination rate. Conidia returned to terrestrial gravity after a long-term exposure to simulated microgravity (CoCl) show germination rate reduction starting from 12 hours. A decrease in germination rate was observed also in conidia collected from colonies

always kept in terrestrial gravity and exposed to simulated microgravity for a few hours (ClCo), compared to those that have never been subjected to microgravity (fig. 8).

DISCUSSION

Filamentous fungi may threaten long-duration space missions, such as a 500-day human mission to Mars or the Moon colonisation, on human physiology and spacecraft materials (Novikova, 2006; Cortesao et al., 2020). To evaluate biodeterioration activity, infections and pathogenicity by fungi developed under microgravity conditions, it is necessary to understand and predict the growth in this environment and how fungal characteristics can change in space. We investigated the effect of simulated microgravity on microscopic morphology, growth and germination rate of *Penicillium chrysogenum*. Little information is available on how fungi are affected and on changes due to growth under reduced gravity conditions and, in particular, once returned to Earth. In this work colonies of *P. chrysogenum*, which were kept in microgravity conditions for 60 days, were used to inoculate malt agar plates. These plates were again subjected to microgravity conditions in order to understand fungal adaptation capacity. In this way it is possible to observe the effects of long-term simulated microgravity exposure both on colonies constantly kept under simulated microgravity (ClCl) and on colonies returned in static condition for a few days (CoCl). These data were compared with those from colonies kept always in static conditions (CoCo) and colonies that have experienced simulated microgravity for a few days (ClCo).

Penicillium chrysogenum colonies aspect suggests that the growth conditions did not influence the morphology of the colonies, in contrast to what is observed by Gomoiu et al. (2013) and Jiang et al. (2019) for *Ulocladium chartarum* and *Aspergillus carbonarius*, respectively. Regardless, simulated microgravity influenced the growth of filamentous fungi over time. Romsdhal et al. (2019) reported an increase in growth rate for the colonies of *Aspergillus niger* exposed to real microgravity. Fungi exposed to stress conditions probably activate molecular pathways involved in the interruption of dormancy and fungal growth (Romsdal et al., 2018). Moreover, other studies highlight that microgravity induces a pathway regulation that leads to a more active metabolism, which could play an essential role in adaptation under these conditions (Taheri-Talesh et al. 2008; Takeshita et al. 2014; Wosten et al. 1991). Until today, no

more specific information was available in the literature about germination and growth behaviour regulation under altered gravity conditions.

Usually, colony growth is typically sigmoidal, with a lag phase at lower growth rates, followed by an exponential growth phase and a stationary phase, after which the fungus dies (Deacon, 2006). Our data showed the most significant slow-down in growth rate, probably due to increased gravity force (from 10^{-6}g in the RPM to 1g on the ground). The short exposure to simulated microgravity doesn't seem to influence the fungal colony growth that comes from static conditions (ClCo). The microgravity environment allows the growth of these filamentous fungi; however, the total length of the mycelium is always shorter in colonies that come from microgravity conditions (ClCl and CoCl) compared to static control plates (CoCo) at the same time. Indeed, in simulated microgravity conditions, it was possible to observe that fungi maintained growth more than when returned in normal gravity conditions, almost indicating a possible environmental adaptation. Data indicate that simulated microgravity reduces fungal growth, and this effect increases when *P. chrysogenum* returns at a static condition.

The growth slowdown observed for colonies in RPM and ground seems to be preceded by hyphal branching and loss of the dominance of the main hyphae, leading to apical branching and chaotic lateral branching. Several enzymes involved in chitin recognition and degradation were found up-regulated in fungi exposed to simulated Mars conditions, and this could allow morphological changes during germination and growth (Blachiwicz et al., 2019). Under normal gravity conditions, lateral branching takes place behind the apex of main hypha, which maintains its growth. Therefore, the diameter at the base of the branch does not show broadness. What causes branching is one of the fascinating questions in fungal biology. Katz et al. (1972) concluded that ‘‘a new branch is formed when the capacity of the hypha to elongate exceeds that of the existing tips.’’ Previous studies showed that the position and behaviour of the Spitzenkörper determine the growth, morphology, and direction of growth in fungal hyphae (Bartnicki-García, 2002). Our static samples show a canonical pattern of lateral branching with a new Spitzenkörper formed without affecting the primary Spitzenkörper; the elongation rate of the dominant hypha continued undisturbed while the branch emerged and developed. The most evident differences between RPM and

control samples in static condition is the presence of chaotic lateral branching and an apical growth interruption of the main hypha with lateral branching formation. These lateral branchings emerge close to the arrested tip attempting to restore the apical dominance. The increase in branching formation was also described in *Ulocladium chartarum* (Gomoiu et al., 2013) after short-term exposure to real microgravity. In *Neurospora crassa* (Riquelme et al., 2004), in terrestrial condition, were described the presence of some apical ramifications besides to the usual lateral ramifications. In our experiments the main tips stopped growing and produced two lateral branching, really close to the main tip, that carried on the growth. Moreover, main tips often swelled into an enlarged and rounded shape probably due to mechanical unloading. New branches followed an interruption of apical growth of the main hypha. In particular, it seems that this process is characterised by a retraction and disappearance of the Spitzenkörper, during which the elongation rate dropped sharply. In some cases, the main hypha doesn't stop the growth but it gets narrower in the apical zone or swells up in an irregular way sausage-like. This feature could be related to an aberrant cytoskeletal organisation strictly involved in apical growth in a simulated reduced gravity environment. The Spitzenkörper's formation is a mechanism largely unknown but is well known that is deeply tied with cytoskeleton components (Bartnicki-García, 2002). Therefore, morphological alterations, such as growth rate and germination pattern, could be influenced by septins, evolutionarily conserved GTP binding proteins, and cytoskeleton elements. The septins are involved in various cellular processes, including cytokinesis, vesicular trafficking, cytoskeleton organisation, polarity and formation of diffusion barriers. Given their role, swings in septins may cause abnormal morphologies in hyphae and aberrant germination patterns, such as increasing germinative tubes and branches (Hernández-Rodríguez et al., 2022).

The germination tests showed a higher number of germinative tubes in conidia exposed to simulated microgravity for a long time (ClCl and ClCo) than in conidia in static condition (CoCo) at the same time-point. First stages of germination rate seems to be enhanced by simulated microgravity exposure, with significant differences at 8h between conidia collected from colonies always grew under terrestrial condition (CoCo) and colonies kept for two months under simulated microgravity. However, in samples exposed in a new gravity condition (simulated microgravity, ClCo, or returned

in terrestrial gravity, CoCl) a slow down over-time is observed, mainly in conidia returned to terrestrial condition after a long period of simulated microgravity (CoCl). Changes in germination rate and germ-tube production can be related to different growth rates. Taking the current data together, *P. chrysogenum* exposed to long-term simulated microgravity revealed changes in germination rate, growth rate and hyphal tip organisation, compared to static controls. The germination rate increases with branching formation, while the radial growth rate decreases after long-term simulated microgravity exposure. Moreover, the longer the colonies are grown in simulated microgravity conditions, more significant are the differences with the colonies constantly kept under static or microgravity conditions.

CONCLUSION

The fungi have developed an extraordinary ability to adapt to changing environments and thrive under a wide range of conditions. The adaptation mechanism of filamentous fungi to spacecraft environments isn't completely understood. Different fungal species exposed to real or simulated microgravity show different behaviours (Gomiou et al., 2013; Blachowicz et al., 2018; Jiang et al., 2019; Tesei et al., 2021). Data collected up to now suggest that some fungal species, as *P. chrysogenum,* respond to adverse environmental conditions altering their growth and development. One common theme is that the ability to grow in extreme environments involves the adaptation of the whole organism. Clearly, integration with morpho-physiological data is needed with the growing number of molecular and cytologic findings associated with the onset of hyphal morphogenesis and branching under simulated microgravity conditions. In this work it was shown that long-term exposure to simulated microgravity can induce important differences when the fungi returned to terrestrial condition.

Data obtained in this work evaluated the response of *P. chrysogenum* conidia, collected from colonies previously exposed to static and simulated microgravity conditions for 60 days, to short-term (4 and 10 days) gravity vector changes. Results suggest that fungi exposed to long-term simulated microgravity adapt themselves to this condition and show disruption in colony growth when they experience terrestrial conditions once again. Colonies exposed for short-term (4 or 10 days) to simulated microgravity conditions (ClCo), by contrast, don't seem to show alteration in parameters evaluated.

Gravity vector changes adaptation mechanism is probably strictly related to cytoskeletal organisation, as shown by apical dominance drop and by irregular lateral branching. Germination tests highlight changes in germinative tube production that increase in conidia subjected to simulated microgravity conditions. A major challenge could be to discern cause-effect hierarchy in this complex phenomenology to elucidate the origin and the sequence of events triggering gravity response.

REFERENCES

Bartniki-García S. Hyphal tip growth: outstanding questions. In: Osiewacz HD, editor. Molecular Biology of Fungal Development. New York: Marcel Dekker; 2002. pp. 29–58.

Blachowicz A, Chiang AJ, Elsaesser A, Kalkum M, Ehrenfreund P, Stajich JE, Torok T, Wang C and Venkateswaran K. Proteomic and Metabolomic Characteristics of Extremophilic Fungi Under Simulated Mars Conditions. *Front. Microbiol.* 2019; *10*, 1013. Doi:10.3389/fmicb.2019.01013

Boberg JB, Finlay RD, Stenlid J, Ekblad A and Lindahl BD. Nitrogen and carbon reallocation in fungal mycelia during decomposition of boreal forest litter. *PLoS One.* 2014; 9, 1–12.

Checinska A, Probst AJ, Vaishampayan P, White JR, Kumar D, Stepanov VG, Nilsson HR, Pierson DL, Perry J, Fox GE and Venkateswaran K. Microbiomes of the dust particles collected from the International Space Station and Spacecraft Assembly Facilities. *Microbiome* 2015, 3, 50.

Chunmei J, Dan G, Zhenzhu L, Shuzhen L, Junling S, Dongyan S. Clinostat Rotation Affects Metabolite Transportation and Increases Organic Acid Production by *Aspergillus carbonarius*, as Revealed by Differential Metabolomic Analysis. *App. Env. Microb*. 2019, 85 (18) e01023-19;

Cortesão M, Schütze T, Marx R, Moeller R, Meyer V. Fungal Biotechnology in Space: Why and How? In: Nevalainen, H. (eds) Grand Challenges in Fungal Biotechnology. Grand Challenges in Biology and Biotechnology. 2020; Springer, Cham. Doi:10.1007/978-3-030-29541-7_18

Deacon, J. W. *Fungal biology*. 2013, John Wiley & Sons.

Fisher EK and Roberson RW. Hyphal tip cytoplasmic organization in four zygomycetous fungi. *Mycologia*, 2016; 108:3, 533-542, doi: 10.3852/15-226

Fricker MD, Heaton LLM, Jones NS and Boddy L. The mycelium as a network In *The Fungal Kingdom* (eds J. Heitman, B. J. Howlett, P. W. Crous, E. H. Stukenbrock, T. Y. James, and N. A. R. Gow.) pp. 335–367. American Society of Microbiology, 2017 Washington DC.

Fricker MD, Lee JA, Bebber DP, Tlalka M, Hynes J, Darrah PR, Watkinson SC and Boddy L. Imaging complex nutrient dynamics in mycelial networks. *J. Microsc.* 2008; 231, 317–331.

Galland P. The sporangiophore of Phycomyces blaskesleeanus: a tool to investigate fungal gravireception and graviresponses. *Plant Biology*, 2013; 16 (1): 58- 68.

Gomoiu I, Chatzitheodoridis E, Vadrucci S, Walther I. The effect of spaceflight on growth of Ulocladium chartarum colonies on the international space station. *PLoS One*. 2013; 24;8(4):e62130. doi: 10.1371/journal.pone.0062130.

Harding MW, Marques LLR, Howard RJ and Olson ME. Can filamentous fungi form biofilms? *Trends Microbiol*. 2009; 11, 475-80

Hernández-Rodríguez Y., Hastings S., Momany M.. (2022). The Septin AspB in Aspergillus nidulans Forms Bars and Filaments and Plays Roles in Growth Emergence and Conidiation. *Eukaryotic Cell* p. 311–323.

Jiang C, Guo D, Li Z, Lei S, Shi J, Shao D. Clinostat Rotation Affects Metabolite Transportation and Increases Organic Acid Production by *Aspergillus carbonarius*, as Revealed by Differential Metabolomic Analysis. Appl Environ Microbiol. 2019 29;85(18):e01023-19 doi: 10.1128/AEM.01023-19.

Katz D, Goldstein D, Rosenberger RF. Model for branch initiation in Aspergillus nidulans based on measurements of growth parameters. *J Bacteriol*. 1972; 109(3):1097-100. doi: 10.1128/jb.109.3.1097-1100.1972.

Lew RR. How does a hypha grow? The biophysics of pressurized growth in fungi. *Nat. Rev. Microbiol.* 2011; 9, 509–518.

Lichius A, Zeilinger S. Application of Membrane and cell wall selective fluorescent dyes for live-cell imaging of filamentous fungi. *J. Vis. Exp.* 2019; 153.

Moore D, Hock B, Greening JP, Kern V D, Frazer LN and Monzer J. Gravimorphogenesis in agarics. *Mycological Research* 1996; 100, 257– 273.

Naranjo-Ortiz MA, Gabaldón T. Fungal evolution: cellular, genomic and metabolic complexity. *Biol Rev Camb Philos Soc*. 2020 ;95(5):1198-1232. doi: 10.1111/brv.12605.

Novikova N., De Boever P., Poddubko S., Deshevaya E., Polikarpov N., Rakova N., Coninx I. and Mergeay M. Survey of environmental biocontamination on board the International Space Station. *Res. Microbiol.* 2006; 157**,** 5–12.

Novikova ND. Review of the knowledge of microbial contamination of the Russian manned spacecraft. *Microb. Ecol.* 2004; 47 (2): 127-132.

Riquelme M, Bartnicki-Garcia S. Key differences between lateral and apical branching in hyphae of Neurospora crassa. Fungal Genet Biol. 2004 Sep;41(9):842-51. doi: 10.1016/j.fgb.2004.04.006.

Romsdahl J, Blachowicz A, Chiang AJ, Singh N, Stajich JE, Kalkum M, Venkateswaran K, Wang CCC. Characterization of Aspergillus niger Isolated from the International Space Station. *mSystems*, 2018; 3(5): 1-13.

Sathishkumar Y, Velmurugan N, Lee HM, Rajagopal K, Im CK and Lee YS. Effect of low shear modeled microgravity on phenotypic and central chitin metabolism in the filamentous fungi *Aspergillus niger* and *Penicillium chrysogenum*. *Antonie van Leeuwenho*ek 2014; 106, 197–209

Sielaff AC, Urbaniak C, Mohan GBM, Stepanov VG, Tran Q, Wood JM, Minich J, McDonald D, Mayer T, Knight R. 2019. Characterization of the total and viable bacterial and fungal communities associated with the International Space Station surfaces. *Microbiome* 7:50.

Simonin A, Palma-Guerrero J, Fricker M and Glass NL. Physiological significance of network organisation in fungi. *Eukaryotic Cell* 2012; 11, 1345–1352.

Schneider CA, Rasband WS and Eliceiri KW. NIH Image to ImageJ: 25 years of image analysis. *Nature Methods*. 2012; *9*(7), 671–675. doi:10.1038/nmeth.2089

Taheri-Talesh N, Horio T, Araujo-Bazán L, Dou X, Espeso EA, Peñalva MA, Osmani SA, Oakley BR. The tip growth apparatus of *Aspergillus nidulans*. *Mol Biol Cell*. 2008;19(4):1439-49. doi: 10.1091/mbc.e07-05-0464.

Takeshita N. Coordinated process of polarized growth in filamentous fungi. *Biosci. Biotech. Biochem.* 2016; 80, 1693–1699.

Tesei D, Chiang AJ, Kalkum M, Stajich JE, Mohan GBM, Sterflinger K, Venkateswaran K. Effects of Simulated Microgravity on the Proteome and Secretome of the Polyextremotolerant Black Fungus *Knufia chersonesos*. *Front Genet*. 2021 Mar 18;12:638708.

Tlalka M, Bebber DP, Darrah PR, Watkinson SC and Fricker MD. Emergence of self-organised oscillatory domains in fungal mycelia. *Fungal Genet. Biol.* 2007; 44, 1085–1095.

Wösten HA, Moukha SM, Sietsma JH, Wessels JG. Localization of growth and secretion of proteins in *Aspergillus niger*. *J Gen Microbiol*. 1991;137(8):2017-23. doi: 10.1099/00221287-137-8-2017.

Chapter 5

Effect of long-term simulated microgravity on *Penicillium chrysogenum:* deterioration activity of technopolymers employed on International Space Station

Effect of long-term simulated microgravity on *Penicillium chrysogenum:* deterioration activity of technopolymers employed on International Space Station

INTRODUCTION

Life on Earth in its present biodiversity and complexity has developed under constant changing environmental conditions. The gravitational force, however, is one of the most constant factors guiding and affecting the evolution of all organisms (Volkmann and Baluska, 2006).

Interest in long-term effects of altered gravity on living organisms and cells has also intensified in recent years due to the increase in interplanetary travels. Planets suitable to inhibition by Earth-based life are of actual interest, and most of them are predicted to have variable gravitational forces (Kalb and Solomon, 2007; Horneck, 2008; Oczypok et al., 2012). Additionally, astronauts and biological samples sent into space are routinely subjected to microgravity once in orbit and reaching the Space Station (Hu et al., 2008).

Fungi are sensitive to changes in the direction of the gravity vector (gravitropism). However, there is limited information available on the effect of simulated microgravity conditions on fungal species responses. The relationship of a fungus with its immediate environment is defined by an array of secreted proteins and metabolites. When microorganisms are involved in the degradation of synthetic polymers, they form a surface coating to attach hyphae to hydrophobic substrates, and to enhance their cellular ability to penetrate three dimensional substrates. The release of digestive enzymes by exocytosis outside of their hyphae, induces a breakdown of macromolecules and organic molecules into smaller organic compound in order to absorb them back up, releasing CO_2 and H_2O, under aerobic conditions, and CH_4, under anaerobic conditions, if mineralization of the substrate occurs (Pathak and Navneet, 2017). Synthetic polymeric materials are often denoted as ‘‘non-degradable’’ or ‘‘bioresistant’’. However, highly stable polymeric materials such as PE, nylon and PVC have been shown to be degradable by free radicals or enzyme (Deguchi et al., 1997) The degraded polymer chains can then be used by the microorganism community as a source of nutrients. Furthermore, production of these enzymes is tightly regulated and localised within the mycelial network, which saves resources, protects the fungus from damage from highly toxic intermediate metabolites and opens up a wide array of phenotypes in their interactions with other organisms. Several studies conducted with different strains of imperfecti fungi coming from *Penicillium* genus have demonstrated their ability to

degrade different xenobiotic compounds with low co-substrate requirements (Leitão, 2009). *Penicillium chrysogenum*, in particular, is one of the species found on board the ISS (Novikova et al., 2004). Moreover, it exhibited important activities in recalcitrant compound degradation (e.g. lignin, carbon nanotubes.). The aim of this study is to understand how low gravity environments could affect fungal behaviour and how fungi interact with materials employed in spacecraft development. Ground-based methods have been developed to simulate microgravity conditions. One of these methods is the one that simulates microgravity by the random orientation of objects relative to the gravity's vector is Random Positioning Machine (RPM) and it is utilised in this research. The gravitational vector present in the bioreactor is averaged over time near zero (van Loon). Findings obtained could be potentially interesting to assure biosafety of the astronauts preventing biodegradation of spacecraft materials and provide new insights for sustainable solutions for plastic pollution and pollutant transformation challenge.

MATERIALS AND METHODS

Biological Material

Penicillium chrysogenum Thom (P28, isolate from dust in Mycology Laboratory, DiSIT, UPO) inocula were prepared as a spore suspension, collecting spores from the surface of one-week-old Petri dish culture on MEA (Malt Extract Agar, Oxoid) using sterile physiological solution (NaCl, 0,9%). The suspension was adjusted to a concentration of 10^6 spores/ml.

Materials samples

Materials samples were selected among those employed on the ISS. These materials were supplied by Etan Laboratory (Engineering Technological Area for Nanotechnologies for Space; Thales Alenia Space, Turin). The samples were classified as technopolymers according to their chemical nature, their types of processing, and their practical applications. Technopolymers characteristics are listed, as below.

Technopolymer (PU) is a polyurethane ethylene-vinyl acetate polymer with two different sides, the blue one (rough) and the grey one (smooth).

PU + PES + EVOH + PU

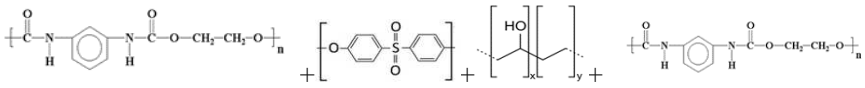

Technopolymer (PA) is a poli-para-fenileneterephatalamide, an heat-resistant synthetic para-aramid fibre with numerous inter-chain bonds that increase the resistance.

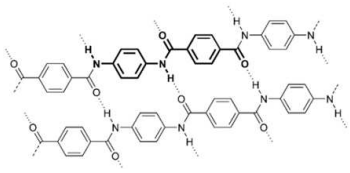

In particular, the network of hydrogen bonds provides a tensile strength 10 times greater than steel for the same weight. Known for its use in bulletproof vests, it also lends itself to numerous other applications thanks to its high tensile strength to weight ratio. Provides a strong protective barrier against rips, cuts and punctures. It is intrinsically flame resistant, the fibres do not melt, do not drip and do not favour combustion, protecting against thermal risks up to 426.667.

Technopolymer (PI) is a polyimide film obtained from the polycondensation of an aromatic acid and an aromatic diamine; the resulting structure gives the material excellent physical, chemical and electrical properties. It has an aluminium coating.

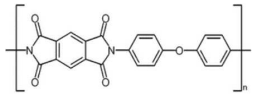

It has excellent mechanical strength and excellent thermal resistance (from -269 ° C to +400 °C). It is used in all electrical equipment that requires excellent electrical insulation and as a pipe insulator.

Technopolymers samples were cut into small pieces of 6*1 cm and autoclaved at 120°C for 5 minutes (PU and PI) or sterilised in 100% EtOH for 10 minutes (PA) and washed twice with sterile deionized water for 10 minutes. The initial study was completed along with a morphological examination.

Simulated microgravity condition

Microgravity conditions were simulated using an RPM connected to a control console through standard electrical cables (Dutch Space, Leiden, The Netherlands). The apparatus is a 3D clinostat consisting of two independently rotating frames. This device does not eliminate gravity, but the RPM is a micro-weight simulator based on the principle of "gravity-vector averaging": it allows a 1 g stimulus to be applied omnidirectionally rather than unidirectionally, and the sum of the gravitational force vectors tends to equal zero ($1x10^{-6}$ G). The effects generated by the RPM are comparable to the impact of real microgravity, provided that the direction changes are faster than the system's response time to the gravity field. The desktop RPM used was positioned within an incubator to maintain the temperature.

Experimental Setup

The technopolymers were placed in 6 cm in diameter plates ts with low glucose (10 g/l) Potato Dextrose Agar medium (PDA, Oxoid). Three replicates for each material were inoculated with 5µl of 10^6 spores/ml of *P. chrysogenum* suspension and placed into the 3D-RPM inner frame. The same has been done for plates with materials without inocula. Controls for all tests were cultured in the same conditions without rotation. All incubations were carried out at 24±2°C for 60 days.

Mycodegradation Analysis

Mycodegradation analysis was performed on 9 points for each side of materials. The samples used were washed, to remove both the culture medium and the fungus, dried carefully (4h at 37 °C). If the materials had two sides with different composition and/or morphology, the analyses were carried out on both sides (PU and PA). The technopolymer samples were processed with CA (optical Contact Angle**)**, SEM (Scanning Electron Microscopy) and ATR (Attenuated Total Reflectance).

CA measurements

The wettability of the material surface was obtained by measuring the optical contact angles (CA) that was performed on materials before and after biotic exposure. Wettability of each surface was determined by drop measurements of the advancing water contact angle (θ) using a CAM 200 from KSV Instruments. The analyses involve

one drop of 4µl of Millipore grade distilled water on the surface of the material. Advanced contact angles are presented as mean ± standard deviation. The measurements were made at 20 ± 2 °C. The average of these points will give the final contact angle that will allow to define material as hydrophobic or hydrophilic. For tissues materials, it was not possible to perform the CA test, given the presence of empty spaces.

Scanning electron microscopy (FE-SEM) analysis

The surface morphology before and after biotic exposure was investigated using Keysight U9320B. The samples were coated with a gold thin layer (10-20 nm) after passing the pure and dry argon gas in the coating chamber, under vacuum for a sputtering time of 30s. The plate voltage was 2000 V and the current passed was 25 mA. The samples were settled on carbonious stabs.

Scanning electron microscopy (ESEM-EDX) analysis

Element analyses to detect the presence of aluminium were carried out on technopolymers before and after biotic exposure and also on mycelia far from the material samples. The analyses were carried out with 10KeV EDS landing energy using a FE-SEM Keysight U9320B.

Fourier transform infrared (FTIR) spectroscopy combined with attenuated total reflectance (ATR) analysis

Sample analyses are performed directly using ATR-FTIR (Thermo Fisher Nicolet iS50); there is no preparation of samples. The analyses are superficial and the depth corresponding to the spectral region covered is less than 4 µm.

RESULTS

PU is a polyurethane ethylene-vinyl acetate polymer with two different sides, the blue one (rough) and the grey one (smooth); analyses were performed on both sides. CA values were evaluated for both sides of PU before sterilisation (with autoclave), before inoculation and after inoculation. Each of these experimental replicates was performed in terrestrial gravity and simulated microgravity conditions. The rough surface of PU had a contact angle of ΘL 89° and ΘR 90° which did not change after autoclaving (fig.1a). In the culture medium-only samples, a slight decrease in angle (ΘL: 75° and - ΘR: 76°) was observed. However, the decrease in presence of the fungus in terrestrial gravity was higher (ΘL 62° and ΘR 62°; fig.1b) than under simulated microgravity (ΘL 69° and ΘR 71°). In conjunction with the reduction of the angle, the reduction of the

roughness of the material was also noted macroscopically. The CA of the smooth surface did'n show any differences in all conditions tested (fig.1c, d).

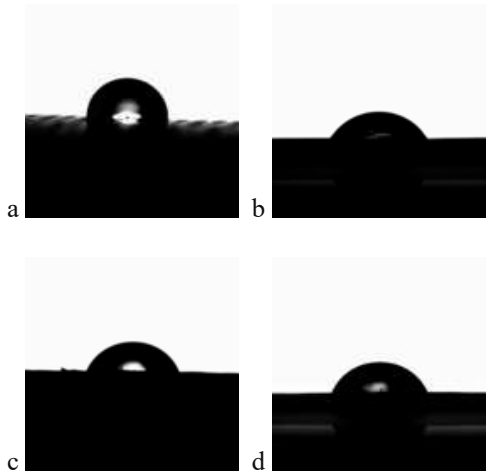

Fig.1 Comparison of PU blue (a and b) and grey (c and d) before any treatment (a and c), after the fungal inoculum (b and d). Contact angle measurement and roughness are reduced on the blue side inoculated with *P. chrysogenum*.

Physical alterations, such as roughness of the surface and the formation of holes, cracks, and crumbling were performed by scanning electron microscopy (SEM). Changes on the PU surface were visible both on the rough side (blue; fig.1c, d) and on the smooth side (grey; fig.1e, f) in the samples where the fungus was developed. The surfaces appeared to be corroded on samples inoculated with *P. chrysogenum* kept both under static conditions and in simulated microgravity.

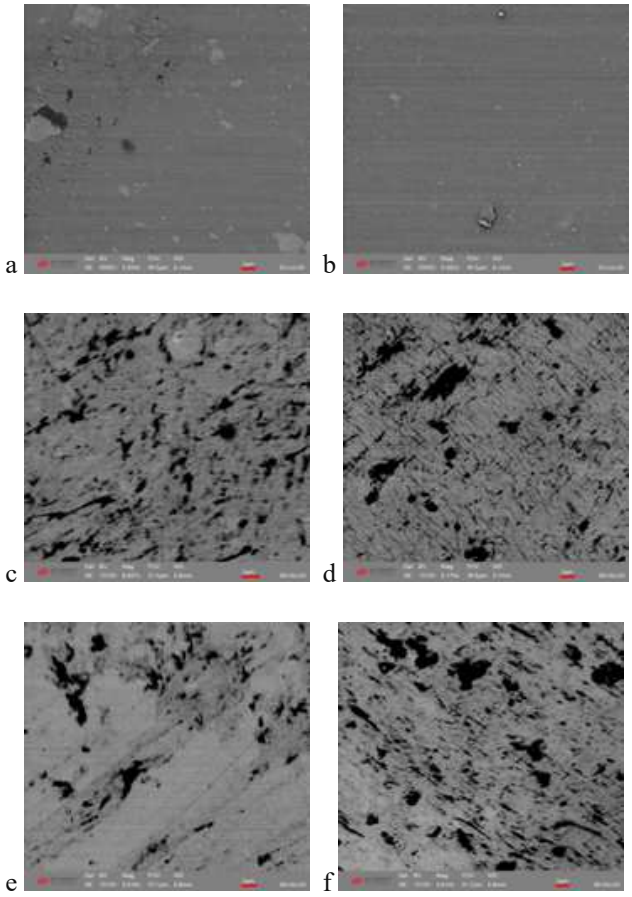

Fig.2 SEM micrograph of blue side (a, c, e) and grey side (b, d, f) of PU. Analyses have been performed on samples before the fungal inoculum (a, b), used as controls, and on samples inoculated and kept under terrestrial gravity (c, d) or under simulated microgravity (e, f). Scale bar: 2 μm.

Chemical changes induced by fungal activity were evaluated by Fourier transform infrared spectroscopy (FTIR) coupled with ATR were determined (fig.3). These alterations were a reduction at 3325,97 cm^{-1} (blue side, fig.3b) and at 3332,25 cm^{-1} (grey side, fig.3c) which could correspond to an N-H stretching of a secondary amine (Silverstein, 2005). The newly appearing peaks at 1472.42 cm^{-1} (blue side, fig.3b) and 1471.98 cm^{-1} (grey side, fig.3c) wavenumbers could be traced back to a primary amine (Silverstein, 2005) and CH_2 bending (Hu et al., 2008). In addition, following the fungal inoculum, it was possible to observe the disappearance of the peak at 1729.13 cm^{-1}, attributed to the stretching of the carbonyl, both in the spectrum relative to the blue side and that close to the grey side (Russel et al., 2011). In both spectra (blue and grey, fig. 3b, c), the absence of the peak at 1529.06 cm^{-1} suggests a N-H bending vibration attributable to a secondary amine (Silverstein, 2005). Spectra of samples inoculated

with *P. chrysogenum* suspension and kept under simulated microgravity showed no difference compared to control growth under static condition.

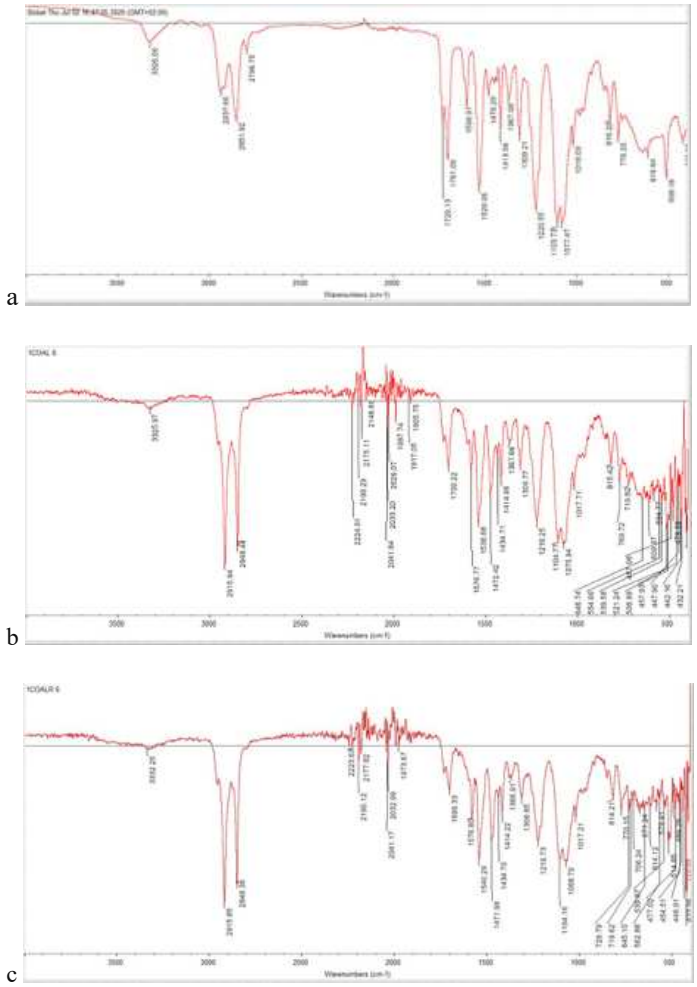

Fig.3 ATR-FTIR spectra of PU samples before (a) and after fungal inoculation: blue side (b) and grey side (c) inoculated with *P. chrysogenum*

PI is a two-sided material: an aluminium coated side and an orange one with polyimides exposed. The values of the angles measured with the CA analyses of PI shown differences between the surface covered by a layer of aluminium (ΘL: 76° and ΘR: 76°; fig.4) and the polymer surface (ΘL: 67° and ΘR: 67°). The surface covered by a layer of aluminium has undergone variations involved the aluminised surface of both samples placed in medium without the fungus (ΘL:84° and ΘR: 84°; fig.4b) and the samples inoculated with the fungus not exposed to microgravity (ΘL:87° and ΘR: 87°). PI has been altered after sterilisation in autoclave, so the experiments were carried out

by sterilising the material with ethanol. The values of the contact angles were also carried out after sterilisation with ethanol, and there was a decrease on the metal surface to ΘL: 60° and ΘR: 61° (fig.4b), but not on the polymer surface (ΘL: 65° and ΘR: 65°).

Samples subjected to simulated microgravity did not have the metallic layer, so it was impossible to measure the CA of the metallic layer altered by the presence of the fungus. However, it was possible to obtain the value corresponding to the contact angle of the eroded surface, which is varied concerning the unaltered polymeric surface, showing values of ΘL: 47° and ΘR: 47° for the samples inoculated with the fungus exposed to simulated microgravity and of ΘL: 46° and ΘR: 46° with the fungus not exposed to microgravity (fig.4c).

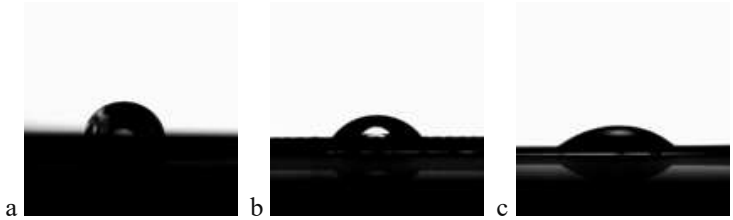

Fig.4 Comparison of PI aluminized side before any treatment (a), after the sterilisation in ethanol (b), and after *P. chrysogenum* inoculum cultured in static condition (c). Contact angle measurements are reduced on inoculated samples.

By scanning electron microscopy (SEM) coupled with X-ray diffraction physical alterations such as stripings were analysed on the aluminised surface of PI before any treatments (fig.5). After inoculum with *Penicillium chrysogenum,* there were numerous cracks and crumbling only on the aluminised surface. The surfaces appear to be more corroded under simulated microgravity (aluminised surface of PI was completely absent in larges area) than in static conditions.

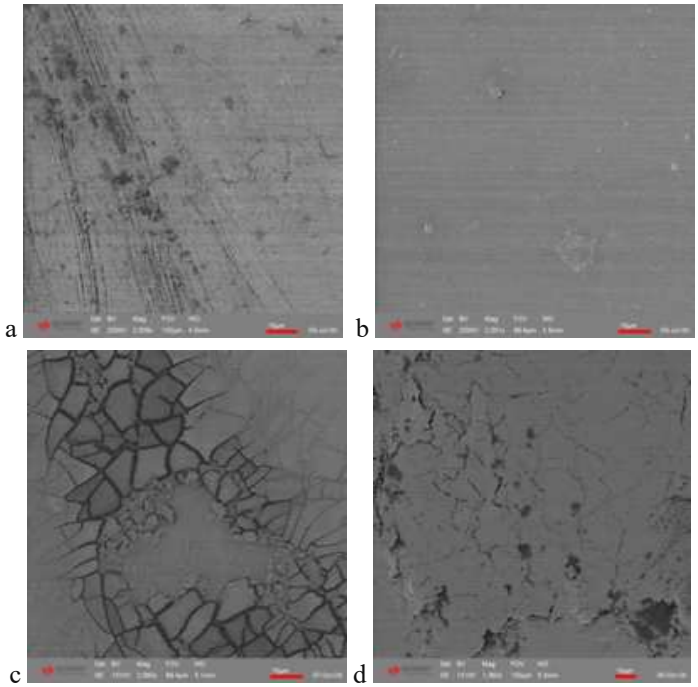

Fig. 5 SEM micrograph of aluminized side (a, c, d) and polymeric orange side (b) of PI. Analyses have been performed on samples before the fungal inoculum (a, b), used as controls, and on samples inoculated kept under terrestrial gravity (c) and under simulated microgravity (d). Scale bar: 10µm.

The analysis of the mycelium that was far from the PI sample by X-ray diffraction also showed Aluminium presence in hyphae of *Penicillium chrysogenum* (fig.6a, b). EDX analyses were performed on mycelia samples on nine random areas of 581µm^2 (fig.6c).

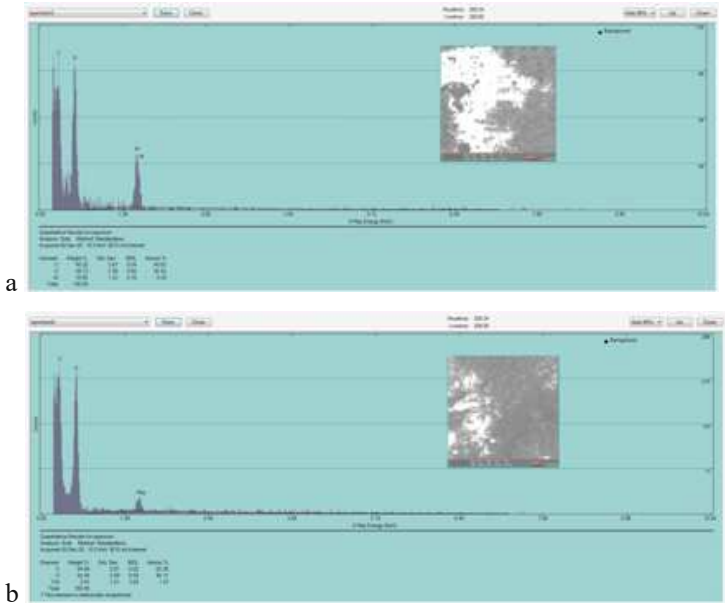

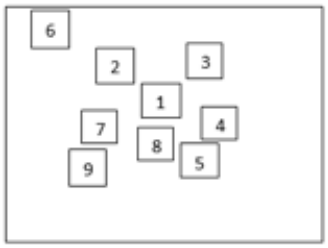

c

Fig.6 EDX spectra to detect aluminium presence in *P. chrysogenum* mycelium (a, b). Random areas of 581µm^2 analysed in 9 different fields of view (c).

Considering results collected with previous analyses, FTIR-ATR was performed in order to evaluate PI chemical changes. Based on the data reported by Corregidor et al. (2019), it was possible to allocate the peaks of the spectrum of the aluminium side. Analyses performed on the aluminized side highlight more changes in samples inoculated with fungus. The aluminium layer in some cases completely disappears and the characteristic polyamide peaks (similar to those found on the orange side) appear. No significant variations of the orange side spectra are observed, except for strong attenuation of the peak at 2923.32 cm^{-1} attributed to C-H asymmetric stretching (Zieba-Palus et al., 2017) in simulated microgravity condition.

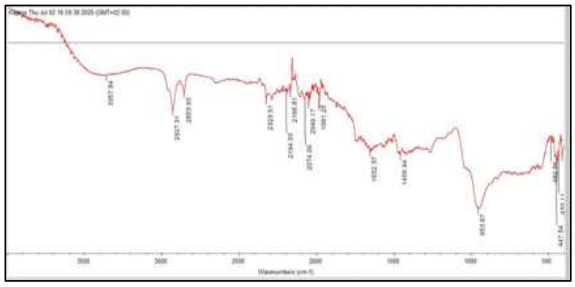
a

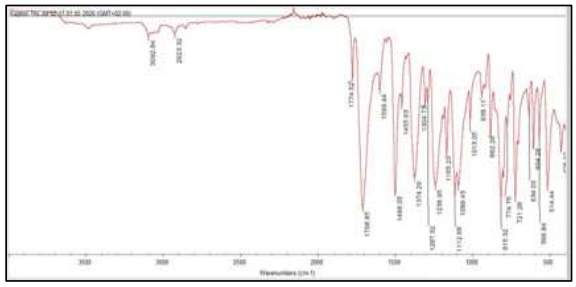
b

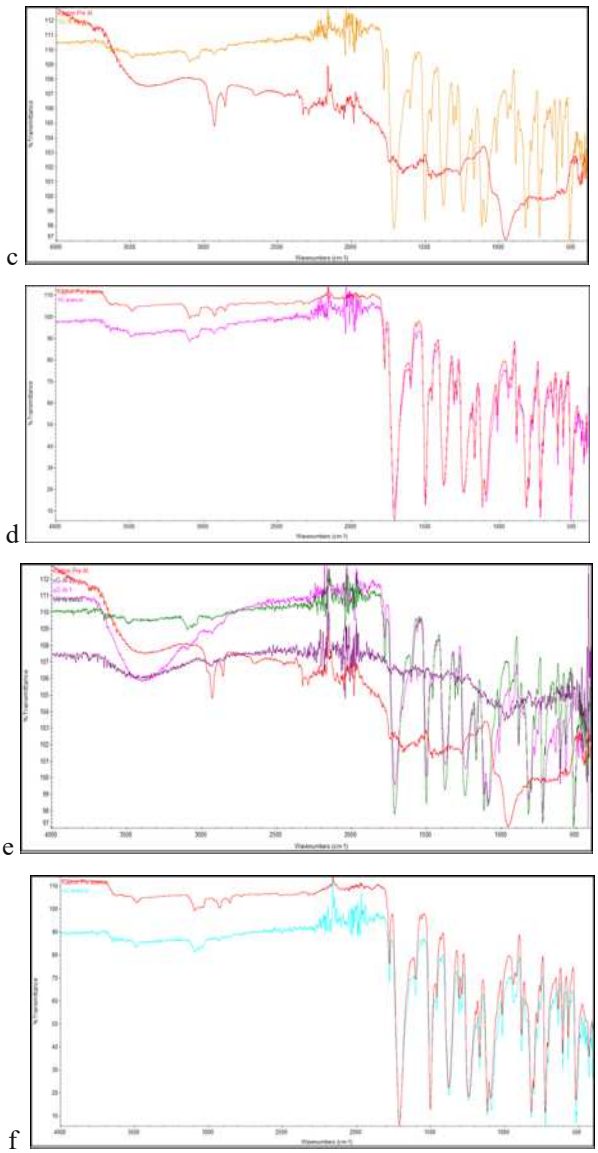

Fig.7 ATR-FTIR spectra of PI aluminized side (a, c, e) and polymeric orange side (b, d, f). Analyses have been performed on samples before (a and b) and after the *P. chrysogenum* inocula kept in terrestrial condition (c and d, red line) or in simulated microgravity condition (e, violet and pink line, and f, red line). Analyses on the aluminized side in degraded areas were performed on samples inoculated with *P. chrysogenum* and kept under simulated microgravity conditions (e, green line).

PA is a para-aramid, aromatic polyamide. It is a tissue and was not possible to perform the CA test, given the presence of empty spaces. PA control samples observed by scanning electron microscopy (SEM, fig.8) show fibres of different sizes; in particular, the largest fibres have a smooth surface before the fungal inoculum. Alterations of the largest fibres have been observed in samples tested with the fungus. Areas of erosion,

holes and cracks due to fungal development appeared both in conditions of terrestrial gravity and in simulated microgravity, even thought with different pattern of erosions.

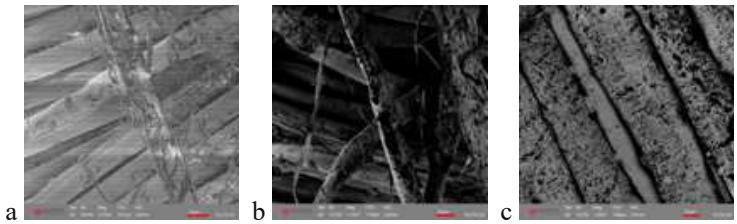

Fig.8 SEM micrograph of PA before (a) and after fungal inocula developed under terrestrial (b) and simulated microgravity condition (c). Scale bar: 10µm.

Following the fungal inoculum, FTIR-ATR analysis shows no significant variations in spectra (fig.9), except for the disappearance of the peak at 2921.17 cm^{-1} attributed to C-H synthetic polymers asymmetric stretching (Zieba-Palus, 2017) in spectra related to both terrestrial gravity and simulated microgravity tests.

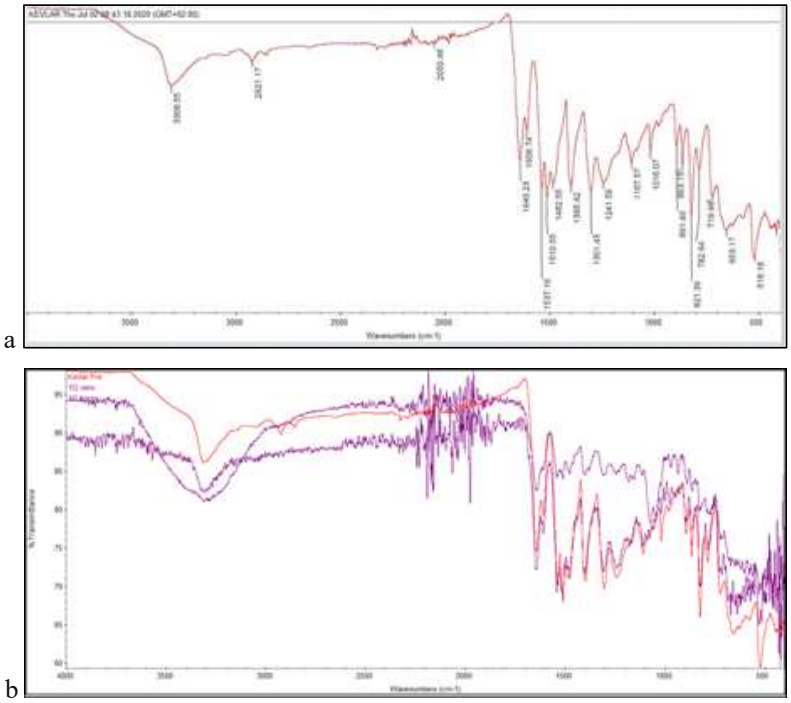

c 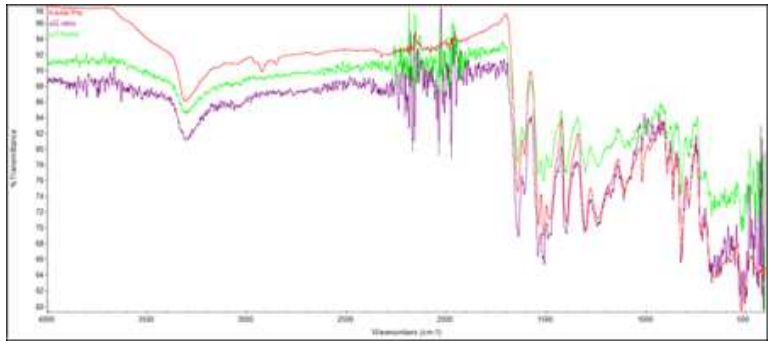

Fig.9 ATR-FTIR spectra of PA samples before (a, red line) and after *P. chrysogenum* inocula kept in terrestrial (b, violet line) and in simulated microgravity conditions (c, green and violet line).

DISCUSSION

The Russian experience with the Mir orbiting station (1986-2001) has shown that long-duration space missions present a series of problems related to the health of the crew and the integrity of the materials constituting the station. Among these problems, those associated with the microbial communities present on board have particular implications (Mishra et al., 1992; Pierson et al., 1994; Novikova, 2004). Direct damage occurs when the material is used as a nutritional source by the microorganism growing on the surface; indirect damage results from the production of various enzymes and organic acids resulting from the metabolism of microorganisms and fungi (Klintworth et al., 1999). Although procedures aimed at minimising the microbial load are applied to each ISS module and to all cargo spacecraft, during production and shipping to orbit, bacterial and fungal colonies are still present and capable of surviving and reproducing in the space environment. In orbit, corrosion induced by biological agents pose a very significant risk factor, especially in long-term missions (Klintworth et al., 1999). It has been seen that both fungi and bacteria are capable of colonising a wide range of high-strength polymeric materials. These materials have an important structural function for spacecraft, moreover some of these polymers, used as electrical insulators, are fundamental in flight control operating systems (Gu et al., 2007). A well documented example of microorganism's ability to colonise spacecraft materials was the progressive degradation of a window in quartz of Mir station module. This event was largely due to the growth of *Bacillus polymira*, *Penicillium chrysogenum* and several species of *Aspergillus* (Pierson et al., 1994; Zaloguyev et al., 1985). Fungal species identified as responsible for the deterioration materials employed on Mir Station are the same isolated from ISS and belong to the genera *Penicillium*, *Aspergillus* and *Cladosporium* (Alekhova et al., 2005). *Penicillium chrysogenum,* with its degradation

activity, has been selected for tests carried out in this work under terrestrial and simulated microgravity conditions, exploiting Random Positioning Machine (RPM). Analyses performed on technopolymers inoculated with *P. chrysogenum* suspension indicate that some technopolymers can be altered by fungal metabolic activities, which can be influenced by simulated microgravity.

Based on their chemical structure, composition synthetic polymers can be potential substrates for the growth of heterotrophic microorganisms. The biodegradability of polymers also depends on their molecular weight, their crystalline structure and their physical characteristics. Moreover, the initial adhesion of bacteria and fungi to the material could be mediated by some characteristics of the material surface, such as texture, hydrophobicity and smoothness (Gu et al., 2007). The analysed polymers, especially those that appear as fabrics, were found to be susceptible to fungal attack due to the easy adhesion of the hyphae to the material. Polymers mycodegradation was evaluated through physical and chemical testing methods. In some cases, such as that of PU, the observation of the surface before and after the development of *P. chrysogenum* through the CA analysis revealed differences in surfaces hydrophobicity attributable to fungal development in terrestrial gravity and simulated microgravity conditions on the rough side. PU appears to be modified by the development of *P. chrysogenum* under both gravity conditions. Indeed, SEM analysis performed on inoculated PU samples kept for 60 days at 25 °C in conditions of terrestrial gravity and simulated microgravity, showed considerable differences in surfaces attributable to fungal development on materials. The ATR spectra confirmed alteration observed and revealed evident attenuations of the peaks at 3325.97 cm^{-1} (blue side) and at 3332.25 cm^{-1} (grey side) that probably correspond to N-H stretching. Related to this phenomenon is the appearance of new peaks at 1576.77 cm^{-1} (blue side), at 1576.80 cm^{-1} (grey side) and at 1472.42 cm^{-1} (blue side) and at 1471.98 cm^{-1} (grey side). According to the information reported by Silverstein (2005), the peak attenuation could correspond to a secondary amine, while the new peaks could correspond to an N-H bending vibration of a primary amine and to the scissoring mode of $–CH_2$ (Garidel et al., 1999). These results suggest that urethane bond degradation could have occurred. According to Malikova et al. (2010) this dissociation mechanism could be explained by the reaction that determines the dissociation of the polyurethane bond into primary amine, carbon dioxide and alkene:

$$-R\text{-}CH_2\text{-}NH\text{-}CO\text{-}O\text{-}CH_2\text{-}CH_2\text{-}R' \rightarrow -R\text{-}CH_2\text{-}NH_2 + CO_2 + CH_2{=}CH\text{-}R'$$

Malikova et al. (2010) reported that this reaction occurs in an acidic environment and begins with ester or ether oxygen attacked by hydrogen ions. In an advanced stage of degradation, the unsaturated group CH_2=CH- could become an oxidation site by free radicals. An acid environment is in agreement with mycelial development and ROS could be produced by fungi under stress situations, such as simulated microgravity. Moreover, Chunmei and collaborators (2019) showed that the concentration of organic acids, in particular the intermediate products of the TCA cycle, such as citric acid and isocitric acid, is greatly increased in the colonies exposed to simulated microgravity. The observed decrease of the secondary amine could be explained by assuming that the hydrolysis of the urethane bond took place by proteases, able to break the urethane group amide bond (Magnin, 2020). Mccarthy et al. (1997) also report the appearance of a minor peak relative to the absorbance of N-H stretching close to 3300 cm^{-1} as an index of material degradation. The PU spectrum obtained with ATR-FTIR analyses shows also the disappearance of the peak at 1729 cm^{-1} attributable to the stretching of the carbonyl. A progressive reduction in the relative intensity of this peak, up to its complete loss, is associated with the hydrolysis of the ester bond in the urethane connection. This phenomenon was reported by Russel et al. (2011) who identified the *Pestalotiopsis microspora as* species able to synthesise serine-hydrolase enzymes for PUR degradation, in order to exploit the polymer as a carbon source in anaerobic conditions. Biodegradation could induce variation in molecular structure of materials evaluated by FTIR spectroscopic analysis. Alvarez-Berragàn et al. (2016) showed a loss of carbonyl groups (C=O) (1,729 cm^{-1}) and bonds C-N-H (1,540 e 1,261 cm^{-1}) performing FTIR and gas chromatography (GC-MS) analysis on degraded impranil by *Cladosporium spp., Aspergillus fumigatus* and *Penicillium chrysogenum*. Results collected showed a decrease in ester compounds and an increase in alcohols and di-isocyanate, suggesting hydrolysis of ester and urethane bonds. The degradation of the ether bond described in the literature could be related to monooxygenases, identified as enzymes able to break this bond in polyurethane polymer. Other studies on fungal degradative activity on polymers, highlight fungal production of extracellular proteolytic enzymes, such as urease, papain and subtilisin (Schink et al., 1992; Howard, 2002). On this material no differences in mycodegradation related to gravity condition were observed.

The mycodegradation was visible also for PI. Samples inoculated with the *P. chrysogenum* show altered FTIR-ATR spectra on the aluminium-coated side; in particular fungal development alters the aluminium layer until it disappears, under simulated microgravity conditions. In some cases, the characteristic peaks of the polyimide, similar to those found on the orange side (without aluminium coating). It is known that fungi are able, through normal growth processes, to acidify the medium. Moreover, the clinostat rotation results in an increase in the accumulation of organic acids and in lower levels of transport of metabolites from the cell to the surrounding substrate. The ESEM analyses carried out in the areas of mycelium developed in the plates containing PI which showed altered areas of the aluminium coating show the presence of aluminium in the fungal mycelium. *P. chrysogenum* is able to move aluminium from the polyimide coating to hyphae far from the PI sample. Jiròn-Lazos et al. (2018) described a mechanism involved in aluminium consumption by fungi. They observed the aluminium alloy AA 6061 break down in correspondence of anodic zones (generating Al^{3+} ions), the resulting electrons are transferred to cathode zones to be used by protons through the fungal activity, reaching a final acceptor, the oxygen. This mechanism supports fungal metabolism and provides energy for growth and synthesis of metabolites. Electron transport maximises the oxygen reduction, improves cellular respiration and accelerates the corrosion process tied to fungal enzymes involved in the synthesis of acids. The acids produced by the fungus can generate protons which maintain the cathodic reaction. Fungal growth and oxygen consumption make the environment microaerobic in different points causing localised corrosion, that seems to be enhanced under simulated microgravity.

These results, together with those of Huang et al. (2018), demonstrate that simulated microgravity through the use of the clinostat has an important effect on the metabolism of microorganisms; furthermore, the analysis of the metabolic pathways has shown that the simulated microgravity has an effect mainly on the metabolism of amino acids and on the pathways associated with the production of energy in *A. carbonarius* (Chunmei et al., 2019). The ability of fungi to solubilize insoluble metals depends on the excretion of organic acids such as oxalic acid and citric acid which not only lower the pH of the medium but are also able to complex the metals making them more soluble (Gadd, 2017).

PA is a para-aramid, aromatic polyamide. This is an intertwined tissue and it does not present a surface due to this peculiar characteristic it was not possible to assess the

hygroscopicity with CA. SEM images confirm that the fungus has been able to break down the complex polymer, as observed for PU and PI. The observed grooves and cracks highlight the low resistance of these two materials to fungal activity. In particular PA observed with SEM shows fibres of different sizes, the larger ones exhibit a smooth surface before the fungal inoculum. The analysed tissue presented fibres with different dimensions, the larger ones were those that showed greater alterations in the samples inoculated with fungi. Alteration of fibres surfaces caused by fungal development occurred in all samples inoculated with *P. chrysogenum*, cultured in terrestrial gravity and in simulated microgravity. Except for the disappearance of the peak at 2921.17 cm^{-1} attributed to C-H_2 asymmetric stretching in spectra related to fungal inoculated samples in both terrestrial gravity and microgravity conditions, FTIR-ATR analysis on PA materials shows a slight general decrease in the intensity of all peaks, compared to control samples (Zieba-Palus, 2017). Spectra explanations are difficult because of a high background noise due to the nature of this material, which, being a woven fabric made of fibres, presents discontinuities that could cause light to pass through and disturb the recording of the spectrum.

Molecular analyses performed on *P. chrysogenum* growth on technopolymers and kept under microgravity conditions can help to identify enzymes and pathways involved in materials degradation, allowing to better explain results obtained.

CONCLUSION

The gravitational force is one of the most constant factors guiding and affecting the evolution of all organisms. Fungi are sensitive to changes in direction of the gravity vector (gravitropism). Nowadays there is limited information available on the effect of simulated microgravity conditions on fungal species responses. In the present study, *P. chrysogenum* inoculated on different technopolymers, employed on ISS, was kept on simulated microgravity for a long time (60 days) in order to evaluate its deterioration activity on technopolymers. To assess mycodegradation we evaluated physical and chemical changes in synthetic polymers induced by fungal activities. The materials analysed appear to be susceptible to *Penicillium chrysogenum* degradation activity under terrestrials and simulated microgravity conditions.

These data suggest an influence of simulated microgravity on fungal metabolic activities, that seems enhanced on PI samples. However, results collected lead the way to in-depth analyses in order to identify the production of enzymes and better characterise mycodegradation processes under simulated microgravity.

REFERENCES

Alekhova TA, Aleksandrova AA, Novozhilova TIu, Lysak LV, Zagustina NA and Bezborodov AM. Monitoring of microbial degraders in manned space stations. *Prikl Biokhim Mikrobiol*. 2005; 41(4):435-43. Russian. PMID: 16212041.

Álvarez-Barragán J, Domínguez-Malfavón L, Vargas-Suárez M, González-Hernández R, Aguilar-Osorio G, Loza-Tavera H. Biodegradative Activities of Selected Environmental Fungi on a Polyester Polyurethane Varnish and Polyether Polyurethane Foams. *Appl Environ Microbiol*. 2016; 82(17):5225-35. doi: 10.1128/AEM.01344-16.

Corregidor F, Cuesta PM, Acosta DE, Destefanis HA. Composite ZSM-5/MCM-41 material obtained from a green re source and its enhanced catalytic performance in the reaction of vinyl acetate and isoamyl alchol, *Applied Catalysis A: General*, 2019; 587: 1-11.

Deguchi T, Kakezawa M, Nishida T. Nylon biodegradation by lignin-degrading fungi. *Appl Environ Microbiol*. 1997 ;63(1):329-31. doi: 10.1128/aem.63.1.329-331.1997.

Gadd GM. Geomycology: biogeochemical transformations of rocks, minerals, metals and radionuclides by fungi, bioweathering and bioremediation. *Mycol Res*. 2007 ;111(Pt 1):3-49. doi: 10.1016/j.mycres.2006.12.001.

Garidel, P., Blume, A., Hubner, W., 1999, A Fourier transformation infrared spectroscopic study of the interaction of alkaline earth cations with the negatively chared phospholipid 1,2-dimyrisitoyl-sn-glycero-3-phosphoglycerol, Biochimica et biophysica Acta (BBA)-Biomembranes,1466: 245-259.

Gu J.-D., 2007, Microbial colonization of polymeric materials for space applications and mechanisms of biodeterioration: A review, International Biodeterioration and Biodegradation, 59: 170-179.

Horneck, G., Klaus, D.M., and Mancinelli R.L., 2010, Space Microbiology, Microbiology and Molecular Biology Review, 74 (1): 121-156.

Howard, G. T., 2002, Biodegradation of polyurethane: a review, International Biodeterioration and Biodegradation Journal, 49:245–252

Hu C, Hao H, Ma B, Yuan Y, Liu F, Li L. A new respiratory training system for astronauts. In: Peng, Y., Weng, X. (eds) 7th Asian-Pacific Conference on Medical and Biological Engineering. *IFMBE Proceedings*. 2008; vol 19. Springer, Berlin, Heidelberg. Doi:10.1007/978-3-540-79039-6_46

Huang B, Li DG, Huang Y and Liu CT. Effects of spaceflight and simulated microgravity on microbial growth and secondary metabolism. *Mil Med Res* 2018;5, 18.

Jiròn-Lazos, U., Corvo, F., De la Rosa, S. C., Garcìa-Ochoa, E. M., Bastidas, D. M., Bastidas, J. M., 2018, Localized corrosion of aluminium alloy 6061 in the presence of Aspergillus niger, International Biodeterioration and Biodegradation, 133: 17-25.

Kalb R, Solomon D. Space exploration, Mars, and the nervous system. Arch Neurol. 2007 ;64(4):485-90. doi:10.1001/archneur.64.4.485.

Klintworth, R., Reher , H.J., Viktorov, A.N., Bohle, D., 1999, Biological induced corrosion of materials. II. New test methods and experiences from MIR station, Acta Astronautica, 44 (7-12): 569–578.

Leitão AL. Potential of Penicillium species in the bioremediation field. *International journal of environmental research and public health*, 2009; *6*(4), 1393-1417.

Magnin A, Pollet E, Phalip V and Avérous L. Evaluation of biological degradation of polyurethanes. *Biotechnology Advances*, 2020; *39*, 107457.

Malíková M, Rychlý J, Matisová-Rychlá L, Csomorová K, Janigová I, and Wilde HW. Assessing the progress of degradation in polyurethanes by chemiluminescence. I. Unstabilised polyurethane films. *Polymer Degradation and Stability*, 2010; *95*(12), 2367-2375.

McCarthy SJ, Meijs GF, Mitchell N, Gunatillake PA, Heath G, Brandwood A and Schindhelm K. In-vivo degradation of polyurethanes: transmission-FTIR microscopic characterization of polyurethanes sectioned by cryomicrotomy. *Biomaterials*, 1997; *18*(21), 1387-1409.

Mishra SK, Ajello L, Ahearn DG, Burge HA, Kurup VP, Pierson DL, Price DL, Samson RA, Sandhu RS, Shelton B. Environmental mycology and its importance to public health. J. Med. Veterin Mycol. 1992; 30 (1): 287–305.

Novikova ND. Review of the knowledge of microbial contamination of the Russian manned spacecraft. *Microbial Ecology*, 2004; 47 (2): 127-132.

Novikova ND, De Boever P, Poddubko S, Deshevaya E, Polikarpov N, Conix I, Mergeay M. Survey of enviromental biocontamination on board the International Space Station. *Research in microbiology*. 2005; 157: 5-12.

Oczypok EA, Etheridge T, Freeman J, Stodieck L, Johnsen R, Baillie D, Szewczyk NJ. Remote automated multi-generational growth and observation of an animal in low Earth orbit. *J R Soc Interface*. 2012; 7;9(68):596-9. doi: 10.1098/rsif.2011.0716.

Pathak, V. M., Navneet, 2017, Review on the current status of polymer degradation: a microbial approach, Bioresources and Bioprocessing, 4 (15): 1- 31.

Pierson DL, McGinnis MR, Viktorov AN. Space Biology and Medicine, Vol. II: Life Support and Habitability in: F.M. Sulzman, A.M. 1994; Genin (Eds, American Institute of Aeronautics and Astronautics,Washington, DC, pp. 77–93.

Russell JR, Huang J, Anand P, Kucera K, Sandoval AG, Dantzler KW and Strobel SA. Biodegradation of polyester polyurethane by endophytic fungi. *Applied and environmental microbiology*. 2011; *77*(17), 6076-6084.

Schink B, Janssen PH, Frings J. Microbial degradation of natural and of new synthetic polymers FEMS *Microbiology Reviews*, 1992 103(2/4):311–316.

Silverstein RM, Webster FX, Kiemle DJ. Spectrometric Identification of Organic Compounds, 7° edn, 2005; JOHN WILEY and SONS, INC., Hoboken (USA).

Van Loon JJWA. Some history and the use of random positioning Machine, RPM, in gravity related research, Advances in Space Research, 2007; 39: 1161-1165.

Volkmann D and Baluška F. Gravity: one of the driving forces for evolution. *Protoplasma*, 2006; *229*(2), 143-148.

Zieba-Palus and Neeved. The usefulness of infrared spectroscopy in examinations of adhesive tapes for forensic purposes. *Forensic Science and Criminology*. 2017; 2(2):1-9.

Chapter 6

Micodegradetion of multilayer polyurethane: could long-term simulated microgravity affect this process?

Micodegradetion of multilayer polyurethane: could long-term simulated microgravity affect this process?

INTRODUCTION

Fungi are ubiquitous microorganisms able to colonise different closed environments, such as the International Space Station (ISS). Human space exploration is envisioning long-term spaceflight missions. In this scenario it becomes really important to know the effects of long-term microgravity conditions on microorganisms, able to grow in Space, to preserve crewed spacecraft safety and to prevent biodegradation of spacecraft materials. More than 126 species of fungi belonging to the genera *Penicillium*, *Aspergillus*, *Cladosporium* and *Candida* have been isolated on Space Station (Sielaff et al., 2019). Previous works reported that some fungi proliferate more rapidly under microgravity conditions, increasing their pathogenicity (Rosenzweig et al, 2010; Wang et al. 2020). Altered physiology and virulence could be not only a potential threat to astronauts' health, but also for the Space Station materials integrity. Moreover, opportunistic pathogens and species involved in biodeterioration of structural materials have been identified in food and waste storage and recycling systems (Novikova et al., 2004).

Thanks to the notable enzyme set, fungi are able to germinate and develop on different substrates (e.g. life support systems, windows, control panel, etc.) changing their structural properties (Klintworth et al., 1999; Checinska et al., 2015). Their growth is usually associated with materials degradation due to the biofilms formation and with direct and indirect damages, causing ageing of material and alterations in the functioning of technical systems and equipment. Direct damage occurs when the material is used as a nutritional source by the microorganism growing on the surface; indirect damage results from the production of various enzymes and organic acids resulting from the metabolism of fungi (Klintworth et al., 1999). As a result of biological damage, some characteristics such as colour, strength, resistance and structure of the materials can change thus resulting in the formation of leaks and perforations. In the recycling pipes of life support systems, biofilms and aggregates of microorganisms have been described, this resulted in a blockage of water filtering and ventilation systems (Klintworth et al., 1999).

Nowadays, polymers are very popular and widely available materials. The main reasons for their popularity are the great diversity of synthetic polymers available, the variety of processing techniques that can be applied to them, and the possibility of adding substances to them as they are manufactured. There are currently a wide variety of synthetic materials on the market. The chemical composition of the polymer is responsible for its properties. However, the chemical nature of the polymer is not the only factor that influences its properties and its long-term behaviour. Various processing methods can lead to films, fibres, foams, corrugated plastics, sheets, multilayers, composites, blends, and reinforcing materials (Chércoles et al., 2009). Multilayer polyurethane (PU) is a technopolymer widely used also in aerospace engineering because of its ability to provide high bending stiffness coupled with light weight (Vijay Kumar, Bhimasen Soragaon, 2014). In the present study we evaluated the effect of simulated microgravity on degradative activity of *Cladosporium cladosporioides, Aspergillus niger* and *Mucor plumbeus* on PU samples. The purpose of this research is to investigate how simulated low gravity environments could affect fungal behaviour and how fungi interact with materials employed in spacecraft development.

MATERIALS AND METHODS

Biological Material

Aspergillus niger van Tieghem, *Cladosporium cladosporioides* de Vries and *Mucor plumbeus* Bonorden (isolates from dust in Mycology Laboratory, DiSIT, UPO and indentified throught morphological characteristics) inocula were prepared as a spore suspension, collecting spores from the surface of one-week-old Petri dish culture on MEA (Malt Extract Agar, Oxoid) using sterile physiological solution (NaCl, 0,9%). The suspension was adjusted to a concentration of 10^6 spores/ml.

Materials samples

Multilayer polyurethan samples employed on the ISS were supplied by Etan Laboratory (Engineering Technological Area for Nanotechnologies for Space; Thales Alenia Space, Turin). The material was classified as technopolymers according to its chemical nature, its types of processing, and its practical applications. Technopolymer characteristics of polyurethane ethylene-vinyl acetate polymer are the presence of two

different sides, the blue one (rough) and the grey one (smooth). The technopolymer is a four-layer material composed as follow:

PU + PES + EVOH + PU

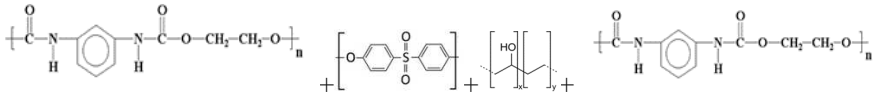

Technopolymers samples were cut into small pieces of 6 x 1cm and autoclaved at 120°C for 5 minutes. The evaluation of micodegradation has been performed with morphological analysis of samples surfaces.

Simulated microgravity condition

Microgravity conditions were simulated using the RPM connected to a control console through standard electrical cables (Dutch Space, Leiden, The Netherlands). The apparatus is a 3D clinostat consisting of two independently rotating frames. This device does not eliminate gravity, but the RPM is a micro-weight simulator based on the principle of "gravity-vector averaging": it allows a 1 g stimulus to be applied omnidirectionally rather than unidirectionally, and the sum of the gravitational force vectors tends to equal zero ($1x10^{-6}$ g). The effects generated by the RPM are comparable to the impact of real microgravity, provided that the direction changes are faster than the system's response time to the gravity field. The desktop RPM used was positioned within an incubator to maintain the temperature.

Experimental Setup

The PU samples were placed in 6cm in diameter plates with low glucose (10 g/l) Potato Dextrose Agar medium (PDA, Oxoid). Three replicates for each experimental condition were inoculated with 5µl of 10^6 spores/ml of fungal suspension and placed into the 3D-RPM inner frame. The same has been done for plates with material without inocula. Controls for all tests were cultured in the same conditions without rotation. All incubations were carried out at 24±2°C for 60 days.

Mycodegradation Analysis

Mycodegradation analysis will be performed on 9 points for each side of materials. The samples used were washed with distilled water to remove both the culture medium and the fungus, dried carefully (4h at 37 °C). The material examined has two sides with different colour and morphology, the analyses were carried out on both sides. The technopolymer samples were processed to asses mycodegradation with CA (Contact Angle**)** measurements and Scanning Electron Microscopy (SEM) observations.

CA measurements

The wettability of the material surface has been assessed by measuring the contact angles (CA) on each surface material before and after biotic exposure through drop water contact angle (θ) measurements using a CAM 200 from KSV Instruments. The analyses involve one 4µl drop of Millipore grade distilled water on the material surface. Advanced contact angles (CA) are presented as mean ± standard deviation. The measurements were made at 20 ± 2°C. The average of these points will give the final contact angle that will allow to define material as hydrophobic or hydrophilic.

Scanning electron microscopy (SEM) analysis

The surface morphology before and after biotic exposure were investigated using Keysight U9320B. The samples were coated with a gold thin layer (10-20 nm) after passing the pure and dry argon gas in the coating chamber, under vacuum for a sputtering time of 30s. The plate voltage was 2000 V and the current passed was 25 mA. The samples were settled on carbonious stabs and analysed.

RESULTS

Mycodegradation Analysis

All fungi inoculated on PU were developed on almost the entire surface of both blue and grey side. Mycelia and reproductive structures were present already after 7 days in all samples.

CA measurements

First of all, analyses on PU samples without fungal inoculum were carried out with the CA detector and these values have been used as controls. Subsequently measures were taken on nine different points for each material side and for all points evaluated a drop image has been taken (fig.1). In figure 1, the blue and grey sides show respectively their

characteristic roughness (fig.1a) and smoothness (fig.1b). The CA values are different for the two material sides, in particular the blue side roughness entails higher CA values than those grey sides (the grey smooth surface has a contact angle of ΘL 76,44° and ΘR 77,13°, while the blue rough surface has a contact angle of ΘL 83,03° and ΘR 81,07°). Gravitational conditions don't impact on materials wettability without fungal inocula.

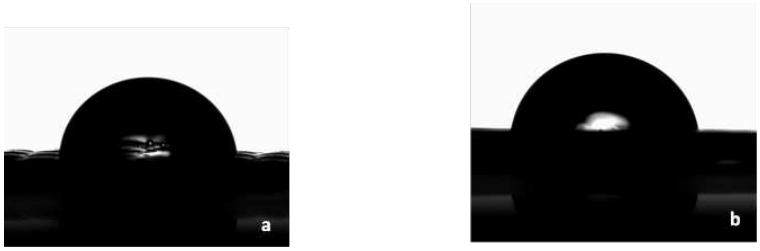

Fig 1. Control PU contact angle measurement, (a) blue side and (b) grey side.

SEM analysis

Surface morphology has been observed through Scanning Electron Microscope (SEM). Each side of multilayer PU without fungal inocula in order to obtain images used as controls (fig.2).

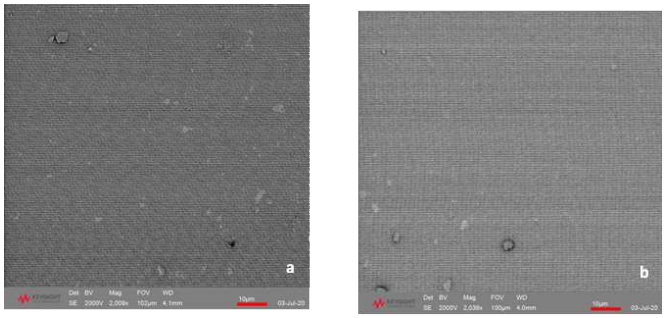

Fig.2 SEM micrograph of blue side (a) and grey side (b) of PU before the fungal inoculum used as controls. Scale bar: 10 µm.

Analyses of PU samples inoculated with *Aspergillus niger*

CA measurements

The CA data and images (Tab.1 and fig.3) show very different contact angle values in comparison to those measured on the control surfaces without the fungus. The values of samples inoculated with *Aspergillus niger* decrease more in samples placed in simulated microgravity than those cultured in terrestrial gravity condition. In addition, the grey side registers values lower than those of the blue side.

Table 1
CA values of the water drop on the PU surface inoculated with *Aspergillus niger* grown in terrestrial gravity conditions and in simulated microgravity conditions

Polyurethane (PU)				
A. niger	Blue side		Grey side	
	Left θ	Right θ	Left θ	Right θ
Terrestrial gravity	70,05±1,27	70,09±1,72	58,7±3,65	58,8±3,43
Simulated microgravity	67,96±	68,76±3,59	54,49±3,43	54,82±6,99

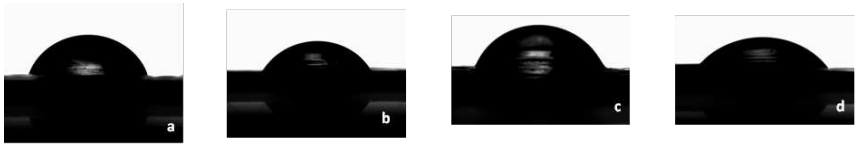

Fig. 3 Comparison of PU blue side (a,c) and grey side (b,d) inoculated with *Aspergillus niger* and cultured in terrestrial condition (a, b) and in simulated microgravity (c, d) conditions.

SEM analysis

The images obtained at SEM show the surfaces of PU samples. Surface cracks are visible on blue side samples inoculated with *Aspergillus niger* and subjected to simulated microgravity (fig. 4 c), while on grey sides there are discontinuities and morphological irregularities in some areas of surface in both growth conditions (terrestrial and simulated microgravity conditions).

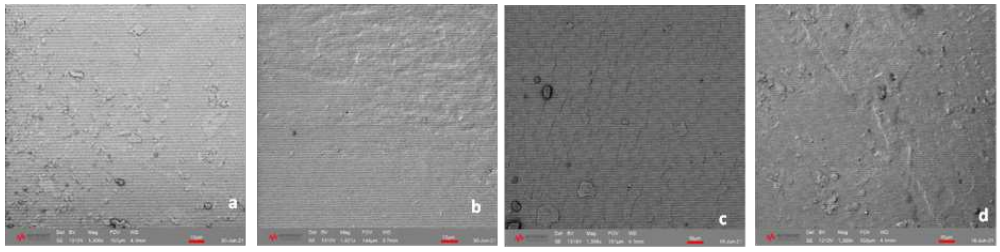

Fig. 4 SEM micrograph of blue side (a, c) and grey side (b, d) of PU. Analyses have been performed on samples inoculated with *A. niger* kept under terrestrial gravity (a, b) or under simulated microgravity (c,d). Scale bar: 10μm.

Analyses of PU samples inoculated with *Cladosporium cladosporioides*

CA measurements

The CA measures, as images (Tab.2 and fig.5), showed how PU samples inoculated with the *Cladosporium cladosporioides* exhibit interesting reduction of drop contact angle values compared to control samples. In particular, grey side inoculated with *C.*

cladosporioides and exposed to long term simulated microgravity has the biggest difference compared to the control.

Table 2
CA values of the water drops on *Cladosporium cladosporioides* PU inoculated surfaces under earth terrestrial condition and simulated microgravity.

Polyurethane (PU)				
C. cladosporioides.	Blue side		Grey side	
	Left θ	Right θ	Left θ	Right θ
Terrestrial gravity	69,24±3,18	69,6±3,18	69,20±4,09	69,10±3,70
Simulated microgravity	74,82±5,38	74,18±4,71	66,78±2,90	66,5±2,02

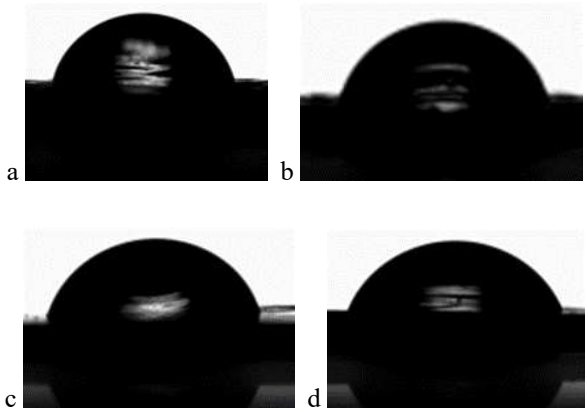

Fig. 5 Comparison of PU blue side (a,c) and grey side (b,d) inoculated with *Cladosporium cladosporioides* and cultured in terrestrial condition (a, b) and in simulated microgravity (c, d) conditions.

SEM analysis

The SEM images (fig.6) also show in general how the fungus changed the morphology of the surface. Simulated microgravity exposure induces cracks and pits formation on the PU blue side inoculated with *C. cladosporioides* (fig.6c). The grey side inoculated with *C. cladosporioides* show surface abrasions in both gravity conditions.

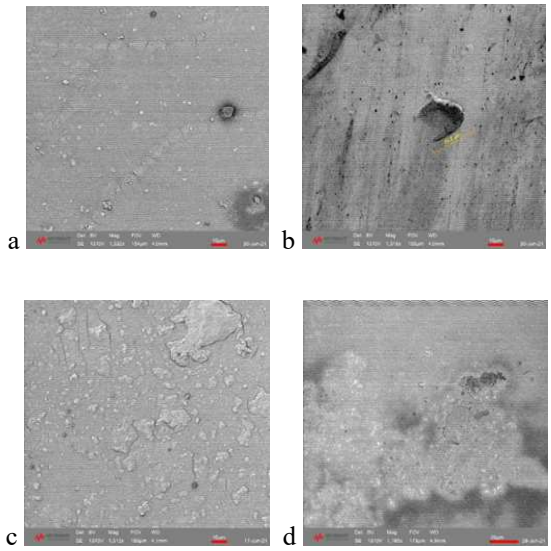

Fig. 6 SEM micrograph of blue side (a, c) and grey side (b, d) of PU. Analyses have been performed on samples inoculated with *C. cladosporioides* kept under terrestrial gravity (a, b), or under simulated microgravity (c, d) Scale bar: 10 μm.

Analyses of PU samples inoculated with *Mucor plumbeus*

CA measurements

With the data and images obtained from and images obtained by CA measurement (Tab. 4 and fig.7) of the PU inoculated with *Mucor plumbeus* we were able to highlight some differences in PU outcomes to fungal exposure between blue and grey side. In fact, the grey side data show the highest increase in material hydrophobicity ever. On the other hand, the blue side data show a slight decrease in CA values compared to the control sample.

Table 4
Water drop CA values on the PU surface inoculated with *Mucor plumbeus* under terrestrial gravity condition and simulated microgravity.

Polyurethane (PU)				
M. plumbeus	Blue side		Grey side	
	Left θ	Right θ	Left θ	Right θ
Terrestrial gravity	73,84±6,47	74,20±6,35	83,00±4,43	83,3±5,35
Simulated microgravity	76,97±6,17	76,79±7,76	83,13±7,32	83,48±6,72

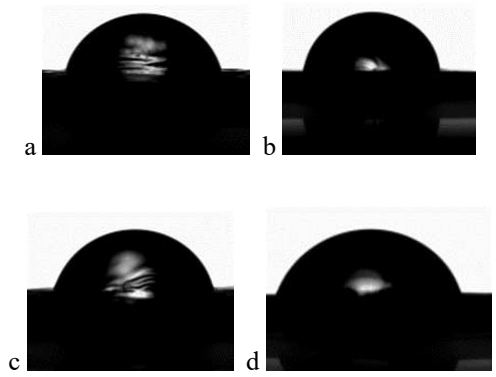

Fig. 7 Comparison of PU blue side (a,c) and grey side (b,d) inoculated with *Mucor plumbeus* and cultured in terrestrial condition (a, b) and in simulated microgravity (c, d) conditions.

SEM analysis

SEM images (Fig. 8) of the surfaces of samples inoculated with *Mucor plumbeus* present in all the experimental conditions (blue side, grey side, terrestrial gravity and simulated microgravity) a marked smoothing of the surface with the almost total loss of the morphological roughness characteristics of the surfaces of the material.

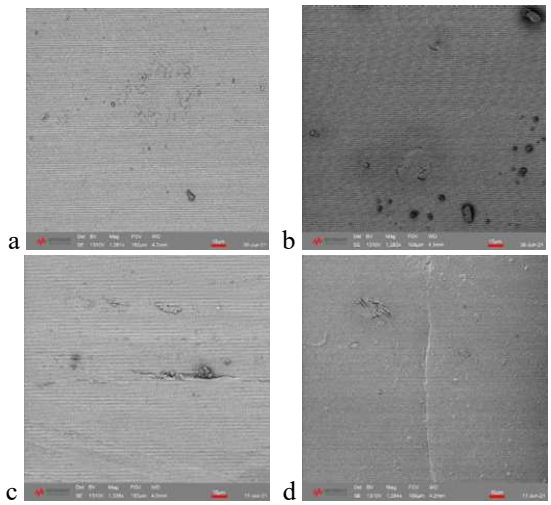

Fig.8 SEM micrograph of blue side (a, c) and grey side (b, d) of PU. Analyses have been performed on samples inoculated with *M. plumbeus* kept under terrestrial gravity (a, b), or under simulated microgravity (c, d) Scale bar: 10 μm.

DISCUSSION

Biodegradation and biodeterioration are common phenomena in nature. The fungi are responsible for many damages on both natural and synthetic materials. The release of digestive enzymes by exocytosis outside of their hyphae, induces the breakdown of

macromolecules into smaller organic compounds the fungus is able to absorb, releasing CO_2 and H_2O (Pathak, 2017). This process allows fungi to extend hyphae and form complex filamentous networks in order to reach recalcitrant nutrient sources often unavailable for other microorganisms. Their powerful enzymatic system, together with the ability of adsorption and the production of natural biosurfactants (e.g. hydrophobins) enables them to use polymers (i.e. plastics) as a source of carbon and electrons, providing them an energy source (Sànchez, 2020). The multilayer PU used in this work is a technopolymer widely used on Earth but also employed for Space applications (Vijay Kumar, Bhimasen Soragaon, 2014). Preserving Space Station materials integrity is essential for envisioning human interplanetary Space exploration advances, as long-term space missions to reach Mars and the Moon. However, based on their chemical structure and composition, synthetic polymers, as multilayer PU, can be a possible substrate for heterotrophic microorganisms growth. Filamentous fungi represent a potential risk for biodeterioration of these materials as shown by analyses performed in this research. El-Morsy et al. (2017) reported the pool of enzymes involved in polyurethane biodegradation carried out by *Monascus sp*. (i.e. protease, esterase and lipase). Polyester polyurethane (impranil) micodegradation has been reported by *Pestalotiopsis* microspore serine hydrolase synthesis enhanced when impranil was the sole carbon source (Russell et al., 2011). In addition, the ascomycetes *Zalerion maritimum* and *Gloeophyllum trabeum* were able to degrade microplastics (Krueger et al. 2015; Paço et al. 2017). *Aspergillus* and *Cladosporium* species are known to participate in aliphatic hydrocarbon degradation while *Mucor* spp. have been shown to be able to deteriorate some recalcitrant aromatic hydrocarbons (Amend et al., 2019). Moreover, these genera have been commonly found as a part of the ISS microbial community (Grizzaffi et al., 2011; Vesper et al., 2008).

In the present work degradative activity of *A. niger*, *C. cladosporioides* and *M.plumbeus* has been evaluated. Degraded polymer samples are explained by changes in wettability and surface fractures and such alterations examined by analysing contact angle θ (CA), formed between the sample surface and the tangent of micro-droplet on it, and scanning electron microscopy (SEM). Degraded polymer shows conformational changes in its texture.

The CA measures indicate that the values of samples inoculated with different fungi decrease more when exposed to simulated microgravity than those cultivated in terrestrial conditions. *Aspergillus niger*, in particular, displays a remarkable lowering

of the CA values on the grey side compared to the other fungi. The surface hygroscopicity increase is probably due to the degradative fungal activity. *A. niger* produces a pool of enzymes involved in polymer degradation as acetyl xylan esterase efficient for xylan degradation and proteolytic enzymes for polyurethane degradation (Pathak and Navneet, 2017). The images obtained with SEM showed numerous cracks and surface discontinuities on PU samples inoculated with fungi, compatible with the enzymatic action of the fungi. As for *A. niger*, samples inoculated with *Cladosporium cladosporioides* present an alteration in the wettability of the material. SEM micrographs confirmed surface alteration with cracks and pits formation, more emphasised in samples kept under simulated microgravity. *Cladosporium spp.* have been isolated by polyethylene materials and different plastics suggesting to be involved in pollutant degradation (Pathak and Navneet, 2017; Spina et al., 2021).

For samples inoculated with *Mucor plumbeus* we have observed different behaviours in mycodegradation between the blue and the grey side. In fact, the *M. plumbeus* inoculated grey side data present an increase in the hydrophobicity of the material that has never been observed for the other fungal strains tested. CA values of blue side showed a mild decrease in both clinostat and terrestrial conditions if compared to control samples, as observed in experiments with the other fungal strains. SEM images of the surfaces of samples inoculated with *M. plumbus* presented, in all the experimental conditions (blue side, grey side, simulated microgravity and terrestrial gravity), a marked smoothing of the surfaces with losing almost total roughness of the material surfaces. The species of the genus *Mucor* constitute a group of microorganisms characterised by a high production of extracellular enzymes (Alves et al., 2002). Several studies described *Mucor spp.* degradative activities on plastic materials as surface fractures, bond scratching and other changes like colour and texture of materials (Mahalakshmi et al. 2012; Eubeler et al. 2009).

In the course of our experiments we observed the ability of all strains tested to deteriorate the PU surfaces. Despite the degradation activity was observed in both the experimental conditions, the long term microgravity exposure (60 days) seemed to have enhanced the degradation process of both the surfaces. Current studies concerning the metabolic responses of microorganisms exposed to real and modelled microgravity concern only short time (from hours to a few days) exposure to weightlessness (Sathishkumar et al., 2014; Chunmei et al., 2019). It is well known that fungi are sensible to changes in direction of the gravity vector (Chunmei et al., 2019). Until now

limited information is available on the effect of simulated microgravity cellular and metabolic responses of fungal species. The relationship of a fungus with its immediate environment is defined by an array of secreted proteins and metabolites. Molecules secreted form a surface coating in order to attach hyphae to hydrophobic substrates and enhance their cellular ability to penetrate three dimensional substrates. Therefore, these secreted molecules form a biofilm that can exert a potential risk for the materials onboard of the ISS (Harding et al., 2009; Ammala et al. 2011).

CONCLUSION

Data collected in the present work indicate that fungal activities affect the surface of the PU, the fungus development modifies the material surface and can make it more absorbent. PU degradation could lead to changes in mechanical properties, as reduction in tensile strength. Earth-based experiments show us that fungi are producers, decomposers and recyclers. Fungi take part in the deterioration process via modification of their metabolic functional pathways in order to utilise xenobiotic compounds, according to environmental conditions. In fact, our results indicate that fungi growth on PU in simulated microgravity conditions exhibit a different degradative behaviour. Further analyses focused on metabolic activity and enzymes production can discern the sequence of events triggering long-term simulated microgravity impact.

REFERENCES

Alves MH, Campos-Takaki GM, Porto ALF and Milanez AI. Screening of Mucor spp. for the production of amylase, lipase, polygalacturonase and protease. *Brazilian Journal of Microbiology*, 2002; *33*(4), 325-330

Amend A, Burgaud G, Cunliffe M, Edgcomb VP et al. Fungi in the Marine Environment: Open questions and unsolved problems. *mBio* 2019; *10*, 1–15.

Ammala A, Bateman S, Dean K, Petinakis E et al. An overview of degradable and biodegradable polyolefins. *Progress in Polymer Science*, 2011; *36*(8), 1015-1049.

Checinska A, Probst AJ, Vaishampayan P, White JR, Kumar D, Stepanov VG, Nilsson HR, Pierson DL, Perry J, Fox GE and Venkateswaran K. Microbiomes of the dust particles collected from the International Space Station and Spacecraft Assembly Facilities. *Microbiome* 2015, 3, 50.

Chércoles Asensio, R, San Andrés Moya M, de la Roja JM and Gómez M. Analytical characterization of polymers used in conservation and restoration by ATR-FTIR spectroscopy. *Analytical and bioanalytical chemistry*, 2009; *395*(7), 2081-2096.

Chunmei J, Dan G, Zhenzhu L, Junling S, Dongyan S. Clinostat Rotation Affects Metabolite Transportation and Increases Organic Acid Production by Aspergillus carbonarius, as Revealed by Differential Metabolomic Analysis. *Applied and Enviromental Microbiology*. 2019; 85 (18): 1-16.

El-Morsy EM, Hassan HM and Ahmed E. Biodegradative activities of fungal isolates from plastic contaminated soils. *Mycosphere*, 2017; *8*(8), 1071-1087.

Eubeler JP, Zok S, Bernhard M, Knepper TP. Environmental biodegradation of synthetic polymers I. Test methodologies and procedures. *TrAC Trends Anal Chem* 2009, 28(9):1057–1072

Grizzaffi L, Lobascio C, Parodi P, Saverino A, Locatore I, Perrachon D, Giacosa D and Sampò S. Post-flight analyses of Columbus HEPA Filter. American Institute of Astronautica and Astronomics. 41st International Conference on Environmental Systems 2011.

Harding MW, Marques LLR, Howard RJ and Olson ME. Can filamentous fungi form biofilms? *Trends Microbiol*. 2009; 11, 475-80

Klintworth R, Reher HJ, Viktorov AN, Bohle D. Biological induced corrosion of materials. II. New test methods and experiences from MIR station. *Acta Astronautica*, 1999; 44 (7-12): 569–578.

Krueger MC, Hofmann U, Moeder M and Schlosser D. Potential of wood-rotting fungi to attack polystyrene sulfonate and its depolymerisation by Gloeophyllum trabeum via hydroquinone-driven Fenton chemistry. *PloS one*, 2015; *10*(7), e0131773.

Mahalakshmi V, Siddiq A, Andrew SN. Analysis of polyethylene degrading potentials of microorganisms isolated from compost soil. *Int J Pharm Biol Arch* 2012; 3(5):1190–1196

Novikova ND. Review of the knowledge of microbial contamination of the Russian manned spacecraft. *Microbial Ecology*, 2004; 47 (2): 127-132.

Paço A, Duarte K, da Costa JP, Santos PS, et al. Biodegradation of polyethylene microplastics by the marine fungus Zalerion maritimum. *Science of the Total Environment*. 2017; *586*, 10-15.

Pathak VM. Review on the current status of polymer degradation: a microbial approach. *Bioresources and Bioprocessing*, 2017; *4*(1), 1-31.

Rosenzweig JA, Abogunde O, Thomas K, Lawal A, et al. Spaceflight and modeled microgravity effects on microbial growth and virulence. *Applied microbiology and biotechnology*, 2010; *85*(4), 885-891.

Russell JR, Huang J, Anand P, Kucera K, Sandoval AG, Dantzler KW and Strobel SA. Biodegradation of polyester polyurethane by endophytic fungi. *Applied and environmental microbiology*. 2011; *77*(17), 6076-6084.

Sánchez, C. Fungal potential for the degradation of petroleum-based polymers: An overview of macro-and microplastics biodegradation. *Biotechnology advances*, 2020; *40*, 107501.

Sathishkumar, Y., Velmurugan, N., Lee, H. M., Rajagopal, K., Im, C. K., & Lee, Y. S. (2014). Effect of low shear modeled microgravity on phenotypic and central chitin metabolism in the filamentous fungi Aspergillus niger and Penicillium chrysogenum. *Antonie van Leeuwenhoek*, *106*(2), 197-209.

Chechiska Sielaff A, Urbaniak C, Mohan GBM, Stepanov VG. *et al.* Characterization of the total and viable bacterial and fungal communities associated with the International Space Station surfaces. *Microbiome*, 2019; 7:50

Spina F, Tummino ML, Poli A, Prigione V, et al. Low density polyethylene degradation by filamentous fungi. *Environmental Pollution*, 2021; *274*, 116548.

Vesper SJ, Wong W, Kuo CM, Pierson DL. Mold species in dust from the International Space Station identified and quantified by mold-specific quantitative PCR. Res Microbiol. 2008;159(6):432-5. doi: 10.1016/j.resmic.2008.06.001.

Kumar MV and Soragaon B. Fabrication and evaluation of multilayered polyurethane foam core sandwich panels for static flexural stiffness. *Procedia Engineering*, 2014; *97*, 1227-1236.

Wang, K. A new fractal model for the soliton motion in a microgravity space. *International Journal of Numerical Methods for Heat & Fluid Flow* 2020.

Conclusion and Final Remarks

This thesis collects different research projects conducted during my PhD program which evaluated the impact of gravity vector changes in eukaryotic organisms and cells.

Living organisms are subjected to constant gravitational force; this is presumed to play a crucial role in regulating organisms, tissues and cell homeostasis by inducing mechanical stresses experienced at the cellular level. Thus, mechanical overloading, associated with hypergravity experienced during space launch and reentry or unloading associated with the weightlessness of Space are supposed be able to shift the balance between physiology and pathophysiology, inducing morphofunctional changes at cellular, tissue and organism level, that can lead or accelerate the development and the progression of some disease states.

The increasing number of long-term space missions emphasize the importance to elucidate the role and outcomes of variable gravitational force on biological systems.

Nowadays, it is well known that spaceflight has an enormous influence on space voyagers due to the combined effects of hypergravity (during launch and reentry), microgravity (once they reach outer Space) and cosmic radiation (Nargund, 2015; Mishra and Luderer, 2019). Despite their frequencies, access to spaceflight opportunities continues to be difficult and expensive, for these reasons experiments under real microgravity are limited. However, studies on the effect of gravity variation can be carried out using devices able to simulate microgravity, like Random Positioning Machine (RPM), or hypergravity, as Large Diameter Centrifuge (LDC) (Van Loon, 2001; 2007; 2008). Furthermore, facilities for ground-based research are excellent and reliable tools to identify possible effects of gravity changes before performing costly and time-consuming real microgravity experiments, throughout the Space Shuttle or Space Station (Morita et al., 2015; Frett et al., 2016; Bonnefoy et al., 2021).

Space travels are associated with a set of changes in male reproductive physiology and function, significant body fluid shift causing facial edema, cardiovascular responses and disturbance in hormones and reproductive organs (Merill et al., 1992). Therefore, the plan to establish a colony and pursue normal life in Space has to include a mechanism that preserves and enables the correct reproductive function. In Chapter 1 and Chapter 2 the effects of hypergravity and microgravity were investigated on the mammalian male reproductive system. Since testis is a basic organ of the male reproductive system it is important to evaluate the possibility of spermatogenesis failure

in the space environment. Hypergravity is usually experienced by astronauts during a rocket launch, with a maximum g-force of around 3g. Moreover, increased gravity vector is used for a long time as training for pilots and astronauts, and is proposed as a countermeasure for microgravity disruptions, such as a loss of muscle mass and bone density, impaired vision, decreased kidney function, diminished neurological responses and compromised immune system (Strollo et al., 2000; Monici et al., 2006; Tominari et al., 2019). However, alteration on testes physiology and function induced by high-gravity exposure have been described on mice kept for 14 days under 3g conditions using LDC. In particular, a lack in FSHR and IL-1β expression, together with the specific increase of SHBG expression on Sertoli Cells (SC) was observed. These results could suggest the falling down of physiological function of SC toward a quiescent phase. SC disassembly lining organisation and hormone responsiveness pattern point towards severe consequences for the reproductive axis. This quiescent phase probably evolved in a loss of some SC as evidenced by apoptotic signals, leading to an altered homeostasis of the organ and reduced formation of spermatozoa. Moreover, we observe that hypergravity exposition reduces the expression of enzymes involved in testosterone biosynthesis, suggesting a loss of function of the glandular compartment of the testis. Compared to hypergravity, effects of microgravity on male reproductive system have been better characterised. However, little is known about first responses induced by simulated microgravity exposure at cellular level. For this reason, exploiting RPM, the first stages were evaluated on primary cell culture from rat testis. In this study, we validated our hypothesis that short-term simulated microgravity induces oxidative cellular stress in rat testes primary culture cells, as demonstrated by the response of the antioxidant system and impaired mitochondrial function. Additionally, we found an increase in SHBG/ABP production that together with increase in ROS, morpho-functional and cytoskeletal alteration could have a significant inhibitory effect on germ cell differentiation which may result in male infertility.

Our data on the mammalian male reproductive system ought to provide some insight on mechanisms involved in male infertility, a social concern also on our planet. In addition, testes can be used as a putative model of endocrine gland. Considering data obtained, it could be possible that gravity vector changes could cause deregulation patterns on other glands and organs, revealing strong side effects due to modified gravity conditions.

Interest in the long-term effects of altered gravity on cells and organisms is not only important for preparing humans for longer-term space exploration but may also highlight opportunities to manipulate, correct and improve treatment of certain diseases. Cancer remains one of the most significant diseases worldwide. Despite advances in medical science, no definitive strategies have been found for the prevention of cancer formation or to inform treatment. Pancreatic cancer, in particular pancreatic ductal adenocarcinoma (PDAC) is one of the most severe malignancies, characterised by late diagnosis and/or resistance to the treatments (Konstantinidis et al., 2013). Microgravity revolutionises tumour cell behaviour and metabolism leading to the acquisition of an aggressive and metastatic stem cell-like phenotype, as described in Chapter 3. Results collected describe cell rearrangement dissecting time by time cell transformation toward a more stem and aggressive phenotype induced by simulated microgravity exposure. Information gained improves knowledge in cancer studies in this new dimension and paves the base for altered gravity conditions as new anti-cancer technology. Thus, future works will focus on the evaluation of pancreatic cancer cells' response to anti neoplastic drugs under simulated microgravity.

In this thesis, the effects of long-term simulated microgravity were evaluated on another biological system, that is filamentous fungi. In particular, we evaluated fungal response to simulated microgravity and fungal interaction with materials employed on ISS. The results from these studies are reported in three different chapters (Chapter 4, 5 and 6) confirm that fungi respond to mechanical unloading and should be considered as a possible forward contamination source.

Filamentous fungi such as *P. chrysogenum* are naturally and commonly found as part of microbiota of spacecraft environments (Alekhova et al., 2005). Characterization of *P. chrysogenum*, revealed that gravity vector changes after a long-term exposure to simulated microgravity conditions (60 days) induce modifications in growth rate, germination rate and differences in hyphal tip organisation and branching. In particular *P. chrysogenum* exposed to long-term simulated microgravity conditions develops morphological alteration in hyphae structure with asymmetrical enlargement “sausage-like” and interruption in tip growth, probably related to cytoskeletal reorganisation as demonstrated by vesicle traffic changes. These observations, together with different growth rate slow-down, were enhanced in colonies returned on static condition after a long incubation period under simulated microgravity, if compared with colonies always grown under static or simulated microgravity condition. Changes in growth rate could

be related to germination rate, which is enhanced by exposure to simulated microgravity also if experienced for a few hours. However, going on in the germination process we observed a slowdown in conidia come back to terrestrial gravity and an increase in the number of germ tube formation from conidia exposed to simulated microgravity for a long-time. These data suggest that fungi exposed to long-term simulated microgravity adapt themselves to simulated microgravity and show disruption in colony growth when they experience terrestrial conditions once again.

As reported in literature and in Chapter 4, *P. chrysogenum*, together with other fungi, is able to grow under microgravity environment (Grizzaffi et al., 2011). Considering their ubiquity on board the ISS and their ability to adapt and develop under altered gravity conditions, they could also impair the technological characteristics and completeness of spacecraft materials in long-term missions, causing deterioration in manufactured materials and components (Grizzaffi et al., 2011, Sànchez, 2020).

Materials employed for Space launch vehicles, satellites and spacecraft instruments are technopolymer characterised by high thermal and mechanical performance, used instead of aluminium, base metals and other alloys. Polyesters, reinforced polyamides, acetal resins, polyphenylsulfones, polyurethanes, polyimides and polyetherimides are all defined as technoploymers. Based on their chemical structure and composition synthetic polymers can be potential substrates for the growth of heterotrophic microorganisms (Sànchez, 2020). The heterotrophic nutrition mode, the secretion of extracellular enzymes, the absorption of nutrients through the cell wall and the apical growth are characteristics that demand the fungi to keep close contact with the substrate. Experiments performed under simulated microgravity conditions with *P. chrysogenum* on three different materials employed on ISS (polyurethane, polyimide and para-aramid) might indicate a susceptibility to fungal activity, in addition mycodegradation of synthetic polymers is increased in simulated microgravity conditions. Chemical and physical analyses (CA, FTIR-ATR, SEM) were performed to verify technopolymers deterioration. The data collected highlights the changes in surface hydrophobicity, number of cracks, surface discontinuities shown and chemical changes in synthetic polymer molecules. In particular, micodegradation activity has been further investigated testing other fungal species common on ISS environments (*A. niger, Mucor sp., Cladosporium sp.*) on multilayer polyurethane (PU) technomaterials with carrying out morphological analysis (CA and SEM). Results obtained confirmed degradative action of PU caused by fungal activities. Fungal development modifies

material surface and makes it more absorbent with cracks and abrasion compatible with the enzymatic action of the fungus that is probably enhanced under simulated microgravity. Stress conditions and lack of nutrients could modulate enzymatic activity in order to obtain nutrients by polymeric substrate. However, how low gravity affects fungal behaviour and physiology is still unknown. Future omics-based technologies will be employed to investigate fungal gene expression and metabolic pathways variations in order to provide more information about adaptive changes triggered by microgravity. The information gained can be applicable to the safety and preservation of spacecraft crews, and last but not least can provide new and sustainable solutions for the plastic pollution challenges.

As a general conclusion, it is possible to state that the results obtained in the framework of the present PhD thesis provide insight on biological systems response, acclimatisation and adaptation mechanisms in altered gravity force environments. The future holds exciting prospects for modern Space capabilities to improve life on Earth. Developing integrated physiological models for biology in Space will lead to a better understanding of life on Earth and identify the underlying mechanisms and networks that govern biological processes both in Space and in the terrestrial environment. Moreover, all this knowledge can help to develop new understanding and technology to support human and Earth health.

REFERENCES

Alekhova TA, Aleksandrova AA, Novozhilova TIu, Lysak LV, Zagustina NA and Bezborodov AM. Monitoring of microbial degraders in manned space stations. *Prikl Biokhim Mikrobiol*. 2005; 41(4):435-43. Russian. PMID: 16212041.

Bonnefoy J, Ghislin S, Beyrend J, Coste F, Calcagno G, Lartaud I, Gauquelin-Koch G, Poussier S, Frippiat JP. Gravitational Experimental Platform for Animal Models, a New Platform at ESA's Terrestrial Facilities to Study the Effects of Micro- and Hypergravity on Aquatic and Rodent Animal Models. *Int J Mol Sci.* 2021; 15; 22(6):2961. doi: 10.3390/ijms22062961.

Frett, T., Petrat, G., van Loon, J., Hemmersbach, R., Anken, R.H.: Hypergravity Facilities in the ESA Ground-Based Facility Program – Current Research Activities and Future Tasks. *Micrograv. Sci. Techn.* 2016; 28, 205–214.

Grizzaffi L, Lobascio C, Parodi P, Saverino A, Locatore I, Perrachon D, Giacosa D and Sampò S. Post-flight analyses of Columbus HEPA Filter. American Institute of Astronautica and Astronomics. 41st International Conference on Environmental Systems 2011.

Konstantinidis IT, Warshaw AL, Allen JN, Blaszkowsky LS, Castillo CF, Deshpande V, Hong TS, Kwak EL, Lauwers GY, Ryan DP, Wargo JA, Lillemoe KD, Ferrone CR. Pancreatic ductal adenocarcinoma: is there a survival difference for R1 resections

versus locally advanced unresectable tumors? What is a "true" R0 resection? *Ann Surg*. 2013 ;257(4):731-6. doi: 10.1097/SLA.0b013e318263da2f.

Merrill Jr AH, Wang E, Mullins RE, Grindeland RE and Popova IA. Analyses of plasma for metabolic and hormonal changes in rats flown aboard COSMOS 2044. *Journal of applied physiology*, 1992; *73*(2), S132-S135.

Mishra B and Luderer U. Reproductive hazards of space travel in women and men. *Nature Reviews Endocrinology*, 2019; *15*(12), 713-730.

Monici M, Marziliano N, Basile V, Romano G, Conti A, Pezzatini S and Morbidelli L. Hypergravity affects morphology and function in microvascular endothelial cells. *Microgravity-Science and Technology* 2006; *18*(3), 234-238.

Morita H, Obata K, Abe C, Shiba D, Shirakawa M, Kudo T, Takahashi S. Feasibility of a Short-Arm Centrifuge for Mouse Hypergravity Experiments. *PlosOne* 2015. Doi:10, e0133981.

Nargund V. Effects of psychological stress on male fertility. *Nat Rev Urol* 2015; 12**,** 373–382 doi:10.1038/nrurol.2015.112.

Sánchez, C. Fungal potential for the degradation of petroleum-based polymers: An overview of macro-and microplastics biodegradation. *Biotechnology advances*, 2020; *40*, 107501.

Strollo F, Barger L, Fuller C. Testosterone urinary excretion rate increases during hypergravity in male monkeys. *J Gravit Physiol* 2000; 7:181–82.

Tominari T, Ichimaru R, Taniguchi K, Yumoto A, Shirakawa M, Matsumoto C, Watanabe K, Hirata M, Itoh Y, Shiba D, Miyaura C, Inada M. Hypergravity and microgravity exhibited reversal effects on the bone and muscle mass in mice. *Sci Rep*. 2019 29; 9(1):6614. doi: 10.1038/s41598-019-42829-z.

Van Loon JJ. Hypergravity studies in the Netherlands. J Gravit Physiol. 2001 ;8(1):P139-42.

Van Loon JJWA. "A Large Radius Human Centrifuge: The Human Hypergravity Havitat", in Life in Space for Life on Earth, 2008, vol. 553.

Van Loon JJWA. 2007: Some history and the use of random positioning Machine, RPM, in gravity related research. *Advances in Space Research*, 39: 1161-1165.